

AL.C. 1987-1

Exposure Time Effects on Concentration Fluctuations in Plumes

CANADIANA
C2
JAN - 6 1987



Alberta
ENVIRONMENT



National Library
of Canada

Bibliothèque nationale
du Canada



Canada

EXPOSURE TIME EFFECTS ON CONCENTRATION FLUCTUATIONS IN PLUMES

By

D.J. Wilson

and

B.W. Simms

**Department of Mechanical Engineering
University of Alberta
Edmonton, Alberta, Canada**

prepared for

**ALBERTA ENVIRONMENT
9820 - 106 Street
Edmonton, Alberta T5K 2J6**

**Project Officer: R.P. Angle
Air Quality Control Branch
Pollution Control Division
Environmental Protection Services**

Contract No. 830990

April 1985



Digitized by the Internet Archive
in 2016

<https://archive.org/details/exposuretimeeffe00wils>

TABLE OF CONTENTS

	<u>Page</u>
Acknowledgement	i
List of Tables	ii
List of Figures	iii
Nomenclature	vi
Executive Summary	xii
Chapter 1 - Introduction	1
Chapter 2 - Refinement of Concentration Fluctuation Model	3
Crosswind Spacing of the Variance Source	4
Accounting for Atmospheric Stability	14
Limitations Imposed by Wind Tunnel Simulation	16
Comparison with Full Scale Atmospheric Data	20
Chapter 3 - Sampling, Averaging and Response Time Effects	26
Integral Time Scale τ_c of Concentration Fluctuation	27
Adjustment for Sampling Time - T_s	28
Effect of Averaging Time - T_a	34
Influence of Averaging Time on Intermittency	36
Comparison with Field Measurements of Averaging Time	37
Dosage Fluctuations	40
Fluctuation Damping by Receptor Response Time	42
Correcting for Instrument Time Response	43
Time Constants for Indoor Air Pollution	45
Chapter 4 - Conditional Mean Concentration	46
Conditional Mean for Long Sample Times	49
Required Sampling Times for Conditional Means	52
Variation of Conditional Mean with Distance	52

TABLE OF CONTENTS (con't)

	Page
Chapter 5 - Statistical Distributions and Threshold Crossing	
Probabilities	55
Log-Normal and Exponential Probability	
Distributions	55
The Gamma Probability Distribution	57
Measured Probability Distributions	59
Threshold Crossing Probability	66
Application of Threshold Crossing Probability to Air Quality Monitoring	67
Appendix A - Effect of Receptor Time Constant and Data Averaging	
Time Interval on Effective Fluctuation Variance	A1
System Frequency Response	A2
The Markovian Spectrum	A2
Frozen Turbulence	A3
Frequency Spectrum of Concentration Fluctuations	A4
Observed Spectrum and Variance with Gain Attenuation	A5
Effect of Data Averaging Time Interval on Observed Variance	A8
Effect of Response Time Constant and Averaging Time on Measured Fluctuation Scales	A12
Appendix B - Universal Ground Level Profiles of Mean and	
Fluctuating Concentration	B1
Mean Concentration	B1

TABLE OF CONTENTS (con't)

	Page
Appendix B - (con't)	
Fluctuation Intensity	B1
Conditional Fluctuation Intensity and Intermittency	B6
Variance Source Strength	B7
Appendix C - Length and Time Scales of Concentration Fluctuation	C1
Variation of Length Scale Across a Plume	C2
Alongwind Variation of Concentration Scale	C5
Comparison With Measurements	C7
Appendix D - Effect of Wind Direction Meandering on Mean and Fluctuating Concentration	D1
Accounting for Long Time Averages by Increased Crosswind Spreading	D2
Crosswind Integration to Simulate Long Sampling Times	D4
Crosswind Averaging of Mean Concentration	D7
Crosswind Averaging of Intermittency	D8
Crosswind Averaging of Fluctuation Variance	D10
Influence of Sampling Time on Integral Scales	D13
Relating Meandering Width to Sampling Time	D15
Crosswind Profiles at Long Sample Times	D17
Appendix E - Dosage Fluctuations	E1
Dosage Fluctuations Caused by Concentration Variance	E2

TABLE OF CONTENTS (con't)

	Page
Appendix F - Probability of Threshold Level Crossing During Exposure	F1
Fraction of Time Over a Threshold	F1
Threshold Crossing Probability for a Series of Short Exposures	F2
Steady Release With Long Exposure Time	F4
Generalized Model for Continuous Exposure	F5
Appendix G - Stochastic Model of Gas Concentrations	
Introduction	G1
The Gas Concentration Process	G2
The Discontinuous Gas Concentration Model	G7
First Passage Times	G13
Numerical Routines	G19
References	

ACKNOWLEDGEMENTS

The body of the report and Appendices A through F were prepared by D.J.W. The theory for threshold crossing probabilities and development of the Gamma distribution in Appendices F and G are by B.W.S.

Report graphics were drawn by Marlene Wilson, and the text and numerous revisions were typed by Daphne Panylyk. The research to develop the concentration fluctuation models was supported by grants to D.J.W. from Imperial Oil Ltd. and the Natural Sciences and Engineering Research Council of Canada.

The constructive comments made by D.D.J. Netterville, R. Angle and S. Sakayima on an earlier draft are appreciated.

LIST OF TABLES

	<u>Page</u>
Table 1 Variability of Location of Maximum Ground Level Concentration with Atmospheric Stability for Two Source Heights	17
Table 2 Plume Centerline Concentration Fluctuations from Ramsdell and Hinds (1971) Ground Level Source Field Measurements.	24
Table 3 Plume Centerline Statistics for Ramsdell and Hinds (1971) Ground Level Source Field Data Compared with Model Predictions Corrected for Sample Time.	35
Table 4 Asymptotic Values of Conditional Mean Concentrations Normalized by Three Minute Centerline Value \bar{c}_{po}	50
Table 5 Peak Exceedance Probabilities for Three Frequency Distributions	60
Table 6 Changes in Centerline Conditional Plume Fluctuation Intensities with Sampling Time	65

LIST OF FIGURES

		Page
Figure 1 -	Crosswind variance profiles from an elevated source (normalized by extrapolated centerline variance \hat{c}^2) from Wilson, Fackrell and Robins (1982).	5
Figure 2 -	Effect of source pair spacing β on crosswind intermittency profiles from a ground level source in a wind tunnel. Data of Robins and Fackrell (1979).	6
Figure 3 -	Crosswind profiles of mean and fluctuation statistics at $x/H = 0.83$ in the plume from an elevated source $d = 0.30$ cm in a neutrally stable wind tunnel boundary layer, $H = 120$ cm, $z_0/H = 4 \times 10^{-4}$. Data of Fackrell and Robins (1982a).	8
Figure 4 -	Crosswind profiles of mean and fluctuation statistics at $x/H = 2.88$ in a plume from an elevated source $d = 0.85$ cm at $h = 23$ cm in a neutrally stable wind tunnel boundary layer $H = 120$ cm, $z_0 = 4 \times 10^{-4}$. Data of Fackrell and Robins (1982a).	9
Figure 5 -	Vertical profiles of mean and fluctuation statistics at $x/H = 0.83$ at $h = 23$ cm in a neutrally stable wind tunnel boundary layer $H = 120$ cm, $z_0/H = 4 \times 10^{-4}$. Data of Fackrell and Robins (1982a).	10
Figure 6 -	Vertical profiles of mean and fluctuation statistics at $x/H = 2.88$	11
Figure 7 -	Vertical profiles of mean and fluctuation statistics at $x/H = 4.79$	12
Figure 8 -	Ground level profiles of mean concentration normalized in downwind distance x and plume spread λ coordinates using plume spreads σ_y and σ_z from Angle (1978).	15
Figure 9 -	Sampling time limitations in wind tunnel simulation of atmospheric dispersion	18
Figure 10 -	Field measurements of crosswind variance profiles [at $z = 1.5$ m with combined data from $x = 200$ m and 800 m for a ground level source with $d \approx 0.02$ m, $h \approx 1$ m. Data of Ramsdell and Hinds (1971).]	22
Figure 11 -	Field measurements of crosswind profiles of total and plume intensities and intermittency. Data of Ramsdell and Hinds (1971).	23
Figure 12 -	Crosswind meandering model for sampling time adjustments to plume centerline statistics.	30
Figure 13 -	Gaussian model prediction of intermittency γ across a plume, and for sampling time meander averaging on centerline γ_{0T} , with single variance source $\phi = 0$.	32

LIST OF FIGURES - Cont'd

	Page
Figure 14 - Meandering plume model prediction of sampling time effects on plume centerline statistics for a single variance source ($\phi = 0$) and $p = 0.2$ using equations (D13), (D19) and (D44).	33
Figure 15 - Field measurements of effect of data averaging time on intermittency for a monitor at $x = 1500$ m from a stack $h_s = 50$ m at Chalk River Ontario. Data from Barry (1977).	39
Figure 16 - Response of an SO_2 field monitor to concentration fluctuations.	40
Figure 17 - Gaussian model prediction of conditional (plume mean \bar{C}_{po} across a plume, and for sampling time meander averaging on centerline \bar{C}_{poT} , with single variance source $\phi = 0$.	48
Figure 18 - Normalized plume (conditional) and total mean concentrations for 3 min. samples for neutral stability Class D dispersion.	53
Figure 19 - Log-normal and Gamma probability densities compared with ground level measurements in a wind tunnel boundary layer $h/H = 0.44$, $x/H = 0.44$, $x/H = 3.2$, $\lambda = 0.175$	62
Figure 20 - Field measurements of exceedance probability for diffusion from a ground level source in flat terrain and in the wake of a building immediately downwind of the source, with sample time 6 to 15 min. and averaging time of 5 sec. Data of Hinds (1969) in Barry (1977).	63
Figure 21 - Field measurements of averaging time effects on exceedance probability at $x = 1500$ m from a stack $h_s = 50$ m. Data from Barry (1977).	64
Figure A1 - Attenuation of the High Frequency End of the Concentration Fluctuation Spectrum by Receptor Time Response.	A14
Figure A2 - Influence of Sensor Response on Observed Intermittency in Water Channel Simulation of the Plume from a Ground Level Source.	A15
Figure C1 - Concentration length scales on plume centerline for a ground level source with $d = 15$ mm, in boundary layer thickness $H = 1.2$ m.	C9
Figure C2 - Concentration length scales for an elevated source with $h/H = 0.192$, $d = 8.5$ mm in $H = 1.2$ m.	C10

LIST OF FIGURES - Cont'd

	<u>Page</u>
Figure C3 - Along-wind variation of concentration length scale Λ_{C^∞} above ground surface dissipation region.	C11
Figure C4 - Ground level source: Comparison of concentration length scales with predictions for $h/H = 0$, $d = 15$ mm, $H = 1.2$ m.	C12
Figure C5 - Elevated source: Comparison of concentration length scales with predictions for $h/H = 0.192$, $d = 8.5$ mm, $H = 1.2$ m.	C13
Figure C6 - Turbulence velocity length scales and mean velocity profile for wind tunnel boundary layer of Fackrell and Robins (1982).	C14

NOMENCLATURE

a_y, a_z	= exponents in power law plume spread equations (B2), (B3)
B	= respiration rate of a subject during exposure, breaths/s
c	= $\bar{c} + c'$, the instantaneous concentration; kg/m ³
\bar{c}	= time or ensemble mean concentration; kg/m ³
c'	= concentration fluctuation above and below mean \bar{c} , kg/m ³
$\overline{c'^2}_a$	= concentration variance of data with high frequency fluctuations removed by averaging over time intervals of duration T_a , kg ² /m ⁶
$\overline{c'^2}_a$	= "effective" concentration variance, reduced from the true variance c'^2 by a receptor system time constant τ_s , see (A26); kg ² /m ⁶
\bar{c}_0	= mean concentration at a fixed height z on plume centerplane y = 0, kg/m ³
\bar{c}_{om}	= maximum ground level concentration on plume centerline, for fixed plume height h and windspeed U, see (B4), kg/m ³
\bar{c}_p	= conditional "inside plume" mean excluding periods of zero concentration; kg/m ³
$\overline{c'^2}_p$	= conditional "inside plume" fluctuation variance excluding periods of zero concentration; kg ² /m ⁶
d	= apparent diameter of pollution source at point of release
D	= time integrated dose at receptor for a given exposure time T_e (see (E1)); kg-s/m ³
\bar{D}	= ensemble averaged dose for exposure to many realizations of a fluctuating concentration, see (E6); kg-s/m ³
$\overline{D'^2}$	= ensemble variance of dose D of individual realizations about the ensemble mean dose, \bar{D} , see (E10); kg ² -s ² /m ⁶
D_y, D_z	= constants in power law plume spread equations (B2)(B3)
E_c	= spectral density of concentration variance: $E_c(f)df$ is the amount of variance c'^2 between frequencies f and f+df; kg ² -s/m ⁶

- $E_{c,\text{eff}}$ = the "effective" spectral density after attenuation by a receptor system gain G , see (A15); $\text{kg}^2\text{-s/m}^6$
 f = frequency of sine wave fluctuations; s^{-1}
 G = receptor system "gain": the ratio of input to output amplitudes at frequency f , see (A1)
 H = thickness of the neutrally stable atmospheric boundary layer that is influenced by surface roughness; m
 h = height of plume centerline above ground; m
 h_v = height of the effective variance source above ground, see (B20); m

$i = \sqrt{\bar{c}'^2 / \bar{c}} =$ fluctuation intensity of total concentration variance

$i_p = \sqrt{\bar{c}_p'^2 / \bar{c}_p} =$ conditional fluctuation intensity excluding periods of zero concentration.

- $i_\infty, i_{p\infty}$ = total and conditional fluctuation intensities measured on the plume centerline, $y=0$, $z=h$ for a plume with negligible surface interaction, $\sigma_z \ll h$
 i_D = dosage fluctuation intensity, see E(19)
 k_1 = $2\pi f/U$, wavenumber, a normalized fluctuation frequency; m^{-1}
 p_c = probability density function (pdf): $p_c(c)dc$ is the fraction of concentration readings that lie between c and $c+dc$
 q = hypothetical RMS strength of a variance source; kg/s
 Q = source strength; the pollutant release rate; kg/s
 r = hazard rate: probability per unit time of exposure of exceeding a specified threshold c^* for the first time
 R_c = normalized autocorelation coefficient, see (A7)
 S = probability of not exceeding the threshold concentration c^* during an exposure time T_e

t	= time; s
t'	= time delay in autocorrelation, see (A7); s
T_a	= data averaging time chosen to smooth out high frequency fluctuations in the true variance $\overline{c'^2}$ to reduce it to c'^2_a , see (A30); s
T_e	= exposure time over which a receptor is subjected to concentrations; s
T_s	= sampling time: the continuous time period over which data is collected, and which sets a lower limit on the frequency f of fluctuations that can contribute to the observed variance $\overline{c'^2_T}$, and mean $\overline{c_T}$; s
U	= local mean wind velocity; m/s
U_c	= mean advection (or convection) speed of a plume past a y-z plane; m/s
$\overline{u'^2}$	= along-wind turbulent velocity variance; m^2/s^2
V	= fraction of concentration readings (or fraction of time) that concentration is greater than the specified value c^* see (F4).
$\overline{v'^2}$	= cross-wind turbulent velocity variance; m^2/s^2
$\overline{w'^2}$	= vertical turbulent velocity variance, m^2/s^2
x	= downwind distance from source; m
y	= crosswind distance from plume centerline; m
z	= vertical height above ground; m
z_0	= log-law surface roughness parameter; m

Greek Symbols

- α = sink strength used to simulate ground surface effects on variance c'^2 , see (B18)
- β, β_z = crosswind and vertical displacement of effective variance source pair in δ_y and δ_z units
- ξ = $\sqrt{\delta_y \delta_z}/H$, normalized downwind distance in terms of plume half-width spread.
- δ_y, δ_z = plume half-width spreads: distance to point of half centerline concentration, m
- ϕ = crosswind spacing in σ_y units of effective variance source pair, see (B19)
- ϕ_z = vertical displacement in σ_z units above source height of the effective variance source, see (B20)
- γ = intermittency factor: the fraction of non-zero concentration readings in a sample at a fixed point in space.
- λ = $\sqrt{\sigma_y \sigma_z}/H$, normalized downwind distance in terms of plume spread
- λ_m = normalized distance at which maximum ground level concentration \bar{c}_{om} is observed
- λ_0 = virtual origin of concentration fluctuation variance source, see (B36)
- σ_m = crosswind meandering contribution to plume spread $\sigma_{yT}^2 = \sigma_y^2 + \sigma_m^2$; m
- σ_y = crosswind plume spread (standard deviation) for a short sample time $T_{s,ref}$; m
- σ_z = vertical plume spread (standard deviation) for short sample time $T_{s,ref}$; m
- σ_{yT}, σ_{zT} = plume spreads observed for a finite sampling time T_s which excludes low frequency meandering contributions; m
- τ_s = time constant of a receptor system responding to a sudden change in concentration; s
- Λ_c = integral Eulerian length scale of concentration fluctuations, see (A9); s

- Λ_{C^∞} = integral concentration length scale at a height far above influence of surface turbulence and wind shear on c'^2 , when $\sigma_z \ll h$; m
- $\Lambda_u, \Lambda_v, \Lambda_w$ = along-wind, crosswind and vertical Eulerian integral scales of turbulent velocity fluctuations; m
- Ω = cumulative probability density function; $\Omega(c^*)$ is the fraction of concentration readings less than a specified value c^* see (F2)
- $\bar{\tau}_c$ = integral Eulerian time scale of concentration fluctuations; see (A8); s
- $\bar{\tau}_{ca}$ = integral time scale of concentration fluctuations with high frequencies removed by averaging over time intervals of T_a ; s
- $\bar{\tau}_{ceff}$ = apparent integral time scale of concentration fluctuations that have had their high frequency components attenuated by a receptor system time constant τ_s ; s

Subscripts

- a = for data that has been subjected to averaging over time blocks of length T_a , which removes contributions from high frequency fluctuations
- e = for a dose exposure time T_e (this is equivalent to an averaging time process with $T_a \equiv T_e$)
- eff = "effective" value, with high frequency fluctuations attenuated by the receptor system response time constant τ_s
- m = at the point of maximum ground level concentration for a given source height h and windspeed U
- o = measured on the center-plane of the plume, i.e. at $y = 0$
- p = "inside plume", conditionally sampled value with periods of zero concentration removed
- T = for data taken with a sampling time duration T_s , which excludes contributions from low frequency fluctuations

EXECUTIVE SUMMARY

Objectives

The primary objective of the studies begun in 1979 has been to develop a reliable and easy to use prediction method for estimating ground level mean and peak concentrations of toxic gas from the rupture of sour gas pipelines and well blowouts. The reports "Expansion and Plume Rise of Gas Jets from High Pressure Gasline Ruptures", (April 1981) and the report "Predicting Risk of Exposure to Peak Concentrations in Fluctuating Plumes", (December 1982) together provide the theoretical basis for this model, and verify it using both wind tunnel and atmospheric data. The present study was initiated to carry out more fundamental research into the statistical theory in order to improve the model and allow it to be applied to a wider range of atmospheric and source conditions. Three objectives were set:

1. To develop a form for the fluctuating concentration model that would be suitable for predicting the probability of peak concentrations under continuous stack gas plumes. Extending the model to the longer exposure times that are associated with continuous plumes required methods for dealing with the increase in plume meandering with exposure time, the intermittent periods of zero concentration that occur due to meandering and incomplete mixing, the response time constants of biological receptors, and the effect of atmospheric stability on concentration fluctuations.
2. To use the existing concentration fluctuation model as a method for predicting the mean of all non-zero values of concentration at a receptor. This conditional mean concentration removes intermittent periods when plume meandering reduces the concentration to zero by moving the plume completely off a receptor. Because this conditional mean concentration is a more accurate indicator of the actual dilution within the meandering plume, and also is less sensitive to varying exposure time, its use as a superior indicator of ambient air quality compliance was studied.
3. To develop new statistical techniques which deal efficiently with the time varying risk of exposure for a fixed receptor under a

transient release from a pipeline rupture. Statistical theories were developed to predict the probability of being exposed to a toxic gas plume for a fixed time without ever crossing some set concentration threshold c^* . Atmospheric and wind tunnel data on concentration fluctuations were used to develop an improved probability distribution function to describe fluctuations in intermittent plumes. Simple, closed-form equations for the threshold crossing probability were developed to reduce the time-consuming numerical integrations previously used to evaluate risk of exposure.

The emphasis in the report is to develop statistical and diffusion models which form the basic elements of a risk analysis calculation procedure. Because of this theoretical orientation, the 70 pages in the body of the report are supplemented by 93 pages of material in the appendices A - G show the various theoretical models in sufficient detail to make their assumptions and limitations clear. Where possible, experimental data on concentration fluctuations are used to verify these models.

Model Refinements to Predict Mean Concentration

The existing semi-empirical model for concentration fluctuations uses Gaussian profiles for the mean concentration and the fluctuation variance. A steady emission rate from the source produces a constant mass flux of pollutant at each downwind plume cross-section. In contrast, the model assumes that all concentration fluctuations are produced close to the source and that the flux of concentration variance decays rapidly and continuously in the downwind direction. As a result, the effective source strength of concentration fluctuation variance is a function of downwind distance, while the mean source strength remains constant.

The fluctuating concentration theory developed by Wilson (1982) was originally optimized to produce accurate predictions for the fluctuation intensity and intermittency factor within a plume. One important feature of the original model was the use of a pair of effective variance "sources" located on either side of the plume centerline. However, when the model

was applied to predict conditional mean concentrations it was found that the use of a pair of variance sources gave unrealistically shaped profiles and a poor agreement with measured wind tunnel data. The model was modified to incorporate only a single variance source located at the same point as the mean emission. The use of a single source greatly improved the accuracy of prediction for the conditional mean concentration and the intermittency factor, which is the fraction of time that non-zero concentrations occur. With this small change in source geometry the model was both simpler to use and gave better estimates for the conditional mean and fluctuation statistics.

One major problem in monitoring atmospheric pollution levels is to interpret the highly intermittent concentration records that occur when the wind fails to carry the plume directly over the monitoring station. A possible solution is to set air quality standards on the basis of the conditional mean concentration determined by discarding the time intervals with zero concentration. Because probability distributions used to estimate the fraction of time concentration exceeds some threshold level require the conditional mean concentration and intermittency, it is sensible to express air quality standards in terms of these conditional statistics.

An important result of the present study was the observation that this conditional mean concentration will take on a constant value rather than decaying to zero as the cross wind distance off the centerline increases. This constant value for the conditional mean in the fringes of the plume is typically 1/5 to 1/2 of the centerline conditional concentration, and depends on the amount of meandering that occurs at the plume centerline. This constant value for the conditional mean is physically realistic

because, in the outer edges of the plume the dilution process can be visualized as a series of random steps with a contaminated eddy entraining uncontaminated air. The dilution of these eddies should be a function of travel time, and not how far the puffs are off the centerline.

From the practical standpoint of monitoring ambient concentration, the conditional mean, with zero concentration periods discarded, appears to be a logical choice because it remains large in the fringes of the plume and so gives a better indication of concentrations on the plume centerline for a monitoring station located off the centerline. The major disadvantage of using conditional mean values is the need for long sampling periods. For non-zero values that occur only 10% of the time, a 10 hour data record will be required to extract a one hour conditional mean. The unsteady nature of atmospheric wind and stability conditions may make it very difficult to interpret such long data records.

The Effect of Sampling Time on Concentration

The sampling time, also called the exposure time, is the continuous time interval over which the receptor samples the atmosphere. In most engineering and laboratory situations, the sampling time is long enough to include all the significant turbulent fluctuations, and steady values for the mean and fluctuation statistics are obtained. In the atmosphere, sampling times are typically a few minutes to a few hours in length, and do not sample all the low frequencies in the turbulent spectrum. As atmospheric sampling time increases, both the mean and fluctuating statistics will vary, even though the mean windspeed and atmospheric stability remain constant.

Changing this sample time significantly affects the observed plume spread, mean concentrations and fluctuation statistics. The influence of

sample time is due to the large scale turbulence and unsteadiness of atmospheric conditions which cause plume meandering, mainly in the cross wind direction. As sampling time increases, more of these low frequency fluctuations are included in the sample and the mean concentration is reduced as crosswind spread increases. Plume fluctuation statistics, in particular the intermittency, are also strongly affected by sampling time. As the sampling time increases meandering induced by large scale turbulence and unsteadiness exposes a receptor on the plume centerline to the highly intermittent fluctuations on the fringes of the instantaneous plume.

The theoretical model developed by Wilson (1982) to predict concentration fluctuations was optimized using a data base of wind tunnel observations. The use of wind tunnel data to adjust the model's parameters limit its use to neutral atmospheric stability, and to short sample times a few minutes in duration. To overcome the model's limitation to short sample times, imposed by the use of wind tunnel data, a meandering plume model similar to that suggested by Gifford (1959) was used. Long sampling times were simulated by allowing the crosswind profiles of the short sampling time statistics to meander back and forth with a Gaussian probability distribution over a receptor on the plume centerline. Using this meandering plume model it was found that the centerline becomes more intermittent and the mean concentration decreases with increasing sample time, as expected. In contrast, the conditional mean concentration with zero readings removed is virtually independent of sampling time, which demonstrates that plume meandering mainly affects intermittency and not the pollutant concentration. The weak dependence of conditional mean concentration on sampling time lends further support to its use as a measure of ambient air quality.

Because the concentration fluctuation theory had its adjustable parameters set using wind tunnel data, there is some uncertainty in applying it to situations where the atmospheric stability is not neutral. To help overcome the theory's limitation to neutral atmospheric stability, downwind distance was expressed in terms of a normalized plume spread. Hopefully, the variation of plume spread with changing atmospheric conditions would automatically correct the theory for stability effects. The present study carried out a detailed examination of this normalized spread parameter for varying atmospheric stabilities, and concluded that, at least for mean concentration, this normalization greatly reduces the variability caused by changing atmospheric stability.

Influence of Data Averaging Time and Receptor Response Time

Two other time factors complicate the interpretation of atmospheric concentration fluctuations. The first of these is the receptor response time, which is a measure of the ability of a receptor to respond to sudden changes in concentration. Both biological receptors and measuring instruments have inertia which causes their response to lag behind sudden changes in input conditions. The effect of this response time constant is to cause the system to lose its sensitivity to high frequency concentration fluctuations, (in contrast to sampling time which changes the contribution of low frequency fluctuations).

To account for this insensitivity to high frequency fluctuations methods were developed in the present study to correct the actual concentration fluctuation variance to an effective variance with high frequency fluctuations smoothed out by the averaging time.

One example of receptor time response is apparent in the difference in fluctuation levels observed indoors compared to their outdoor counterparts. Here, the mixing process within a building produces a large time constant whose slow response can reduce the indoor fluctuation intensity to 10% or less of its outdoor level.

To account for this sensitivity to high frequency fluctuations methods were developed in the present study to correct the actual concentration fluctuation variance by reducing it to an effective variance with the high frequencies attenuated. It was found, as expected, that the receptor time constant prevented short intermittent periods of zero concentration from being felt by the receptor and caused the effective fluctuations to be less intermittent when filtered through the receptor's time response.

The second time factor which influences concentration fluctuations is the data averaging time. In a sense, this is an artificial adjustment, because it is simply the time over which we choose to average a concentration record. For example, many ambient concentration records are averaged over successive one hour intervals. This process of hourly averaging removes the high frequency components from the concentration fluctuation data. To compare theoretical predictions from a dispersion model to these hourly averaged values it is necessary to account for the averaging process. Methods are developed for correcting the variance by assuming a frequency spectrum function and then attenuating the high frequency components for a specified averaging time.

Sampling time and averaging time are two quite different parameters that are often confused with one another. The sampling time increases turbulent concentration fluctuations by exposing a receptor to more of the low frequency components in the meandering plume. Averaging time has

exactly the opposite effect, reducing the variance as high frequency components are removed as the data is smoothed by averaging over successive time intervals. Sampling time (also called exposure time) is influenced by the natural process of atmospheric dispersion while averaging time is set to smooth out fluctuations by a conscious choice for an averaging interval to reduce data sets to manageable size.

Probability Distributions and Threshold Crossing Probability

For pollutants whose effects are cumulative, a receptor responds to the total dose integrated over the time of exposure. At the other extreme, the response time to a highly toxic gas such as hydrogen sulfide is rapid enough that the damage may be best described by a threshold concentration level below which there is no response and above which short exposures cause immediate damage.

Two distinctly different probabilities are required to estimate the risk from these hazards. The first is a probability distribution function which uses the conditional mean, conditional variance, and intermittency in the plume to predict the fraction of time that instantaneous concentrations or an integrated dosage will exceed a specified limit. In addition, for receptors and pollutants that produce a rapid response it is also essential to know the probability of being exposed for a specified time without ever once crossing a critical concentration threshold. Analytical relationships are developed between these two probabilities, and it is shown that simple closed form estimates of the threshold crossing probability can be made directly from the fraction of time exceedance probability distribution.

Several probability distribution functions are reviewed as candidates to describe the variability in concentration fluctuations. The Gamma distribution for fraction of time exceedance is shown to be superior to the

more common exponential and log-normal distributions used by previous investigators. The Gamma distribution is tested against several independent data sets from the atmosphere and wind tunnel, and shown to give good estimates of the frequency of occurrence of concentrations both higher and lower than the mean.

Frequency of occurrence probability distributions are skewed, with the most probable concentration occurring at a value somewhat less than the conditional mean value. Because of this skewed frequency distribution, the instantaneous concentration will exceed the conditional mean only 30 to 40% of the time during which non-zero concentrations occur. This result emphasizes the need for an accurate prediction of the frequency of occurrence of concentrations less than the conditional mean, and supports the conclusion that the gamma distribution is a better choice than the log-normal or exponential both of which are less accurate at low concentrations.

A probability model of the dilution process of pollutant released from a point source is developed. The dilution is modeled as a Wiener process, which is a continuous approximation to a random walk sequence of dilutions. The results of the model show that in an initially Gaussian distribution function is rapidly skewed with time of travel, until meandering produces an exponential frequency of occurrence distribution. The Gamma distribution, which reduces to an exponential distribution when the conditional fluctuation intensity approaches unity, is shown to be a reasonable approximation to this downwind distance dependent probability distribution function.

Threshold crossing probability represents a different approach to estimating risk of exposure. Because there is no data available from which

to predict this first time of crossing probability, a simple model was developed to allow their calculation directly from the known probability distribution for fraction of time that concentration exceeds this threshold. By assuming that concentrations in successive time intervals are statistically independent, it is shown that the probability of exceeding the threshold for some fixed exposure time is simply the negative exponential of the product of the length of exposure time and the fraction of time that the probability exceeds the threshold. This simple closed form solution allows a rapid calculation of first threshold crossing probabilities from the fraction of time exceedance distributions.

CHAPTER 1

INTRODUCTION

This report presents the results of efforts to refine and extend the concentration fluctuation model of Wilson (1982) to predict the risk of exposure to peak concentrations in plumes. The model is based on wind tunnel data, which we will show simulates exposure times of a few minutes, to estimate the hazard from short duration transient releases of toxic gas from pipeline ruptures.

Our primary objective is to extend this model to the much longer sampling times of one hour to several days that are useful in evaluating dosage and peak exposure probabilities for continuous plumes typical of industrial sources. To carry out this extrapolation it is necessary to develop a new theoretical model for the effect of long term plume meandering on mean and fluctuation statistics. The concepts of sampling time, data averaging time, and receptor response time must be included so that raw fluctuation statistics in the plume can be adjusted to determine the response of animals and vegetation.

To make the existing model useful for long term exposures, a whole new set of analytical tools were required. This report reflects the development of those tools by the detailed appendices which present their derivation. Each of these appendices deals only with a specific topic, and in the report we will bring them together to show how they interact, and how they can be used to develop realistic predictions.

As the model becomes more complex, one philosophical question is whether concentration fluctuation predictions are really necessary for

continuous plumes. Barry (1977) points out the dramatic increase in the catastrophic extreme value episodes that will be caused by small changes in the long term mean value of concentration. It is only by understanding the statistics that lead to these extremes that we can effectively assess the cost-benefit ratio for pollution control measures to lower this mean value. The need for concentration fluctuation probabilities is also evident when we consider the mean values only predict the concentration that will be exceeded 50% of the time. However, it is the extreme values that occur only a few percent of the time that may be responsible for most problems related to health and vegetation damage. We should determine not only a range of acceptable concentration levels, but also specify the frequency with which these levels may be exceeded.

CHAPTER 2

REFINEMENT OF THE CONCENTRATION FLUCTUATION MODEL

In the preceding report Wilson (1982) developed a model to predict concentration fluctuation statistics across a plume profile. The adjustable constants in this semi-empirical model were set by matching wind tunnel measurements of Fackrell and Robins (1982) who used tracer gases in a neutrally stable wind tunnel boundary layer to simulate atmospheric releases from ground level and elevated sources. The major features of this modified Gaussian dispersion model are:

- The use of variance "source" with a strength proportional to the mean concentration source and to the ratio of source size to turbulent scale. Unlike the mean source which remains constant, the variance source first increases and then dissipates with downwind distance.
- The use of an image sink term for variance to simulate the dissipation of concentration fluctuations in the highly sheared flow near the ground surface.
- The use of a pair of variance sources displaced on either side of the plume axis and located above the actual point of release to account for distributed production of concentration fluctuations in the central region of the plume.

The details are discussed in two papers by Wilson, Fackrell and Robins (1982). It was found later by Wilson (1982) that the theory could be extended to predict conditional plume statistics such as intermittency, conditional intensity and conditional mean without changing any of the adjustable constants used in the original model. This suggests that the model is not simply an exercise in curve fitting with adjustable constants, but has a physical basis.

One important characteristic of the model is that concentration fluctuations do not decrease to zero at the ground surface as might be

expected from physical reasoning. Instead, the wind tunnel data on which the model is based indicates that the fluctuation variance at ground level is about half the magnitude of the variance that would be expected with no dissipating surface present. This result has been confirmed by independent measurements of Bara (1985) in a water channel simulation of a ground level release. Bara's measurements extended close enough to the surface to be within the roughness elements themselves, at a height of about twice the log-law roughness length Z_0 , and demonstrated the existence of large concentration fluctuations in this region. Why do these fluctuations persist at the ground surface where high rates of dissipation should have removed all concentration variance? The reason appears to lie in the crosswind meandering of the plume, which exposes a receptor to concentration fluctuations caused by the crosswind variation of mean concentration. As this crosswind \bar{c} profile meanders back and forth over a receptor it generates the low frequency fluctuations observed near the ground surface, and causes a variance c^2 to appear.

Crosswind Spacing of the Variance Sources

The model uses a pair of variance sources displaced by some fraction ϕ of the crosswind plume spread σ_y on either side of the plume axis (for plumes normalized by their half width $\delta_y = 1.77 \sigma_y$ the displacement is a fraction $\beta = 0.85\phi$). Figure 1 shows that a displacement $\beta = 0.6$ (or $\phi = 0.706$) gives a better prediction of the crosswind profile than a single variance source with $\beta = 0$ (or $\phi = 0$).

Closer examination of the overall performance of the model in predicting conditional plume statistics indicates that a single variance source, first suggested by Csanady (1973) is a better choice. This is apparent in Figure 2 which shows an

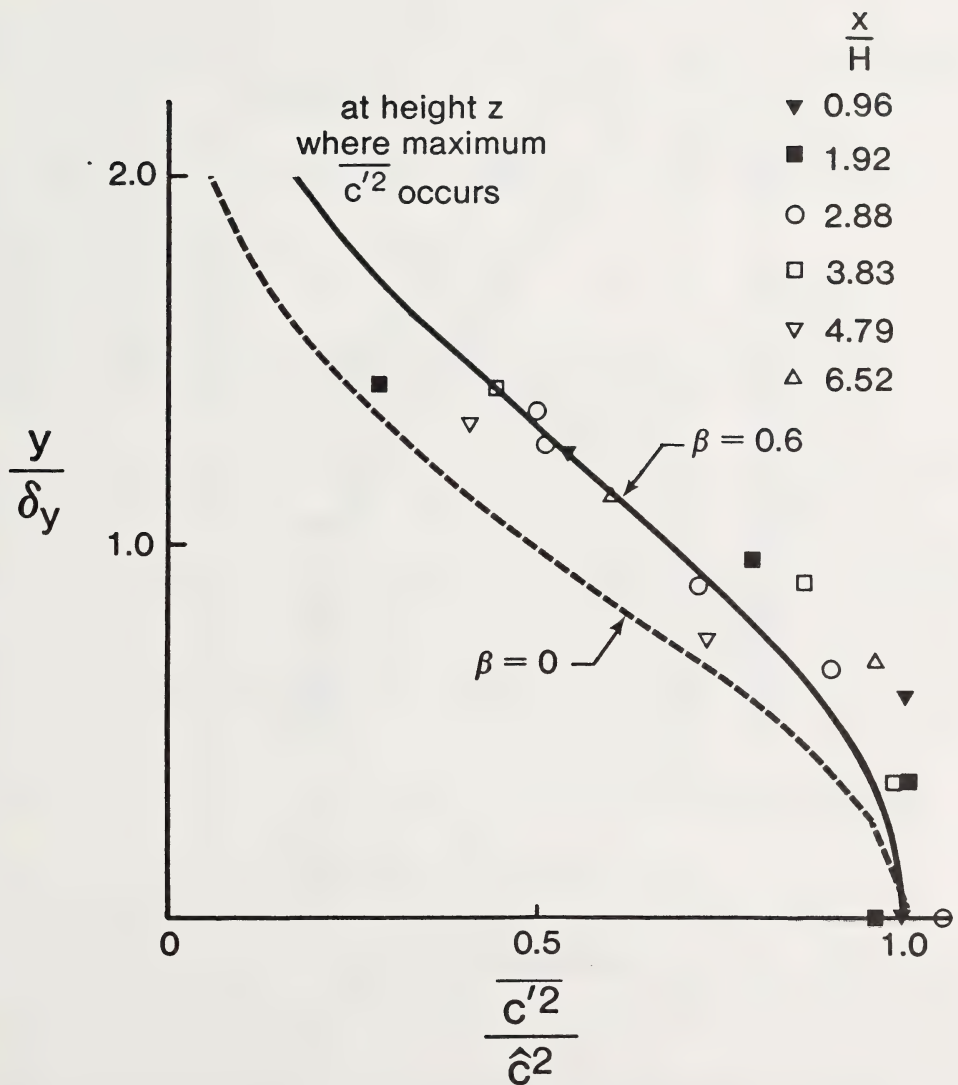


Figure 1 Crosswind variance profiles from an elevated source (normalized by extrapolated centerline variance \hat{c}^2) from Wilson, Fackrell and Robins (1982).

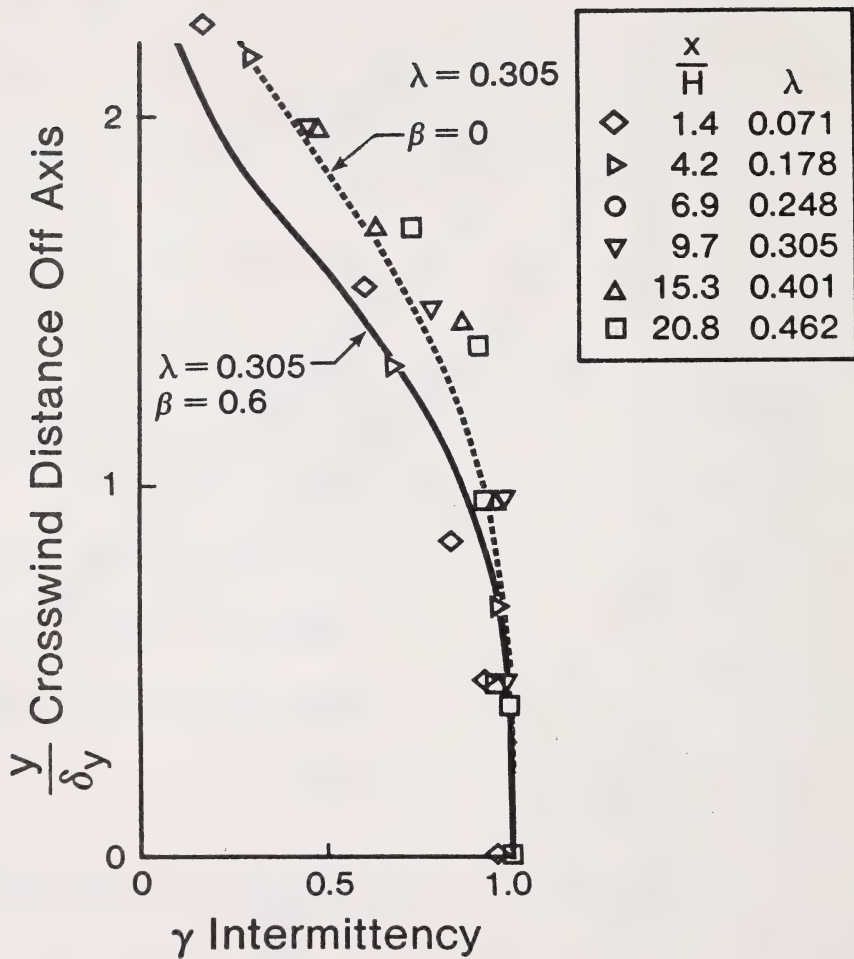


Figure 2 Effect of source pair spacing β on crosswind intermittency profiles from a ground level source in a wind tunnel. Data of Robins and Fackrell (1979).

improved agreement with crosswind intermittency when a single variance source on the plume centreline is substituted for the source pair with spacing $\beta = 0.6$. The three most important parameters predicted by the model are the conditional "plume" mean \bar{c}_p , plume intensity i_p and intermittency γ . These are the required input variables needed for the probability distribution used to predict the risk of exceeding some specified peak level. The choice of variance source spacing has no effect on i_p , which is assumed to be constant across the plume.

Figure 3 shows that the crosswind variation of the conditional plume mean \bar{c}_p is better estimated using the single variance source with $\phi = 0$. In Figure 4 this single variance source continues to give a good fit to the data at a location further downwind, close to the position of ground level maximum concentration. When comparing the model with measurements in the figures, it should be kept in mind that with the exception of mean concentration, none of the predicted profiles are forced to agree with experimental data by normalizing with centreline values. Differences between predicted curves and measurements are due to both data scatter and the deficiencies in predicting variance source strengths in the plume. Considering this, the agreement between experiment and theory is remarkably good.

Because most receptors are on the ground, it is less important to predict accurately vertical plume profiles. On the other hand, predicting vertical profiles provides the most stringent test of the model's ability to simulate dissipation effects on concentration fluctuations near ground level. Vertical profiles of Fackrell and Robins' wind tunnel data are shown in Figures 5, 6 and 7 at three downwind distances from an elevated source. For the source height of $h = 0.192 H$ the maximum mean ground level concentration occurs at

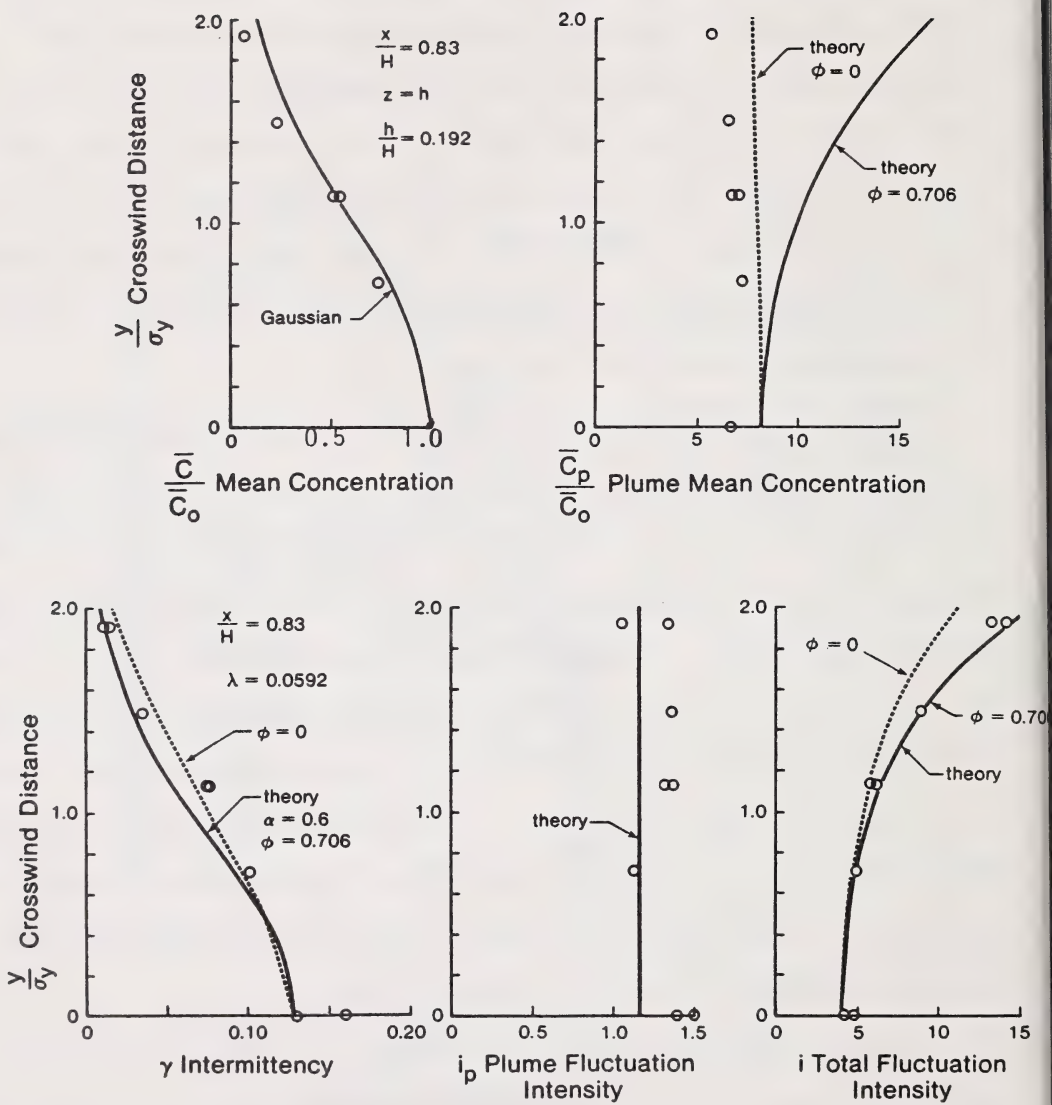


Figure 3 Crosswind profiles of mean and fluctuation statistics at $x/H = 0.83$ in the plume from an elevated source $d = 0.30$ cm in a neutrally stable wind tunnel boundary layer, $H = 120$ cm, $z_0 = 4 \times 10^{-4}$. Data of Fackrell and Robins (1982a).

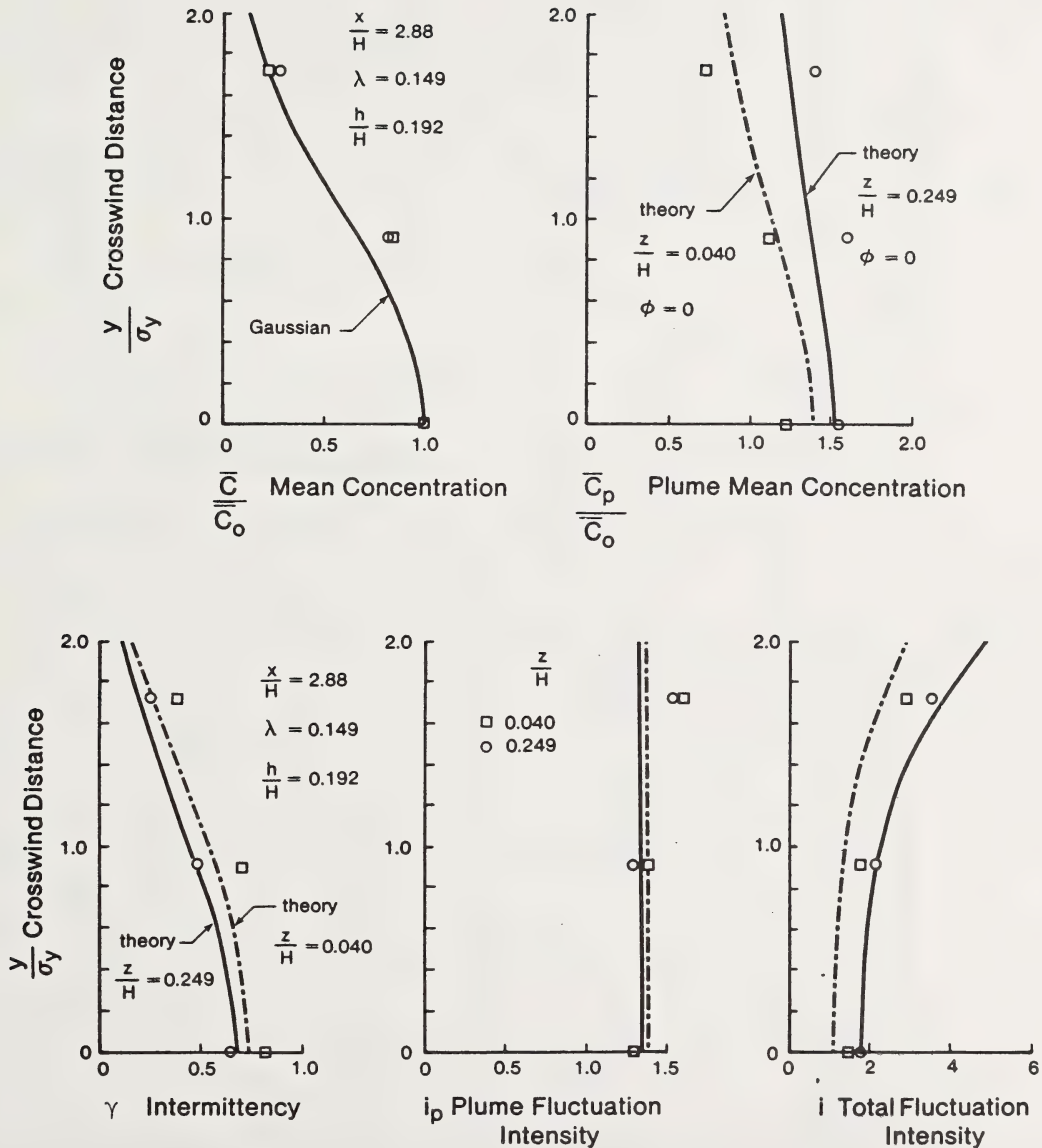


Figure 4 Crosswind profiles of mean and fluctuation statistics at $x/H = 2.88$ in a plume from an elevated source $d = 0.85$ cm at $h = 23$ cm in a neutrally stable wind tunnel boundary layer $H = 120$ cm, $z_0 = 4 \times 10^{-4}$. Data of Fackrell and Robins (1982a).

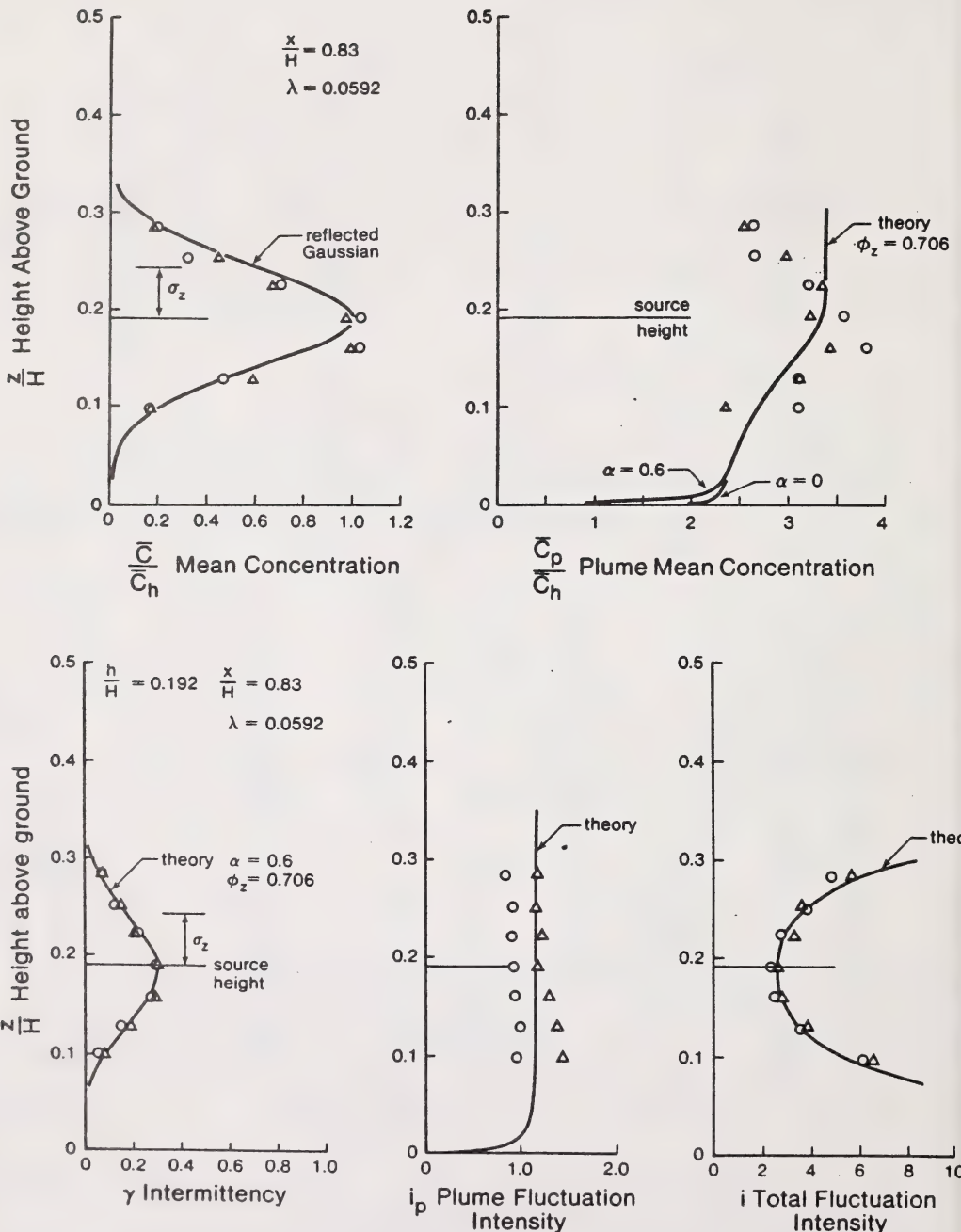


Figure 5 Vertical profiles of mean and fluctuation statistics at $x/H = 0.83$ at $h = 23$ cm in a neutrally stable wind tunnel boundary layer $H = 120$ cm, $z_0 = 4 \times 10^{-4}$. Data of Fackrell and Robins (1982a).

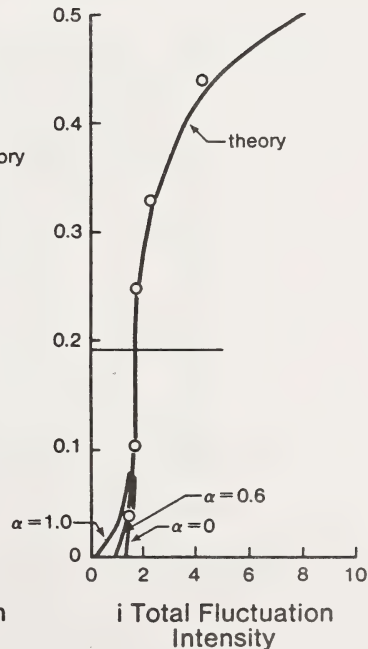
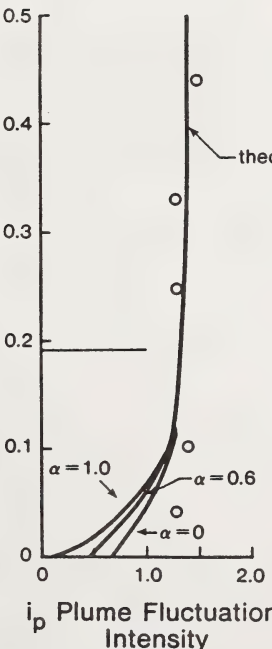
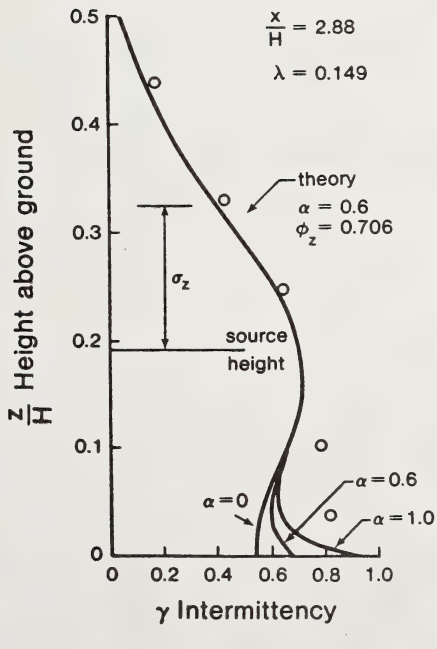
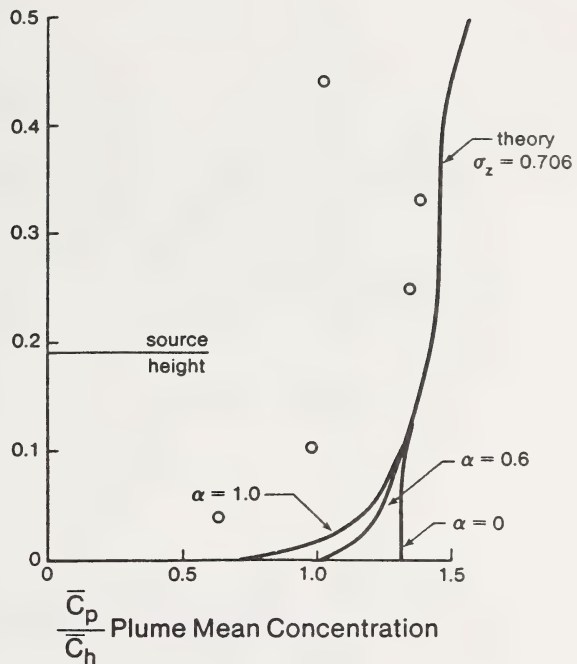
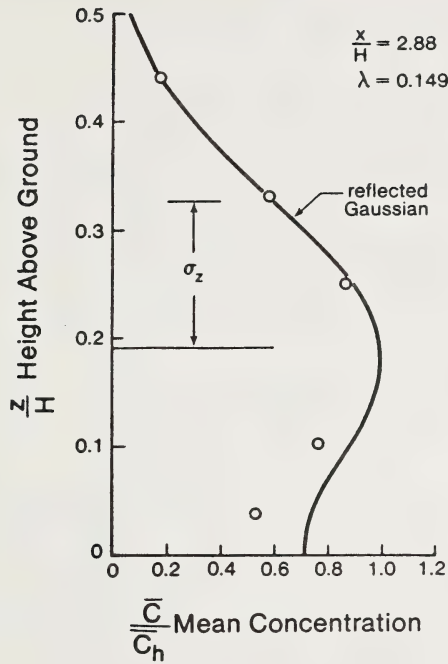


Figure 6 Vertical profiles of mean and fluctuation statistics at $x/H = 2.88$

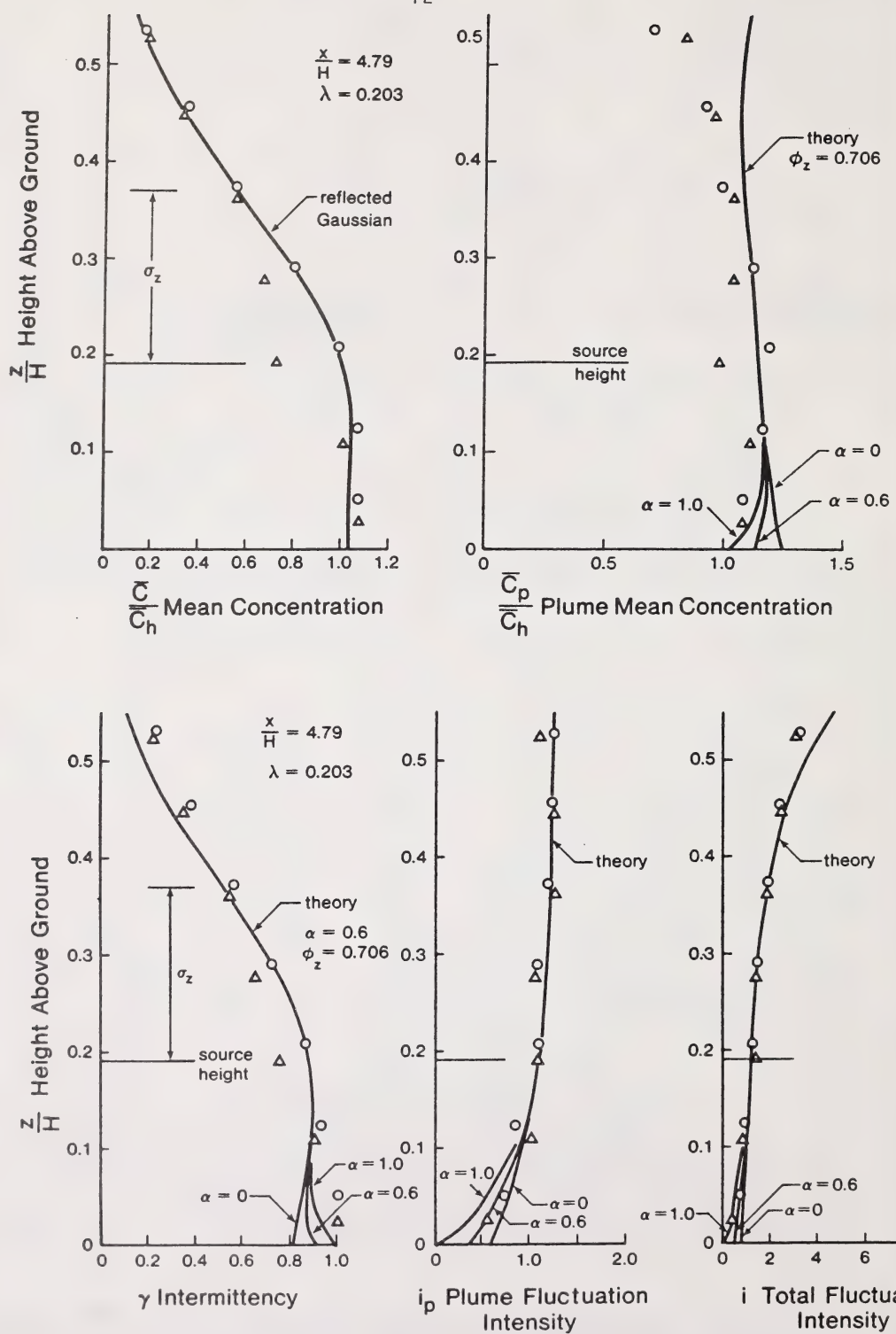


Figure 7 Vertical profiles of mean and fluctuation statistics at $x/H =$

about $x/H \approx 3.0$, with measured profiles shown at $x/H = 0.83, 2.88$ and 4.76 . These vertical profiles are independent of the crosswind source pair spacing ϕ , but do show that a vertical variance source displacement $\phi_z = 0.706$ is still better for predicting variance and intermittency in the upper region of the plume above source height. Because some vertical displacement of the variance source is essential in predicting the vertical profiles for a ground level source, we will continue to use a value of $\phi_z = 0.706$ (or $\beta_z = 0.6$).

In summary, a review of the data indicates that a single variance source with $\phi = 0$, but with vertical displacement $\phi_z = 0.706$ is the best choice. Although a single variance source gives a poor fit to $c^{1/2}$ in the central core of the plume, it gives significantly better agreement for variance, $\overline{c}^{1/2}$, intermittency γ and plume mean concentration \overline{c}_p in the fringes of the plume where $y > 2\sigma_y$. This does not imply that the true profile of variance is Gaussian in the outer regions, because our assumption of constant plume intensity i_p in the outer regions may not hold, and the use of a single variance source may simply provide a compensating error.

Finally, the most important benefit of using a single variance source is that it prevents unrealistic increases in the probability of exceeding a threshold level in the outer crosswind regions. These oscillations in exceedence probability predicted by Wilson (1982), completely disappear when a single variance source is used. From this, we may conclude that simple models are often best, and that correction factors which improve their performance in limited regions often do more harm than good to the overall accuracy.

Accounting for Atmospheric Stability

The concentration fluctuation model expresses the downwind variation of source strength in terms of a dimensionless plume spread parameter λ defined in terms of the vertical and crosswind plume spreads σ_y and σ_z

$$\lambda = \sqrt{\frac{\sigma_y \sigma_z}{H}} \quad (1)$$

where H is the thickness of the atmospheric boundary layer, and may be taken as $H \approx 650$ m. This boundary layer thickness is simply a means of including the scale of atmospheric turbulence, and Wilson, Fackrell and Robins (1982) recommend for neutrally stable wind tunnel boundary layers

$$H \approx 2500 Z_0 \quad (2)$$

in terms of the neutral log law surface roughness length Z_0 .

It is assumed in the model that λ accounts for all effects of turbulence intensity and scale caused by changes in stability and surface roughness. To examine this assumption, the equations for mean ground level concentration along the plume axis are transformed in Appendix B to a coordinate system based on the spread parameter λ . The influence of stability was examined by considering the extremes of "very unstable" (Class A) and "very stable" (Class F) with plume spread parameters recommended by Angle (1978). Normalized ground level concentration profiles shown in Figure 8 confirm that the effects of stability are negligible when downwind distance is expressed in terms of the plume spread parameter λ rather than downwind distance x . In plume spread coordinates the concentration profiles have a maximum variation of about 5%

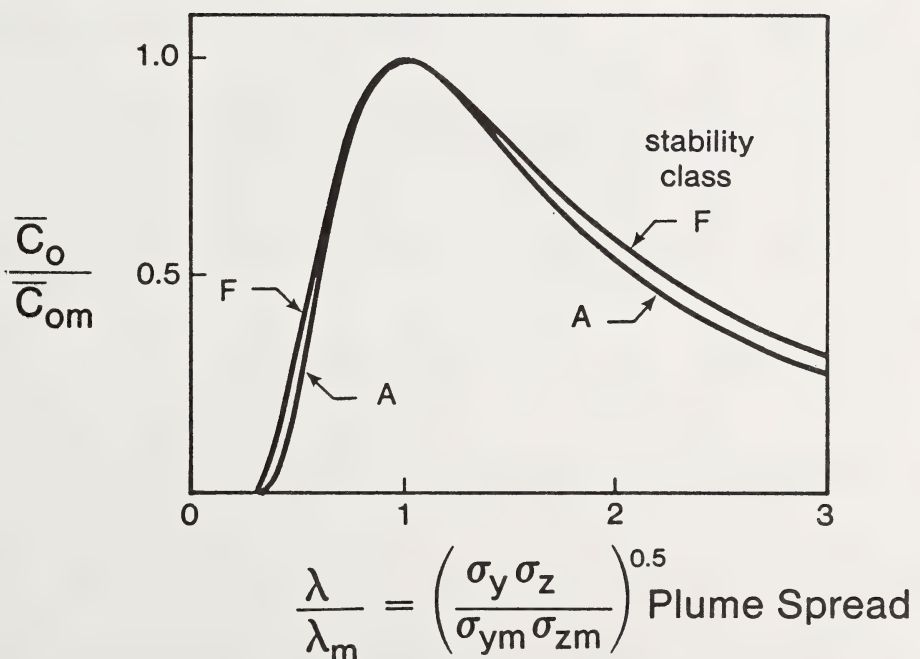
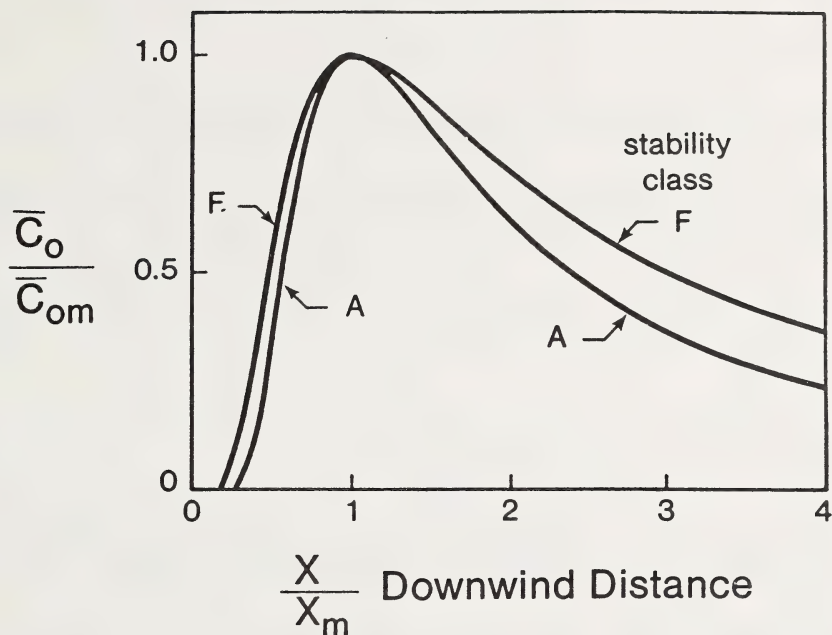


Figure 8 Ground level profiles of mean concentration normalized in downwind distance x and plume spread λ coordinates using plume spreads σ_y and σ_z from Angle (1978).

TABLE 1

Variability of Location of Maximum Ground Level Concentration with Atmospheric Stability for Two Source Heights

Stability Class	Source Height $h = 10 \text{ m}$		Source Height $h = 65 \text{ m}$	
	$\frac{x_m}{X_{m,D}}$	$\frac{\lambda_m}{\lambda_{m,D}}$	$\frac{x_m}{X_{m,D}}$	$\frac{\lambda_m}{\lambda_{m,D}}$
A	0.37	1.16	0.23	0.94
D	1.00	1.00	1.00	1.00
F	3.58	1.20	5.76	1.48

from the neutral stability (Class D) conditions on which our model is based.

Another indication of how well the plume spread parameter λ performs as a universal distance scale is the location of maximum mean concentration λ_m . Table 1 compares the variability of the distance to ground level maximum in both λ and x coordinates. It is clear from this that λ_m is much closer to a universal constant, varying by only about $\pm 20\%$ while the distance to maximum concentration x_m varies by more than $\pm 400\%$ over the same range of stabilities. From this we expect that the concentration fluctuation model might give reasonable predictions for all atmospheric stability classes when downwind distances are expressed in the form of plume spread parameter λ .

Limitations Imposed by Wind Tunnel Simulation

Wind tunnel simulation provides the basis for setting adjustable constants in the concentration fluctuation model developed by Wilson (1982). The working equations for this model are presented in Appendix B for a receptor located at ground level. While a wind tunnel boundary layer is essential to provide the reproducible conditions needed to measure fluctuation statistics accurately, this small scale simulation does not adequately represent atmospheric eddies that cause the plume meandering over periods of a few minutes to a few hours. Also, the wind tunnel is incapable of simulating the long term meandering of wind direction which occurs over sample time periods of a few hours to several days. The mean concentration on the centreline decreases continuously as meandering causes the short term "instantaneous" plume to move back and forth over the receptor. This nonstationary decrease in mean concentration is shown schematically in Figure 9, where the limitation of wind tunnel simulation is clearly evident.

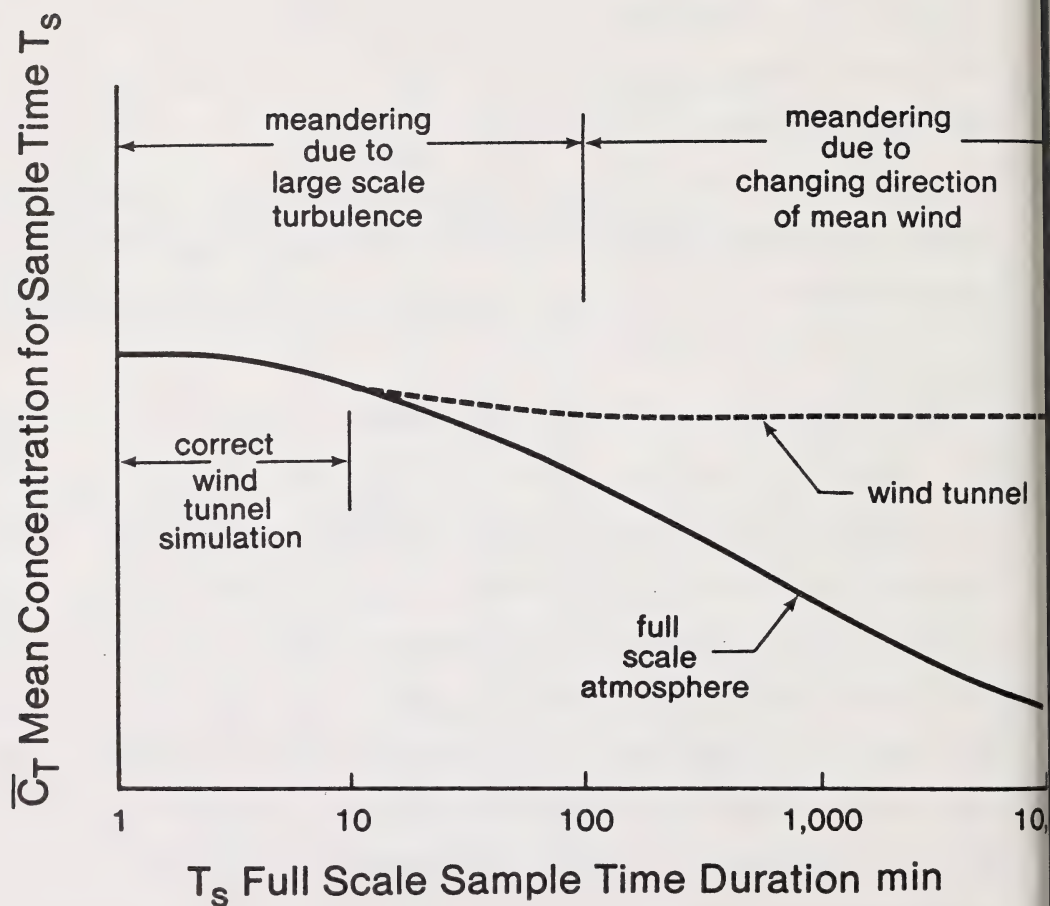


Figure 9 Sampling time limitations in wind tunnel simulation of atmospheric dispersion

The wind tunnel data of Fackrell and Robins are for a boundary layer thickness of $H = 1.2$ m to simulate the atmospheric boundary layer in about 550:1 scale. At a scale downwind distance of about 1.5 km the wind tunnel model produced a full scale equivalent crosswind spread $\sigma_y = 128$ m. The rough surface of the wind tunnel boundary layer generated a mean wind profile with an equivalent full scale log law roughness height of $Z_0 = 26$ cm. Using the power law crosswind spread equations recommended by Smith from Pasquill (1974) p. 375, the predicted crosswind spread for an unspecified sample time is about $\sigma_y = 120$ m. Pasquill suggests that these crosswind spread values in the atmosphere are typical of 3 minute sample times, and the close agreement between the measured and predicted values suggest that the wind tunnel simulation is limited to turbulence scales that are typical of three minute samples in the atmosphere. These short exposure times are exactly what is needed to simulate the passage of a transient plume of toxic gas from a pipeline rupture. On the other hand, long term exposures of several hours to several days that are required for determining damage to plants and animals from continuous releases cannot be predicted from the existing model. In Chapter 3 a procedure will be developed for extrapolating the existing three minute sampling time predictions to estimate concentration statistics for longer exposure times.

Wind tunnel simulation can create the illusion of predicting concentrations for sampling times as long as one hour. If only mean concentration is simulated, the loss of large scale eddies which cause plume meandering can be compensated for by adding an excess of turbulence to the wind tunnel boundary layer. The mean concentration depends only on the vertical and crosswind plume spreads σ_z and σ_y , and the vertical spread remains relatively constant for

sampling times longer than about three minutes in the atmosphere. The crosswind spread σ_{yT} continues to increase with sampling T_s as the effective scale Λ_{vT} of the velocity fluctuations becomes larger. A simple power law is

$$\sigma_{yT} \approx \left(\sqrt{\frac{v'^2}{U}} \right)^{a_y} (B_0 \Lambda_{vT})^{1-a_y} y^a_x \quad (3)$$

where $\sqrt{v'^2}/U$ is the intensity and $B_0 = L_v v'/\Lambda_{vT} U$ is the Lagrangian scaling constant, and Λ_{vT} is the integral scale of crosswind turbulence for a sample time duration T_s . From this it is easy to see that an ingeneous wind tunnel modeller can produce the required crosswind spread for any sample time simply by generating more upstream turbulence v'^2 to compensate for a value of Λ_{vT} that is too small. Typically $a_y \approx 0.88$ so that $\sigma_{yT} \sim \Lambda_{vT}^{0.12}$. This weak dependence requires only a 10% change in turbulence intensity to account for a factor of two error in simulating scale.

However, if a wind tunnel is used to model concentration fluctuation statistics, it can never properly simulate the high intermittency caused by meandering over long sample times. In the atmosphere, crosswind meandering exposes a receptor to the highly intermittent fluctuations in the outer fringes in the crosswind plume profile. Adjustments to wind tunnel turbulence levels will only produce more spread, and not the intermittency needed to simulate sample periods of several hours.

Comparison With Full Scale Atmospheric Data

The most important aspect of the concentration fluctuation model is its ability to predict the crosswind variation of plume intensity and intermittency. The field measurements of Ramsdell and Hinds (1971) used a radioactive tracer

gas to study crosswind profiles from a ground level source. Thirty-nine samplers were located at 200 m and 800 m downwind, and averaged over 38.4 seconds for sampling times of 10 to 20 minutes. Normalized fluctuation statistics were found to be similar at both of the downwind locations, and the data was combined to produce a single normalized data set.

Their crosswind profiles of total variance in Figure 10 show the same trend observed in the wind tunnel measurements in Figure 1. In both cases, the use of a pair of variance sources gives a better prediction in the core of the plume for $y < 2 \sigma_y$. In the fringes beyond two standard deviations a single variance source (source pair spacing $\phi = 0$) gives a better fit. The conditional plume statistics of intermittency γ , plume intensity i_p and total plume intensity i in Figure 11 show good agreement with theoretical predictions normalized by experimental values on the plume centreline. Here, the use of a single variance source gives significantly better estimates of total intensity and intermittency for the crosswind profiles. It is gratifying to find that the field data in Figure 11 showed an approximately constant value for conditional plume intensity i_p . This assumption of constant intensity across the plume is the most important element used in constructing the plume fluctuation model.

Although the shape of crosswind profiles for plume statistics is reasonably well simulated, the model underestimates the magnitude of both i_p and i . A comparison of centreline values is shown in Table 2. Two probable reasons for the model's failure are:

- The predictions are limited to a short sampling time of about three minutes, while the field data was typical of fifteen minute sampling times. These longer sampling times allowed more plume meandering and accounted for the lower value of intermittency factor γ in the measurements.

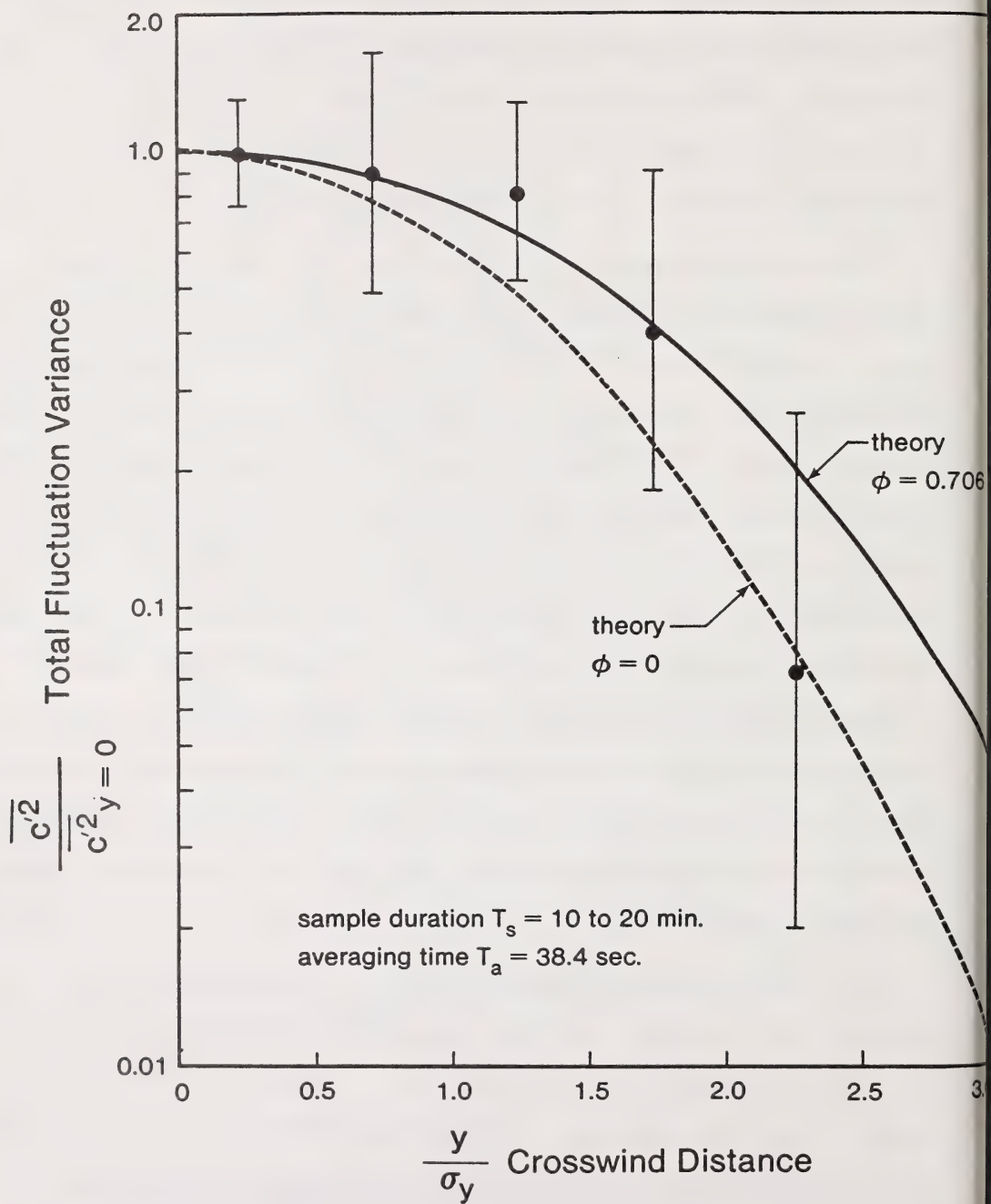


Figure 10 Field measurements of crosswind variance profiles [at $z = 1.5$ m with combined data from $x = 200$ m and 800 m for a ground level source with $d \approx 0.02$ m, $h \approx 1$ m. Data of Ramsdell and Hinds (1971).]

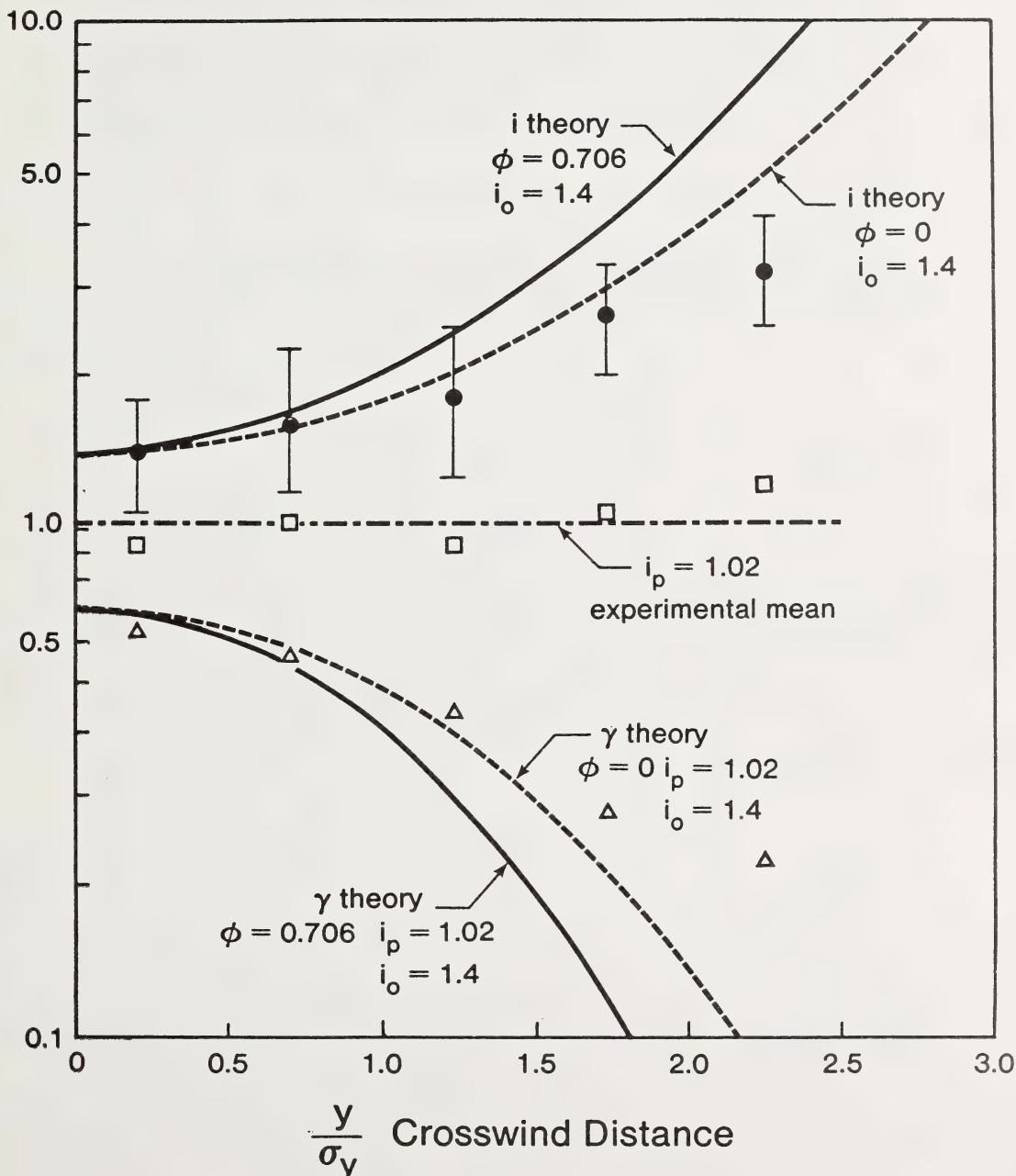


Figure 11 Field measurements of crosswind profiles of total and plume intermittency. Data of Ramsdell and Hinds (1971).

TABLE 2

PLUME CENTERLINE CONCENTRATION FLUCTUATIONS FROM
RAMSDELL AND HINDS (1971) GROUND LEVEL SOURCE FIELD MEASUREMENTS

VARIABLE	FIELD MEASUREMENTS	MODEL PREDICTION*
	Combined Data for $x = 200 \text{ m}$ and 800 m $T_s = 10 \text{ to } 20 \text{ min}$	Sample Time $T_s = 3 \text{ min}$
Intermittency	$\gamma_{T_0} = 0.64$	$\gamma_0 = 1.00$
Plume Intensity	$i_{pT} = 0.95$	$i_p = 0.38$
Total Intensity	$i_{T_0} = 1.40$	$i_0 = 0.38$

*Using average $\lambda = 0.063$ of the two locations, $x = 200 \text{ m}$ ($\lambda = 0.031$) and $x = 800 \text{ m}$ ($\lambda = 0.095$) for $d = 0.02 \text{ m}$, $h = 1.0 \text{ m}$ $\sigma_z = 35 \text{ m}$.

- The model predicts no effect of source size for a ground level release. The wind tunnel simulation on which this was based considered full scale equivalent sources of 1.5 m to 20 m. In the small scale turbulence near ground level the very small source size of $d \sim 0.02$ m in the field measurements may have significantly affected plume meandering.

Neither of these are serious deficiencies, but some adjustment to source size effects in the model are necessary, at least for ground level sources. The effect of sampling time will be accounted for by a crosswind meandering correction presented in the next chapter.

CHAPTER 3

SAMPLING, AVERAGING AND RESPONSE TIME EFFECTS

The theory (Appendix B) for mean and fluctuating concentration assumes that the wind blows directly from the source to the receptor, and that fluctuation statistics are measured over a long enough sampling time to include all relevant large scale meandering effects. These fluctuations are then assumed to act on a receptor with an instantaneous response time which follows the fluctuation peaks. In practice, neither of these idealized limits is ever realized. Barry (1977) suggests that a sample time of about four days in duration would be required to include all fluctuations that contribute to plume dispersion. Current estimates of plume spread parameters σ_y and σ_z apply only for short sample times of about three minutes. While these short sample times are adequate for predicting concentration fluctuations in a brief release of toxic gas, they are inappropriate for long term estimates of dosage and peak concentration levels over several hours.

Accounting for the response time of a receptor is equally important in estimating the effect of fluctuating concentration. The response time of humans and animals to highly toxic gases lies in the range of a few seconds to a few minutes. At the other extreme, the response of slow growing vegetation such as trees to time varying concentration will have a time response measured in hours or in days. The damage to such a slowly responding system is often expressed in terms of the total integrated dose received over the exposure time. When the fluctuating concentration is averaged over these exposure time intervals high frequency fluctuations are

removed and dosage level is much less variable than the instantaneous concentration. The parameters required to account for these time factors are:

T_s - The sampling time duration over which a receptor is exposed to a plume.

T_a - The averaging time over which integrated dosage is computed. T_a will always be less than or equal to the sampling time T_s .

τ_s - The system response time constant of the receptor.

\bar{J}_c - The integral time scale of the concentration fluctuation spectrum.

Integral Time Scale \bar{J}_c of Concentration Fluctuation

In order to estimate the effect of sampling averaging and response times we must specify how the spectrum of c^{-2} varies with frequency. In Appendix A the Markov spectrum is used as the simplest reasonable approximation to the concentration spectrum. This spectrum is consistent with an exponential "inertialess" autocorrelation function, and its scale \bar{J}_c is the only variable required to specify the relative contribution of each frequency to the concentration variance c^{-2} .

The wind tunnel data of Fackrell and Robins is used in Appendix C to estimate the variation of this integral scale with position in the plume and downwind distance. Their data clearly shows a dramatic increase in the size of concentration scale near the ground where the highly sheared atmospheric turbulence dissipates small (high frequency) fluctuations leaving only large scale turbulence to contribute to the variance. The empirical model is used to relate the increase in integral scale \bar{J}_c to the decrease in variance near the ground caused by the same dissipation

effects. The data indicates that in the absence of ground dissipation effects, the scale of concentration fluctuations remains constant across a plume cross-section, and gradually increases with downwind distance as dissipation removes small scale concentration eddies. Because it is the size of eddies, not their time of passage, that remains constant with changing windspeed, the empirical relations in Appendix C are presented in terms of the integral length scale $\Lambda_c = \sqrt{J_c} U$, rather than the time scale. The eddy convection velocity is assumed to the local mean velocity at the height z at which the spectrum is measured.

The empirical correlation for concentration fluctuation length and time scales given in Appendix C is only valid for the sampling time T_s of about three minutes, for which the wind tunnel data is appropriate. When a receptor is exposed for longer sampling times the slow crosswind meandering of the plume will contribute more large scale low frequency turbulence to the variance and cause the time scale J_c to increase. The correction factors necessary to adjust the time scale for sampling times longer than three minutes are developed in Appendix D.

Adjustment for Sampling Time - T_s

For a receptor exposed to a continuous plume we are usually interested in the response over a relatively long exposure time ranging from several hours to several days. Unfortunately, there is no simple method available for extrapolating the mean and fluctuation statistics predicted by the model for an ensemble of three minute sample times to these longer exposures. To allow this extrapolation, a meandering plume model is developed in Appendix D to simulate the effect of long sampling times. The position

of the plume caused by meandering is assumed to have a normal probability distribution with a crosswind standard deviation σ_m which increases with sample time, the same as Gifford's (1959) meandering plume model.

This crosswind meandering process is shown schematically in Figure 12, which shows by the symmetric meander probability about $y = 0$ that the long term average wind direction is assumed to be constant during the sample period. Because we are interested in an ensemble average of many realizations of sample periods of length T_s , this constant wind direction assumption is not a severe limitation for sample times up to several hours. For longer sample durations the effects of topography, drainage flows and synoptic trends should be included by using wind-rose weighting of directions. By using the suggested empirical relation between sample time T_s and meander width σ_m given in (D44), the short term statistics for sampling time T_{sref} are related to longer sampling times as follows:

From (D42) the mean concentration \bar{c}_{oT}

$$\frac{\bar{c}_{oT}}{\bar{c}_o} = \left(\frac{T_{sref}}{T_s} \right)^p \quad (4)$$

where p is an empirically determined exponent. From (D32) and (D44) the total fluctuation intensity i_{To} is

$$i_{oT}^2 + 1 = \frac{\left(\frac{T_s}{T_{sref}} \right)^{2p}}{\left[2 \left(\frac{T_s}{T_{sref}} \right)^{2p} - 1 \right]^{0.5}} + i_o^2 \left(\frac{T_s}{T_{sref}} \right)^p \quad (5)$$

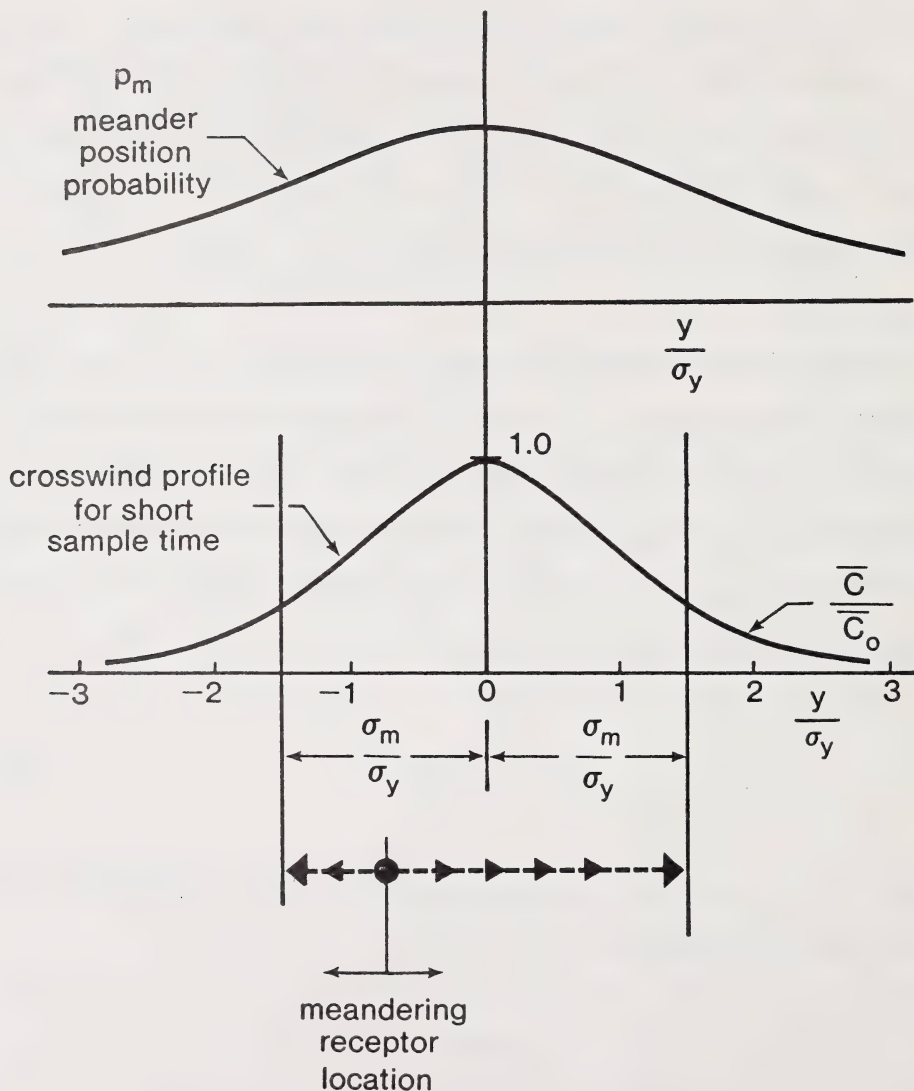


Figure 12 Crosswind meandering model for sampling time adjustments to plume centerline statistics.

For long sampling times where $T_s/T_{sref} > 10$ this may be approximated by

$$i_{oT}^2 + 1 \approx (0.707 + i_o^2) \left(\frac{T_s}{T_{sref}} \right)^p \quad (6)$$

Meandering increases the integral scale \bar{J}_{CT} of concentration fluctuations by the ratio of intensities. From (D41)

$$\frac{\bar{J}_{coT}}{\bar{J}_{co}} = \frac{i_{oT}^2}{i_o^2} \quad (7)$$

The crosswind averaged intermittency γ_{oT} must be found by numerical integration of (D19) in terms of σ_m/σ_y , and then related to sample time with (D44). The conditional "plume" intensity i_{pT} for sampling time T_s is calculated from the values of γ_T and intensity i_{oT} and the relation

$$\gamma_{oT} = \frac{i_{pT}^2 + 1}{i_{oT}^2 + 1} \quad (8)$$

The intermittency γ in the 3 minute plume, and the crosswind average γ_{oT} are shown in Figure 13. When normalized by γ_0 , the 3 minute centerline value, these intermittencies are functions of the centreline intensity i_0 .

For sampling times long enough to make $\sigma_m > 2\sigma_y$, the plume centerline intermittency γ_{oT} falls to about half its three minute value γ_0 . Using the recommended value of $p = 0.2$ for the exponent Figure 14 shows the predicted change in plume centerline statistics. We see the conditional mean value \bar{c}_{po} levels off at a constant value, while the mean concentration \bar{c}_{oT} and intermittency γ_{oT} decrease continuously with exposure time.

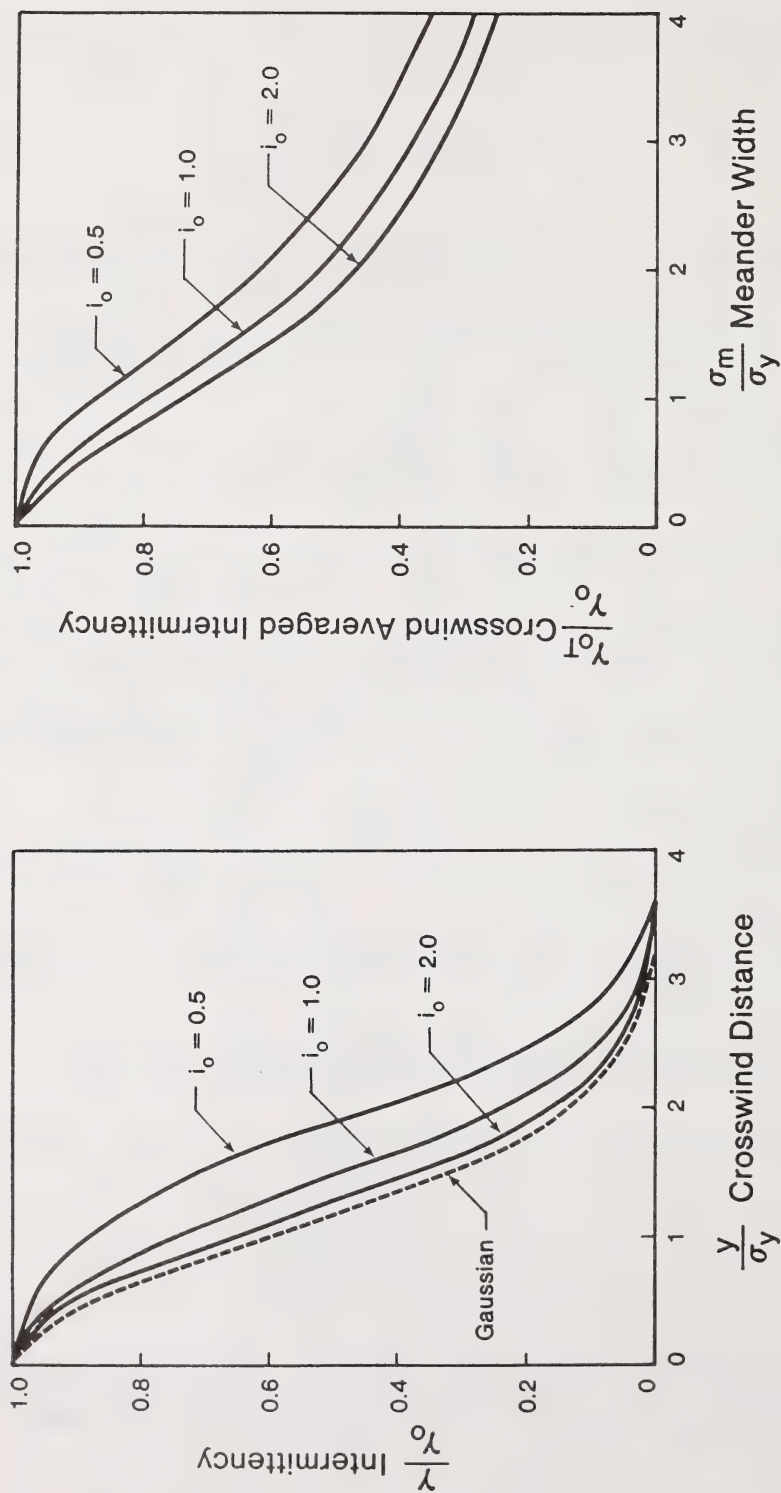


Figure 13 Gaussian model prediction of intermittency across a plume, and for sampling time meander averaging on centerline Y_0/T , with single variance source $\phi = 0$.

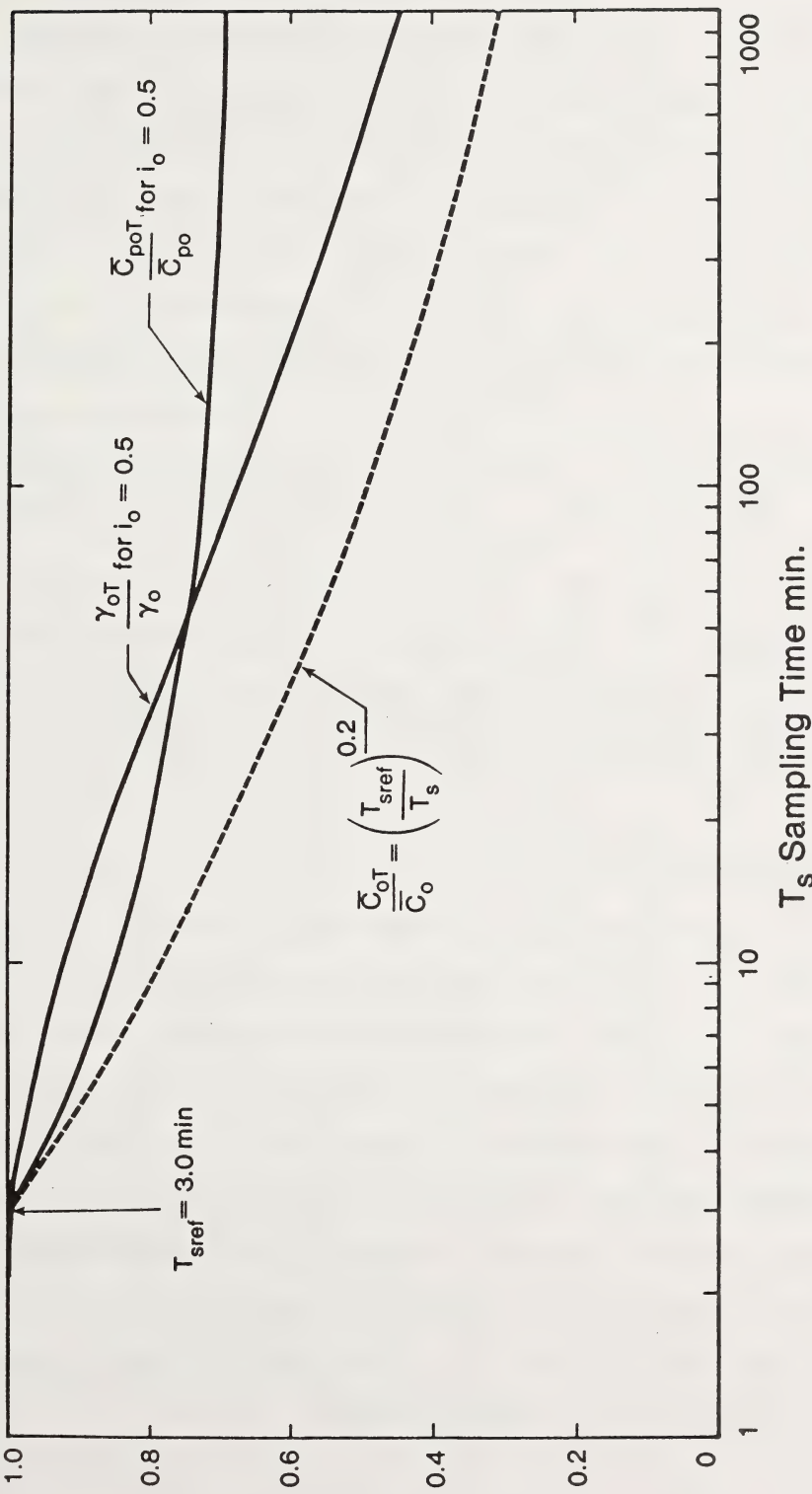


Figure 14 Meandering plume model prediction of sampling time effects on plume centerline statistics for a single variance source ($\phi = 0$) and $p = 0.2$ using equations (D13), (D19) and (D44).

This sampling time adjustment might account for the observed differences between Ramsdell and Hinds field measurements and the model predictions for three minute plumes. Table 3 shows the predicted effect of sampling time on intermittency and fluctuation intensities for the model and ground level field measurements. The values of $p = 0.2$ and 0.3 are reasonable estimates of plume meander exponent. While the correction significantly improves agreement between the model and measurements, the theory still grossly underpredicts conditional and total fluctuation intensity. In turn, this underestimates the intermittency. If $i_p = 0.95$ and $\gamma_0 = 1.0$ are used for the three minute plume, a 15 minute sample time has $i_{OT} = 1.32$ and $\gamma_{OT} = 0.71$ for $p = 0.3$. These are in much better agreement with the measurements, and suggest that the empirical constants in the three minute plume model be adjusted to produce larger ground level intensities and a more intermittent plume.

Effect of Averaging Time - T_a

The averaging time T_a is the time interval chosen by an investigator, over which the instantaneous concentration is averaged to produce a single value for each interval. Because this averaging process removes high frequency fluctuations, the variance of the averaged values will be less than the variance of the instantaneous fluctuations. The attenuation factor for the frequency spectrum is discussed by Pasquill (1974) pp. 12-16, and is applied to the Markov spectrum in Appendix A. For the most common case where the averaging time T_a is much longer than the integral time scale \bar{T}_c of concentration fluctuations, equation (A31) is a good estimate of reduced variance $c_a^{-1/2}$ for averaging time T_a .

TABLE 3

PLUME CENTERLINE STATISTICS FOR RAMSDELL AND HINDS (1971)
GROUND LEVEL SOURCE FIELD DATA COMPARED WITH MODEL PREDICTIONS
CORRECTED FOR SAMPLE TIME

VARIABLE	FIELD MEASUREMENTS $T_s = 10 \text{ to } 20 \text{ min}$	MODEL PREDICTION*		
		$T_s = 3 \text{ min}$	$T_s = 15 \text{ min}$	
			$p = 0.2$	$p = 0.3$
γ_{oT} Intermittency	0.64	1.00	0.92	0.84
i_{pT} Plume Intensity	0.95	0.38	0.47	0.52
i_{oT} Total Intensity	1.40	0.38	0.58	0.71

* At average $\lambda = 0.063$

$$\frac{\overline{c_a^2}}{c_T^2} \approx \frac{\overline{c_a^2}}{c_T^2} \frac{2\overline{J}_{cT}}{\overline{T}_a} \quad (9)$$

for $\overline{T}_a > 5\overline{J}_{cT}$, where $\overline{c_T^2}$ and \overline{J}_{cT} are the variance and scale for a sampling time T_s equal to the averaging time. The time averaged mean \overline{c}_a is by definition the mean \overline{c}_T for sample time $T_s = T_a$. Dividing (9) by the square of these means yields the time averaged intensity $i_a = \overline{c_a^2}/\overline{c}_a$

$$i_a^2 \approx i_T^2 \frac{2\overline{J}_{cT}}{\overline{T}_a} \quad (10)$$

Because increasing sampling time causes the scale \overline{J}_{coT} to increase due to plume meandering, it is more convenient to express (10) in terms of the time scale \overline{J}_{co} of the three minute plume using (7)

$$i_a^2 \approx i_0^2 \left[\frac{i_{oT}^2}{i_0^2} \right]^2 \frac{2\overline{J}_{co}}{\overline{T}_a} \quad (11)$$

for $\overline{T}_a > 5 i_{oT}^2 \overline{J}_{co} / i_0^2$ and the ratio of intensities computed using (6) with $T_s = T_a$. Typically $\Lambda_{co} \approx 200$ m at $z = 10$ m in the atmospheric boundary layer (see Appendix C) so for $U = 3$ m/s at 10 m, $\overline{J}_{co} = \Lambda_{co}/U$ is about 1 minute. Usually we have $i_{oT}/i_0 < 3$, so (11) is valid for $T_a > 45$ min. In most practical situations averaging times of an hour or more are used, and (11) is a good approximation.

Influence of Averaging Time on Intermittency

To produce a zero concentration over an averaging interval the instantaneous concentration must be zero throughout the entire averaging

period T_a . The chance of observing zero concentration will decrease with increasing averaging time, and the intermittency factor γ_a will approach 1.0 for long averaging times. This increase in γ_a arises directly from its definition

$$\gamma_a = \frac{1 + i_p^2}{1 + i_a^2} \quad (12)$$

and the decreasing value of i_a in (11). For total fluctuation intensity of $i_0 \geq 3$, (6) predicts that

$$\frac{i_{pT}^2}{i_0^2} \approx \left(\frac{T_a}{T_{sref}} \right)^p \quad \text{for large } i_0 \quad (13)$$

Also, for $i_p \geq 1.0$ the conditional plume fluctuation intensity i_{pT} is independent of sampling time (see Table 6). So, i_{pa} should also be independent of averaging time, because T_a and T_s have complementary spectral attenuation functions (see Pasquill (1974) p. 16). Using (13) in (11) and the result in (12)

$$\gamma_a = \frac{1 + i_{pa}^2}{1 + \frac{2 i_0^2 \sqrt{c_0}}{T_{sref}} \left[\frac{T_{sref}}{T_a} \right]^{1-2p}} \quad (14)$$

Comparison With Field Measurements of Averaging Time

The full scale data of Barry (1977) in Figure 15 allows us to estimate i_0 and the exponent p in (14). Barry found that the conditional plume intensity was approximately constant at $i_{pa} \approx 1.00$ for averaging times of 1 hour to 100 hour. This confirms the prediction of our sampling time model that i_{pT} remains constant with T_s for large fluctuation intensity i_0 .

on the centerline of the three minute plume. Over the range from $T_a = 1$ hour to 100 hours the data in Figure 15 follows the empirical relation

$$\gamma_a = \frac{2.0}{1 + \frac{13.3}{T_a^{0.4}}} \quad (15)$$

where T_a is expressed in hours. Using the measured value of $i_{pa} \approx 1.0$ in (14) and estimating $\sqrt{J}_{co} \approx 0.02$ hr and $T_{sref} \approx 0.05$ hr we find that $i_0 \approx 7.4$ and $p = 0.3$ by direct comparison of (14) and (15). This is significantly larger than the value $p = 0.20$ recommended by Angle (1978), and close to the inertial subrange value of $p = 0.33$ suggested by Pasquill (1974) p. 65. It is interesting to note that Barry's simple power law fit to the intermittency in Figure 15 predicts that the value of unity will occur for an averaging time of 11 days. Barry suggests that this asymptotic limit should occur within about 4 days, which is the average time for the wind vector to swing through 360° . From our point of view, what is most surprising is that the simple power law model developed for the effective sampling time appears to be valid for sampling and averaging times of at least 100 hours. This conclusion is further supported by the data of McGuire and Noll (1971) who found that a power law with an exponent of $p \approx 0.2$ applied for averaging times from a few minutes to one year. However, their data was for an urban receptor surrounded by multiple point sources, and it does not seem likely that the same exponent should apply over this wide range of T_s for a single source. While such long term extrapolation must be subject to local topography and climate, it appears to be reasonable to use the power law predictions of (4) through (11) for sampling and averaging times up to 4 days.

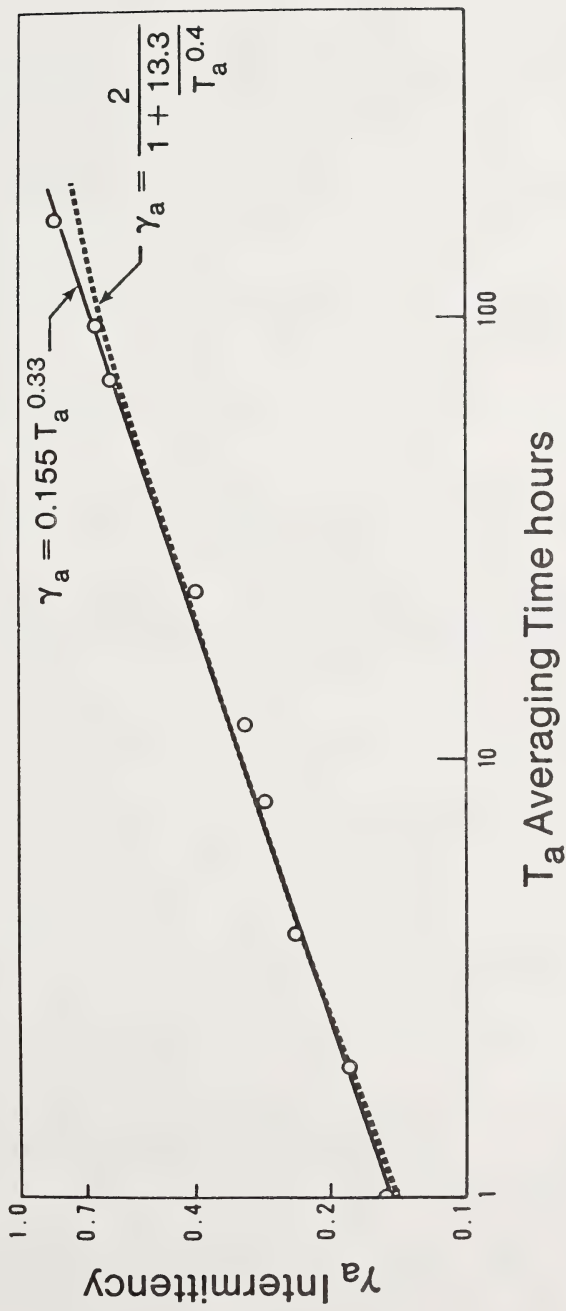


Figure 15 Field measurements of effect of data averaging time on intermittency for a monitor at $x = 1500$ m from a stack $h_s = 50$ m at Chalk River Ontario. Data from Barry (1977).

Dosage Fluctuations

The prime purpose of using an averaging time T_a is to express the concentration as an integrated dose experienced by receptor over a specified exposure time. The implication of using dosage as a measure of damage is that the receptor has a finite response time that integrates the concentration history. The major difference between a dosage concept and a receptor time constant is that dosage provides a memory of all previous events, while the receptor time constant has a receding memory. If for example the receptor is exposed to a fluctuating concentration for several hours, after which the concentration remains at zero, a response function based on receptor time constant τ_s will indicate that the effective concentration is zero after about three time constants. A response factor based on dosage will indicate that the dose received remains constant after the concentration has gone to zero.

It is probably more accurate to express the long term response of a receptor by using an integrated dose based on a concentration fluctuation history that has been attenuated by a short term time constant response. The integrated dose would then represent the irreversible effects that had occurred. A further refinement would be to use a nonlinear function of concentration to represent the increasing sensitivity and damage caused by high concentration. However, given our current state of ignorance on the correlation between a fluctuating concentration field and the long term effects on a receptor, this functional form is difficult to specify.

The smoothing of concentration fluctuations caused by the long exposure time over which the dose is integrated is exactly the same as the effect of averaging time. This relationship between fluctuating dose $D^{\frac{1}{12}}$ and the concentration variance has been derived in Appendix E. The result (E22)

is identical to (11) for an averaging time T_a equal to the exposure time T_e . As the exposure time increases, the fraction of the ensemble that has zero dosage will decrease as it becomes more unlikely that concentration will remain at zero value over the entire exposure time. This dosage intermittency is identical to the time averaged intermittency γ_a given in (14) when the averaging time T_a is equal to the exposure time T_e . The conditional dosage fluctuation intensity is assumed to be independent of exposure time and equal to the plume intensity i_{pT} for $T_s = T_e$. The conditional mean dosage is

$$\overline{D}_p = \frac{\overline{D}}{\gamma_a}$$

where the mean dosage is defined by (E8) for an exposure time T_e

$$\overline{D} = \overline{c}_{oT} T_e$$

with \overline{c}_T the mean concentration for a sample time $T_s = T_e$, from (4). The average intermittency γ_a may be computed from (14) with $T_a = T_e$. Using the value of i_{pT} , \overline{D}_p and γ_a the probability of exceeding some dosage peak D^* may be estimated from the probability distribution.

Fluctuation Damping by Receptor Response Time

The response of physical systems to fluctuating inputs can often be simulated by assuming that the system has a time constant τ_s which causes it to lag behind sudden changes in input conditions. The effect of this time constant is to cause the system to see an effective concentration

fluctuation variance $\overline{c_{\text{eff}}^2}$ that is less than the variance of the instantaneous fluctuations. For biological systems such as trees and other slow growing vegetation, the time constant may be long enough to effectively damp most concentration fluctuations and cause the system to respond to the average concentration. The reduction in total variance for a Markov spectrum of concentration fluctuations is discussed in Appendix A. For this spectrum the effect of time constant on variance produces the remarkably simple result

$$\overline{c_{\text{eff}}^2} = \frac{\overline{c_T^2}}{1 + \frac{\tau_s}{\sqrt{c_T}}} \quad (16)$$

where $\overline{c_T^2}$ and $\sqrt{c_T}$ are variance and scale for sampling time T_s . The mean concentration $\overline{c}_{\text{eff}}$ is unaffected by the time constant so that

$$\overline{c}_{\text{eff}} = \overline{c_T} \quad (17)$$

Dividing (16) by the square of (17) and using (7) to allow the integral scale $\sqrt{J_{co}}$ for the 3 minute plume to be used. The centerline value is

$$\overline{i_{\text{eff}}^2} = \frac{\overline{i_{0T}^2}}{1 + \frac{\overline{i_{0T}^2}}{\overline{i_0^2}} \left(\frac{\tau_s}{\sqrt{J_{co}}} \right)} \quad (18)$$

where i_0 and $\sqrt{J_{co}}$ are intensity and scale in the 3 minute plume. For slowly responding systems, where $\tau_s \gg \sqrt{J_{co}}$ the unity term in the denominator may be neglected and (18) becomes

$$\frac{\overline{i_{\text{eff}}^2}}{\overline{i_0^2}} \approx \left(\frac{\overline{i_{0T}}}{\overline{i_0}} \right)^4 \frac{\sqrt{J_{co}}}{\tau_s} \quad (19)$$

As an illustration consider some vegetation, which might have a time constant of $\tau_s \approx 3$ hour. Typically $\bar{J}_{co} \approx 1$ minute near the ground, and for sampling times of several days $i_{oT} \approx 3 i_o$. Then from (19) $i_{eff} \approx 0.45 i_o$ which is only about a factor of two decrease.

Correcting for Instrument Time Response

Another use for the time constant τ_s is to correct measured data from slowly responding instruments to determine the true concentration variance. Figure 16 shows the response of an SO_2 monitor to concentration fluctuations in a plume. The time constant of the instrument is about $\tau_s = 1.0$ min so the slow rise and fall of concentration at the beginning and end of episodes must be due to plume meander and not instrument response. Equation (16) may be applied to the measured data to determine the true variance $c^{\prime 2}$ over sampling time T_s . Because the instrument time constant will also increase the apparent scale of turbulence, (16) may be put in a more useful form by using (A42) to determine the true integral scale \bar{J}_c from the effective \bar{J}_{eff} found from the measured data. Combining these equations gives the simple correction factor

$$\bar{c}^{\prime 2} = \bar{c}_i^{\prime 2} \left(\frac{\bar{J}_{ci}}{\bar{J}_{ci} - \tau_s} \right) \quad (20)$$

where $\bar{c}_i^{\prime 2}$ and \bar{J}_{ci} are the measured variance and integral scale and $\bar{c}^{\prime 2}$ is the true variance. The true scale is related to the measured scale by

$$\bar{J}_{cT} = \bar{J}_{ci} - \tau_s \quad (21)$$

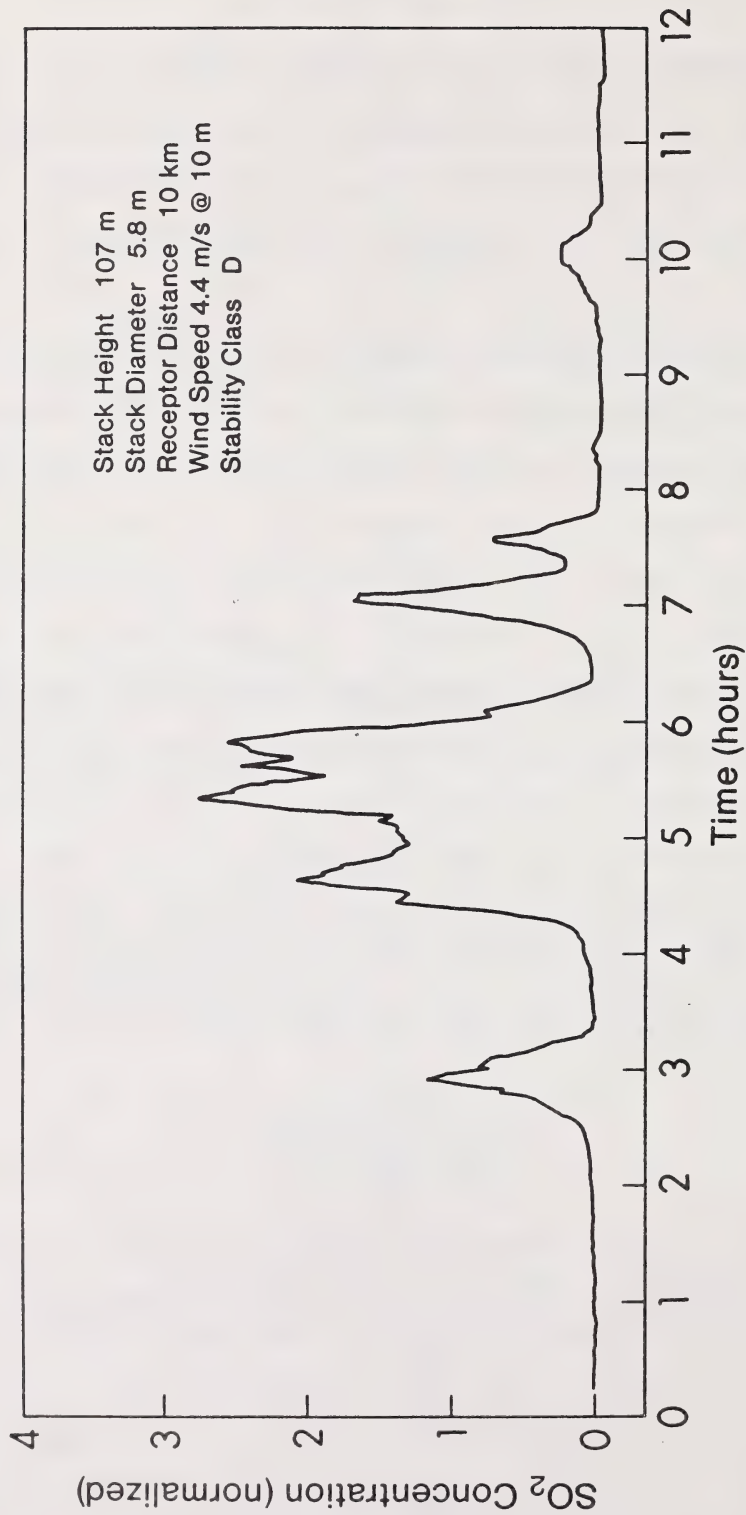


Figure 16 Response of an SO_2 field monitor to concentration fluctuations.

Time Constants for Indoor Air Pollution

A third useful application of the system time constant response is in estimating the effect of fluctuating outdoor concentration on indoor pollution levels. Because buildings are generally tightly sealed and have forced air circulation within them they usually are approximated by a well mixed chamber. If we express the air infiltration into a well mixed volume by the number of air changes per hour (ACH), it is easy to show that the system response time constant is

$$\tau_s = \frac{1}{ACH} \text{ hours} \quad (22)$$

As an illustrative example, consider a house that is exposed to fluctuating concentrations with 3 minute plume intensity $i_o = i_p = 1.0$ so that intermittency factor $\gamma_0 = 1.0$, and fluctuations with an integral scale $\bar{s}_{co} = 1$ minute. For a 12 hour exposure, using an exponent $p = 0.2$ we find from (4), (5), (7), (D19) and (D44) that $\gamma_{oT} = 0.40$, $i_{oT} = 2.04$, $i_{pT} = 1.03$. Then, for a typical house with 0.5 ACH (air changes per hour), $\tau_s = 120$ min. Using (18), we find that the indoor fluctuation intensity i_{eff} is only 18% of the outdoor i_{oT} over a typical (ensemble averaged) 12 hour exposure. It is clearly better to stay indoors, avoiding the high peak concentrations that will be felt outside.

CHAPTER 4

CONDITIONAL MEAN CONCENTRATION

The major problem in monitoring atmospheric pollution levels is the interpretation of the highly intermittent concentration fluctuations when the mean wind direction fails to carry the plume directly over the monitoring station. One possibility is to set air quality standards on the basis of conditional "plume" mean concentration \bar{c}_p which is determined by discarding the time periods with zero concentration. Because the probability distributions used to estimate the fraction of time over some threshold c^* use conditional statistics \bar{c}_p and γ it is sensible to express air quality standards in terms of this conditional value and the intermittency. From the practical standpoint of monitoring concentration readings, the conditional mean concentration is a logical choice because it remains large even in the intermittent fringes off the plume centreline. For a single variance source ($\phi = 0$) the model for short three minute sampling times (D8) and (D14) to (D17) predicts a crosswind variation of

$$\frac{\bar{c}}{c_0} = \exp \left[-\frac{1}{2} \left(\frac{y}{\sigma_y} \right)^2 \right] \quad (23)$$

$$\frac{\gamma}{\gamma_0} = \frac{1 + i_0^2}{1 + i_0^2 \exp \left[\frac{1}{2} \left(\frac{y}{\sigma_y} \right)^2 \right]} \quad (24)$$

where γ_0 and \bar{c}_0 are the plume centreline values for short sample times of $T_{sref} \approx 3$ minutes. By definition, the conditional mean is

$$\bar{c}_p = \frac{c}{\gamma}$$

so from (23) and (24)

$$\frac{\bar{c}_p}{\bar{c}_{po}} = \frac{\exp \left[\frac{-1}{2} \left(\frac{y}{\sigma_y} \right)^2 \right] + i_0^2}{1 + i_0^2} \quad (26)$$

At large distances off the plume centreline both the mean \bar{c} and intermittency rapidly approach zero. However, for $y/\sigma_y \geq 3.0$ the conditional mean concentration has an asymptotic value of

$$\left. \frac{\bar{c}_p}{\bar{c}_{po}} \right|_{y \rightarrow \infty} = \frac{i_0^2}{1 + i_0^2} \quad (27)$$

Figure 17 shows these profiles, which have a constant \bar{c}_p in the outer fringes of the plume. This crosswind variation is physically realistic because we can visualize two distinct types of dilution by entrainment:

- In the outer fringes of the plume, dilution consists of a series of random steps with a contaminated eddy entraining uncontaminated air. The dilution of these eddies should be a function of travel time, and not how far the puffs are off the centerline.
- Contaminated eddies in the central core of the plume near the centerline will experience a similar dilution process, but will mix with other contaminated eddies, and so maintain a higher level of concentration for the same travel time.

The essential difference of puffs of plume material entraining contaminated air on the plume centerline and pure air in the fringes is a plausible explanation for the shape of a crosswind profile shown in Figure 17. The plume fluctuation intensity i_0 , on which the asymptotic value of the conditional mean concentration depends, depends on the plume centerline

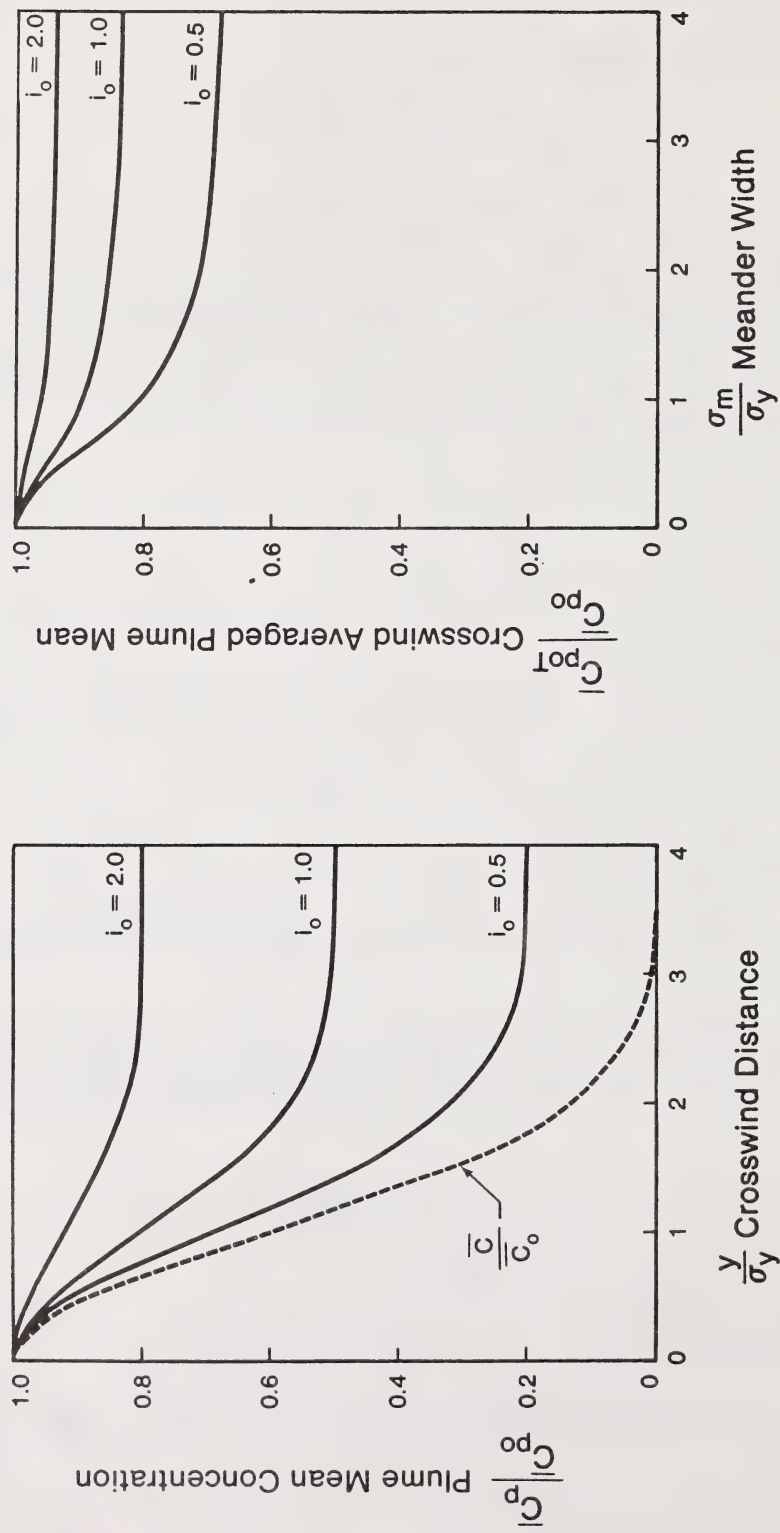


Figure 17 Gaussian model prediction of conditional (plume) means \bar{C}_{po} across a plume, and for sampling time meander averaging on centerline \bar{C}_{poT} , with single variance source $\phi = 0$.

intermittency γ_0 . Because plume fluctuation intensity i_p remains constant across the plume at a fixed downwind position, (D16) shows that the intermittency factor, γ_0 decreases for increasing fluctuation intensity i_0 . When the centerline fluctuations become more intermittent (γ_0 becomes small), the core of the plume has more eddies that are entraining pure air rather than mixing with contaminated material. This causes the diluted eddies in the plume core to have concentrations much the same as those in the outer fringes, which are also mixing with uncontaminated air. Thus, for the high intermittency (small γ_0) consistent with large centerline intensity i_0 we expect less variation in the conditional mean concentration across the plume. This is exactly what we see in (27), plotted in Figure 17.

Conditional Mean for Long Sample Times

The plume centerline concentration for long sample times will be reduced by crosswind meandering as the sample time increases from our reference value of three minutes to several hours. The meandering plume model in Appendix D expresses the meander width in terms of the standard deviation σ_m of the meander position probability distribution. The conditional mean concentration \bar{c}_{pT} on the plume centerline for long sample times may be calculated from the intermittency γ_T obtained from (D19) by numerical integration, and the nonstationary mean \bar{c}_T from (D13). These values are shown in Figure 17, where we see that the centerline conditional mean \bar{c}_{p0T} takes on an asymptotic value for long sampling times. For a sampling time exponent of $p = 0.2$, Figure 14 shows the rapid approach of the plume centerline conditional mean to this constant. Table 4 gives the asymptotic values for two different cases: the far crosswind fringes of

TABLE 4

ASYMPTOTIC VALUES OF CONDITIONAL MEAN CONCENTRATIONS
NORMALIZED BY THREE MINUTE CENTERLINE VALUE \bar{c}_{po}

Centerline Intensity For Reference Sample Time $T_{sref} = 3 \text{ min}$	Conditional "Plume" Mean	
	\bar{c}_p / \bar{c}_{po} Sample Time $T_s = 3 \text{ min}$	$\bar{c}_{poT} / \bar{c}_{po}$ Sample Time $T_s \rightarrow \infty$
	$y/\sigma_y \rightarrow \infty$	$y/\sigma_y = 0$
0.01	0.0001	0.32
0.25	0.059	0.55
0.50	0.20	0.68
1.00	0.50	0.83
1.50	0.69	0.90
2.00	0.80	0.94

the three minute sampling time; and the plume centerline for large sampling times. In most practical situations the centerline intensity i_0 is greater than 0.5 so the plume centerline conditional mean does not vary significantly with sample time. The effect of increased sampling time is mainly to cause the intermittency factor to decrease, without changing any of the other conditional plume statistics.

Crosswind profiles for long sampling times can be computed from (D45) to (D49). These use the same crosswind distribution functions as the three minute plume, but with the time averaged centerline statistics as normalizing factors, and an increased crosswind spread σ_{yT} from the power law in (D2)

$$\frac{\sigma_{yT}}{\sigma_y} = \left(\frac{T_s}{T_{sref}} \right)^p \quad (28)$$

The exponential form of the crosswind distribution in (23) through (26) makes them very sensitive to changes in time averaged crosswind spread. For example, if the mean wind direction places a monitoring station at $y = 3.0 \sigma_y$ off the axis of the 3 minute plume, for $p = 0.2$ it will only be a distance of $y = 1.09 \sigma_{yT}$ off axis after an 8 hour sample time. We see that for long sample times crosswind meandering will make off-axis monitors give a good estimate for the conditional mean value. Taking a typical intensity of $i_0 \approx 1.0$ (26) gives our 8 hour off axis reading as $0.78 \bar{c}_{poT}$. Thus, standards written for 8 hours and based on conditional values are easier to enforce, because compliance is easier to monitor.

Required Sampling Times for Conditional Means

For long sampling times the conditional mean \bar{c}_p remains relatively constant, which suggests that it is a better measure of what is happening on the plume centerline than is the mean concentration \bar{c} which decreases rapidly with increasing sampling time as the plume becomes more intermittent. Unfortunately, we cannot escape the effects of intermittency simply by using conditional averages. If for example, we require one hour of non-zero data to obtain a good estimate for the conditional mean \bar{c}_{pT} , we need only wait an hour when the intermittency $\gamma_T = 1.0$. However, in a highly intermittent plume where $\gamma_T = 0.2$, we must wait five hours to obtain the same data record of nonzero concentrations. The mean wind direction, speed and stability often vary considerably over periods of hours, requiring several measurements to form an ensemble average. For this reason, it may not be any easier to obtain reliable data sets for conditional means than for conventional mean values. What does make the conditional mean value useful is that it is a better representation of plume centerline conditions even when the monitoring station is at an off-axis location.

Variation of Conditional Mean with Distance from a Stack

The model for alongwind variation of plume statistics from Appendix C was combined with the plume spread parameters recommended by Angle (1978) to predict total and conditional statistics for two elevated plumes. The results are shown in Figure 18 for neutral (Class D) atmospheric stability and a 3 minute sample time. When profiles were normalized with the ground level maximum mean concentration \bar{c}_0 and the distance x_m to this maximum, profiles for stability Classes C, D and E were virtually identical. The

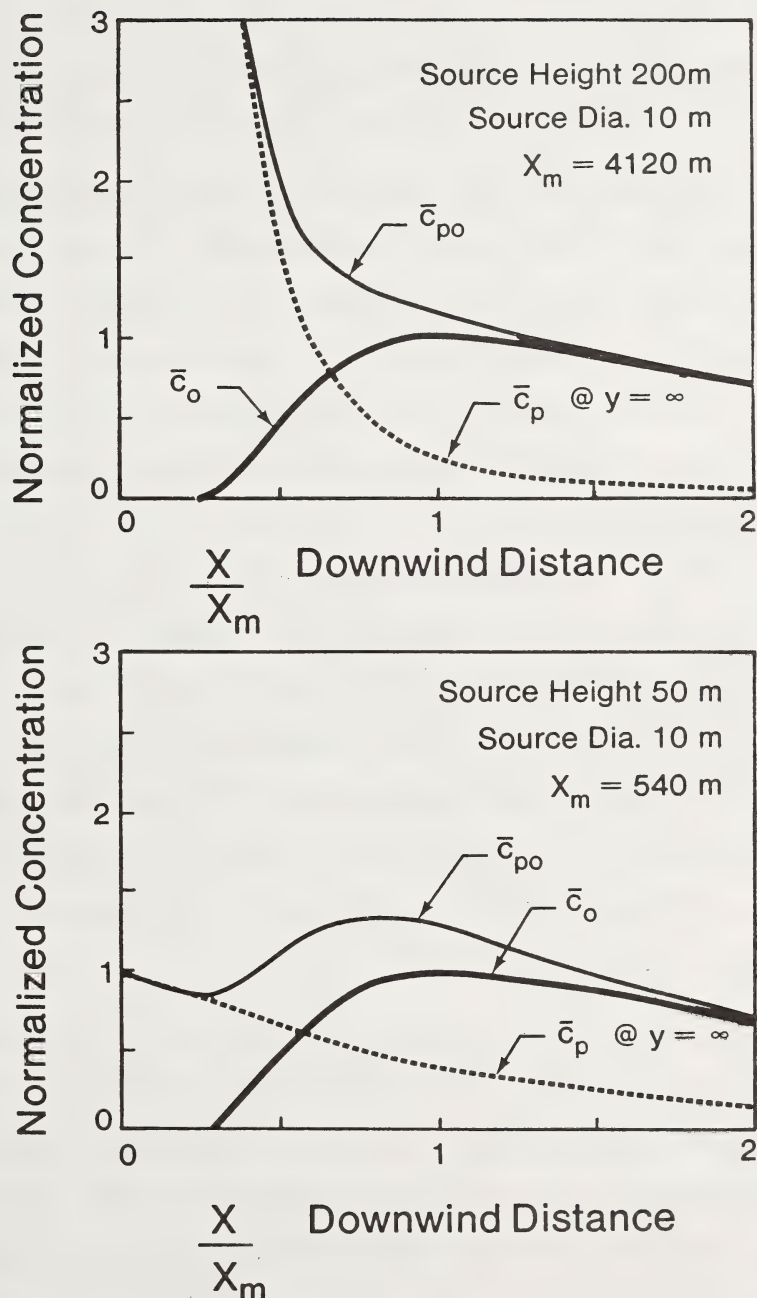


Figure 18 Normalized plume (conditional) and total mean concentrations for 3 min. samples for neutral stability Class D dispersion.

shape of the curves will depend on sampling time, because for large T_s the conditional mean \bar{c}_{pT} becomes constant while the overall mean \bar{c}_T continues to decrease as the plume becomes more intermittent.

It is clear from Figure 18 that the conditional concentration is very sensitive to the ratio of source diameter to source height. When the source is small compared to its effective plume height, ground level concentrations are highly intermittent and conditional mean values are large. However, because ground level receptors lie many standard deviations below the plume axis at positions close to the stack, the model is probably not reliable there. In any case, Figure 18 shows that some care must be taken in estimating the effect of the source size to have any hope of accurately predicting conditional statistics. The asymptotic conditional plume concentration at locations far off the axis is also shown in Figure 18. In the highly intermittent plume from $x = 0$ to $x \approx 0.5 x_m$ the conditional concentration \bar{c}_p is relatively constant across the plume, making it easier to estimate these conditional concentrations when the mean wind direction is not directly from the source to the monitoring station.

Barry (1977) p.366 presents field measurements of conditional plume statistics downwind of the Sudbury, Ontario smelter stack. The ground level conditional mean concentrations remained almost constant over the range of downwind distance of $x \approx 5$ to 40 km, with maximum mean ground level concentration at $x_m \approx 15$ km. This is close to the shape predicted in Figure 18 for five to one ratio of stack height to source diameter, with short sampling time.

CHAPTER 5

PROBABILITY DISTRIBUTIONS AND THRESHOLD CROSSING PROBABILITIES

We now have a plume dispersion model, verified using field data, that allows us to predict the spatial variation of plume mean concentration, its variance and intermittency. These statistics can be adjusted for any sampling time period from a few minutes to several days, and corrected for the smoothing effects of system time response and averaging time for integrated dosage. The final element required for our fluctuation model is a probability distribution function which uses these plume statistics to predict the fraction of time that instantaneous concentration or integrated dosage will exceed a specified limit. For exposure to highly toxic gases it is also essential to know the probability of being exposed for a specified time without even once exceeding a critical concentration limit. We will show in this chapter that these two probabilities, one of which specifies the fraction of concentrations that will exceed some threshold, and the other the probability of not crossing the threshold are related in some situations.

Log-Normal and Exponential Probability Distributions

In the preceding report Wilson (1982) found that measured probability distributions of concentration fluctuations of turbulent mixing suggest that there are two physically different types of dilution process:

- In the core of the plume eddies are diluted by mixing with other contaminated eddies. Here the plume has few intermittent periods, and the intermittency factor $\gamma \rightarrow 1.0$.

- In the intermittent fringes of the plume where the intermittency factor $\gamma \rightarrow 0$, contaminated eddies are isolated from each other and are diluted mostly by entrainment of uncontaminated air.

These two processes should give rise to different probability distributions, with the core of the flow following a log-normal pdf and the highly intermittent fringes an exponential pdf. Barry (1977) supported this approach by noting that

"We cannot expect one single distribution to apply to all cases; a multiplicity of distributions may be pertinent depending on the averaging time or averaging space."

In addition to the different types of dilution process, Barry found that the averaging time used to define an individual sample point will also affect the shape of the probability distribution. For a dilution process which produces a random series of uncorrelated concentration points he showed that an exponential pdf should result. However, when n sequential points were averaged to simulate the effect of grouping data in averaging times, a Gamma distribution resulted. While this indicates that some care must be taken not to extrapolate observed distributions far beyond the range of averaging times for which they were observed, Barry's field measurements downwind of a stack show that for averaging times from $T_a = 1$ to 100 hours there is virtually no effect of averaging time on the shape of the distribution function. Very long averaging times of several hours cause the short term pdf to overestimate the probability of exceeding extreme values.

Wilson (1982) suggested a linear combination of exponential and log-normal distribution functions be used to describe an intermittent plume. While this approach was able to simulate the bimodal pdf's found in a highly

intermittent jet, it is computationally cumbersome and requires the specification of yet another adjustable constant to determine the relative contribution of the two functions. To predict extreme values larger than about twice the conditional mean concentration \bar{c}_p it was found that a simple log-normal distribution gave sufficient accuracy. For concentrations less than the conditional mean \bar{c}_p the log-normal consistently underpredicted the probability of observing low concentrations.

The Gamma Probability Distribution

The Gamma distribution is an attractive compromise between the widely used log-normal pdf for plumes with $\gamma \rightarrow 1.0$, and the exponential pdf observed during highly intermittent conditions when $\gamma \rightarrow 0$. Appendix G presents a detailed discussion of the Gamma distribution and shows it is consistent with a physically realistic model for a dilution process.

The probability density has the functional form

$$p_p(c) = \frac{[k]^k [c/\bar{c}_p]^{k-1}}{\bar{c}_p \Gamma(k)} \exp\left[-k \frac{c}{\bar{c}_p}\right] \quad (31)$$

where the variance appears through k

$$k = \frac{1}{i_p^2} \quad (32)$$

and $\Gamma(k)$ is the gamma function that gives the distribution its name

$$\Gamma(k) = \int_0^\infty x^{k-1} \exp[-x] dx \quad (33)$$

The total pdf including the spike at $c = 0$ due to intermittency is

$$p(c) = (1 - \gamma) \delta(c) + \gamma p_p(c) \quad (34)$$

where $\delta(c)$ is the delta function. The cumulative pdf $\Omega(c)$ is the fraction of concentrations less than c and is the integral of (34)

$$\Omega(c) = (1 - \gamma) + \gamma \Omega_p(c) \quad (35)$$

where

$$\Omega_p(c) = \int_0^c p_p(c) dc \quad (36)$$

and the complementary-cumulative fraction exceeding c is

$$\begin{aligned} V(c) &= 1 - \Omega(c) \\ &= \gamma (1 - \Omega_p(c)) \end{aligned} \quad (37)$$

For the Gamma distribution (31), the integral in (36) must be evaluated numerically using a series approximation to the incomplete Gamma integral, see Appendix G.

When the plume intensity $i_p = 1.0$, $k = 1.0$ the Gamma distribution reduces to the exponential form with $\Gamma(1) = 1.0$

$$p_p(c) = \frac{1}{c_p} \exp\left[\frac{-c}{c_p}\right] \quad (38)$$

It is this feature that allows the Gamma distribution to represent both highly intermittent and continuous concentration fluctuations. Bencala

and Seinfeld (1976) in an analysis of concentration distributions in cities, noted that the Gamma and log-normal distributions predicted similar probabilities for extreme values. This is evident in Table 5 which compares the normal, log-normal and Gamma complementary-cumulative distributions for exceedance probabilities.

Measured Probability Distributions

Wilson (1982) reviewed the observations of several investigators who, with the exception of Barry (1977), fitted their data to log-normal distributions. However, most of this data was for multiple sources in urban areas. For these area sources much of the log-normal behavior can be explained by a log-normal distribution of wind speed, which is the major factor in determining urban pollution levels.

Recent measurements of Berger, Melice and Demuth (1982) tested the log-normal and Gamma distributions on an extensive data set for suspended particulate levels in Gent, Belgium. Typical data sets of more than seven hundred daily averages were used to demonstrate conclusively that the Gamma distribution was superior to the log-normal. They found that the log-normal consistently underestimated the fraction at low concentrations and overestimated the fraction of extreme values at high concentration. For their eleven different measuring stations the conditional fluctuation intensity i_p ranged from 0.5 to 0.8 with an average of 0.64. The multiple distributed fossil fuel sources which contributed to the suspended particulate level, and the long averaging time of 24 hours, allows us to make the assumption that the intermittency factor γ_a was unity.

TABLE 5

PEAK EXCEEDANCE PROBABILITIES FOR THREE FREQUENCY DISTRIBUTIONS

Fluctuation Intensity i_p	Concentration Peak c^* Above Mean $\frac{c^* - \bar{c}_p}{\sqrt{c_p'^2}}$	Fraction of Time Exceeded $V(c^*)$		
		Normal	Log-Normal	Gamma
0.5	0	0.50	0.406	0.433
	1	0.158	0.137	0.151
	2	0.0228	0.0442	0.0424
	3	0.00136	0.0148	0.0103
	4	0.00003	0.00521	0.00229
1.0	0	0.339	0.368	
	1	0.106	0.135	
	2	"	0.0413	0.0498
	3		0.0187	0.0183
	4		0.00940	0.0674
1.5	0	0.294	0.308	
	1	0.0827	0.117	
	2	"	0.0344	0.0501
	3		0.0173	0.0225
	4		0.00977	0.0104

The tendency of the log-normal to underestimate the fraction at low concentrations is apparent in the wind tunnel data in Figure 19, for values less than half the mean concentration. The Gamma pdf gives good agreement for both high and low values, although the peak appears to be somewhat too large. Comparing the areas under the curves suggests that this difference may be due to improper scaling of the probability measurements, rather than any deficiency in either distribution. Both the Gamma and the log-normal distributions are good approximation for the extremes larger than twice the mean \bar{c}_p .

Hinds (1969) measurements of short range diffusion from ground level sources are shown in Figure 20, where the Gamma distribution gives a consistently better estimate than the log-normal, particularly for low concentrations. For long averaging times Barry (1977) found that the conditional intensity i_p was always close to unity, and probability distributions were exponential. Because exponential and Gamma distributions are the same if $i_p = 1.0$, Barry's data in Figure 21 shows that the Gamma distribution is again superior to the log-normal in predicting fluctuations for time averaged data. Barry's observation that plume fluctuation intensity $i_p \approx 1.0$ for long sampling times is properly simulated by the plume meandering model in Appendix D. For long sample times the back and forth meandering causes the crosswind profile of mean concentration \bar{c} to generate fluctuations on the plume centerline. When the "internal" variance in the three minute plume is relatively small, the variance i_0 induced by meandering tends to significantly increase i_{po} for long sample times, as shown in Table 6. We see that if "internal" fluctuations with periods less than three minutes are removed either by

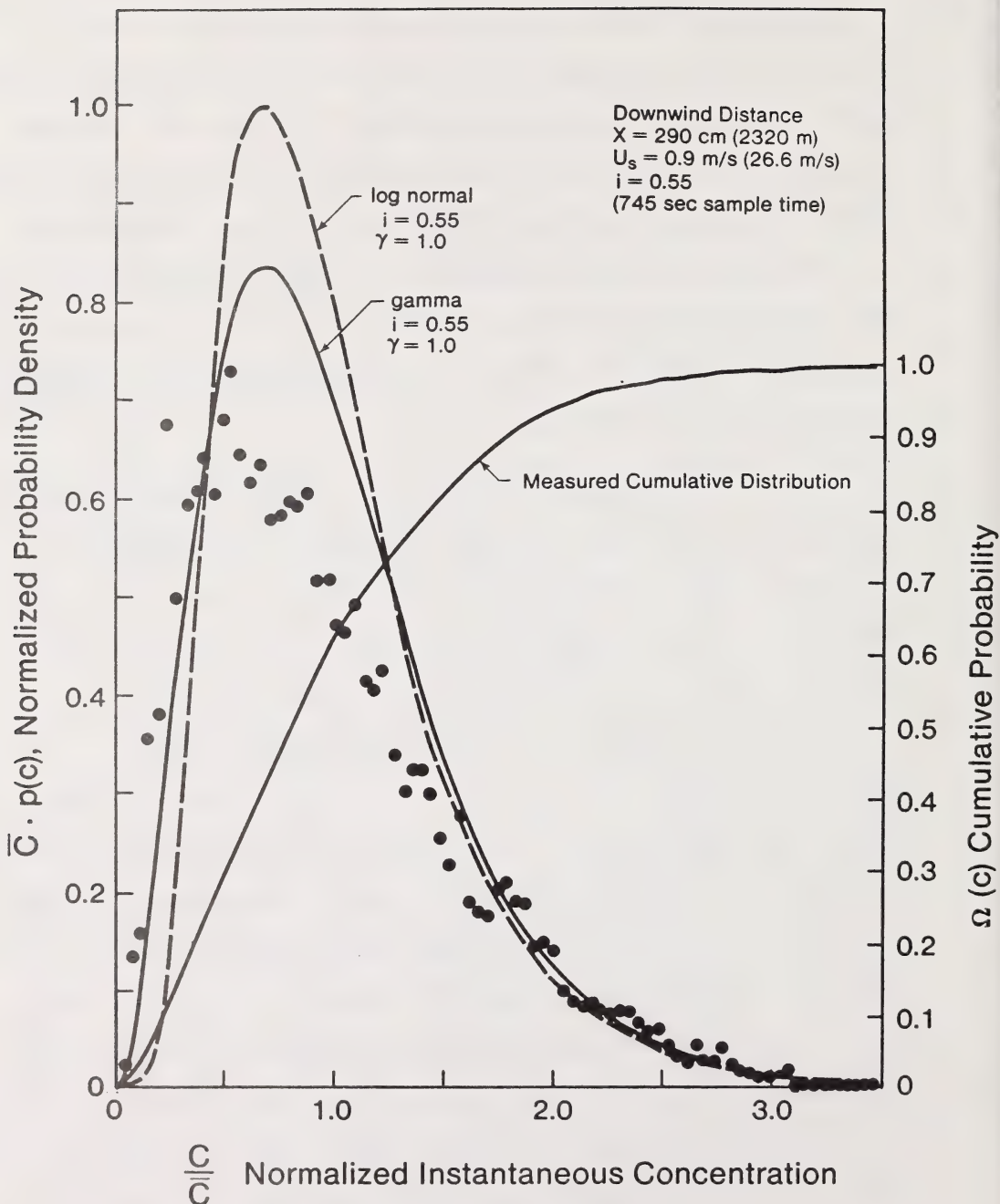


Figure 19 Log-normal and Gamma probability densities compared with ground level measurements in a wind tunnel boundary layer
 $h/H = 0.44$, $x/H = 3.2$, $\lambda = 0.175$.

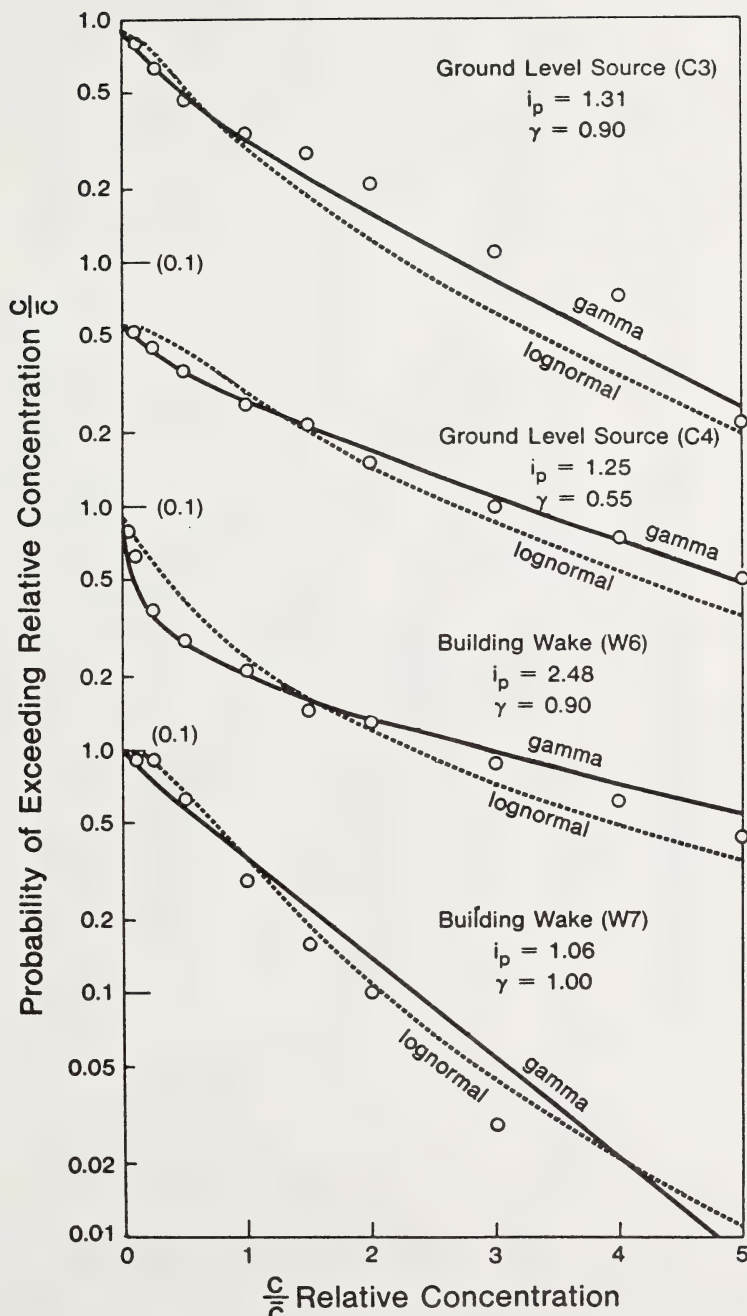


Figure 20 Field measurements of exceedance probability for diffusion from a ground level source in flat terrain and in the wake of a building immediately downwind of the source, with sample time 6 to 15 min. and averaging time of 5 sec. Data of Hinds (1969) in Barry (1977).

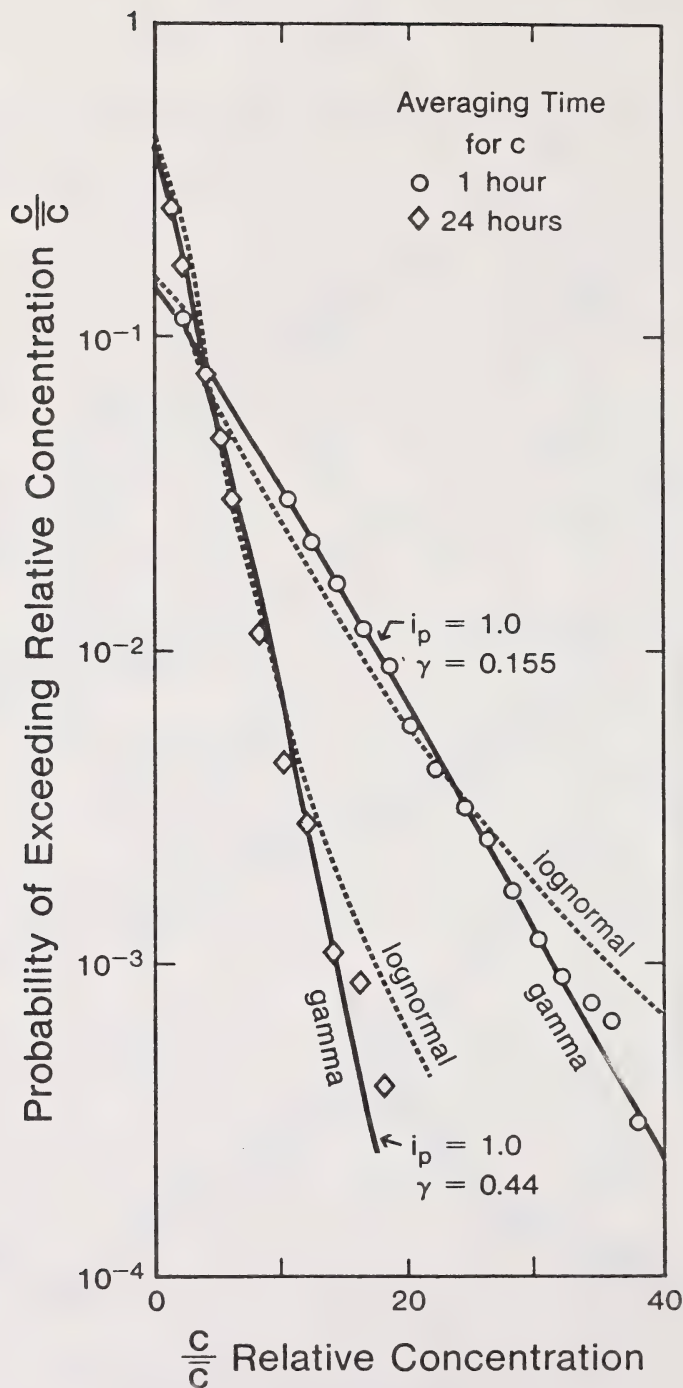


Figure 21 Field measurements of averaging time effects on exceedance probability at $x = 1500$ m from a stack $h_s = 50$ m. Data from Barry (1977).

TABLE 6

CHANGES IN CENTERLINE CONDITIONAL PLUME FLUCTUATION
INTENSITIES WITH SAMPLING TIME

"Internal" Intensity Sample Time $T_s \approx 3 \text{ min}$ $\gamma_0 = 1.00$ $i_0 = i_p$ i_p	Long Sample Time Intensity	
	Conditional i_{pT}	Total i_{oT}
1.50	1.5	3.8
1.00	1.0	2.8
0.75	0.8	2.3
0.50	0.7	1.7
0.10	0.8	1.6
0.05	0.9	1.6
0.01	1.1	1.6

mixing, receptor response, or averaging time, that plume fluctuation intensity tends to values near unity due to the meandering-induced fluctuations from the mean profile. Sawford (1983), using Monte-Carlo methods for particle pair statistics in a dispersing cloud found that the total fluctuation intensity ranged from about 0.5 to 2.0 depending on the initial size of the cloud. This further supports the assumption of plume intensities near unity.

The more accurate prediction given by the Gamma distribution is particularly important when the threshold for damage of a receptor is less than the mean concentration, as might be the case for sensitive vegetation. Even in a continuous plume with no intermittency, Table 5 shows that the concentration exceeds the conditional mean \bar{c}_p only 30% to 40% of the time for log-normal and Gamma distributions. This emphasizes the need for accurate predictions of these low concentrations, and supports our choice of the Gamma distribution.

Threshold Crossing Probability

There are many situations where knowing the fraction of time concentration exceeds a specified threshold c^* is not sufficient to determine risk. What is required in some cases is a knowledge of the probability of exceeding a threshold level at least once during an exposure time T_e . The usefulness of this threshold crossing probability is obvious when we consider exposure to a toxic gas like hydrogen sulfide. In this case, the concept of not once exceeding a threshold is critical. In Appendix F we show that this probability may be estimated from the cumulative exceedence distribution V in (37) using (F24) for the crossing

probability S

$$S(T_e) = \exp \left[- V_{\text{avg}} T_e \right] \quad (39)$$

where the average exceedence probability is for some threshold concentration c^*

$$V_{\text{avg}}(c^*) = \frac{1}{T_e} \int_0^{T_e} V \left(\frac{c^*}{\bar{c}_{pT}}, \gamma, i_{pT} \right) dt \quad (40)$$

The time dependence of the exceedence probability $V(t)$ arises when the concentration statistics \bar{c}_p , γ and i_p vary with time during a transient release of a toxic gas. An alternative way of looking at the probability of threshold crossing is to view $V_{\text{avg}} T_e$ in (4) as the probability "dose" seen during passage of a transient plume.

If the plume is continuous, we will eventually exceed the threshold c^* if we wait long enough. However, because the plume becomes more intermittent as sample time T_s increases, V decreases in direct proportion in (37). Combining (37) and (40),

$$V_{\text{avg}} = \frac{1}{T_e} \int_0^{T_e} \gamma_T dt - \frac{1}{T_e} \int_0^{T_e} \gamma_T \Omega_p \left(\frac{c^*}{\bar{c}_p}, i_{pT} \right) dt \quad (41)$$

Application Of Threshold Crossing Probability to Air Quality Monitoring

The concept of crossing probability can also be directly applied to planning field monitoring programs. The concentration of interest in this case is the sequence of time averaged concentrations \bar{c}_a with an averaging T_a

equal to the time interval over which the air quality standards are set. For this sequence of time averaged values we want to know the length of time we must wait for a violation of the standard c^* to occur. Because plume statistics change as sample time increases, we must carry out an integrated average of (41) to find V_{avg} . This value, determined by numerical integration of (41) is used in (39) to determine the probability of completing the exposure time T_e from the beginning of monitoring to the present moment without having a violation. It is clear from both the probability distribution, and from common sense, that when ground level concentrations \bar{c}_a are a factor of two smaller than the limit c^* , it may be necessary to sample for a long period before seeing the violation on a fixed monitor.

One troublesome approximation in Appendix F is the assumption (F6) that the hazard rate is equal to the fractional exceedence probability. Because this approximation does not explicitly state the time units, we must make a logical choice for the units used for time measurements in (39). One reasonable choice is to take the averaging time over which successive steps are taken as one time unit, so that exposure time for one hour standards is also expressed in hours. For example, if the adjusted statistics for a one hour exposure indicate that the air quality standard will be exceeded 10% of the time, then $V_{avg} = 0.1$, and (39) indicates that we must wait a total of 46 hours to be 99% certain of seeing this violation. However, this choice of time units is rather arbitrary and illustrates the difficulty in inferring the time series behavior from the fractional exceedence pdf without making many restrictive and often questionable assumptions.

APPENDIX A

EFFECT OF RECEPTOR TIME CONSTANT AND DATA AVERAGING TIME INTERVAL ON EFFECTIVE FLUCTUATION VARIANCE

All measuring systems have a limit to their frequency response, usually expressed as the -3dB attenuation point in their amplitude gain, G. For a response (i.e. "output") amplitude A_{out} to a system input amplitude A_{in} the "gain" is

$$G \equiv \frac{A_{out}}{A_{in}} \quad (A1)$$

Using the definition of attenuation decibels

$$\text{dB} = 10 \log G \quad (A2)$$

and we see that the -3dB point on the frequency response curve is the location where $G = 0.5$, and the amplitude has decayed by a factor of two. For many electronic systems this definition is often confused with the "power bandwidth" of the device. Here, the amplitude A is voltage, and because power output into a constant resistive load is proportional to the square of the voltage A^2 , the -3dB attenuation on the power occurs when

$$\frac{A_{out}^2}{A_{in}^2} = 0.5$$

or

$$G = \frac{A_{out}}{A_{in}} = 0.707$$

The listed frequency response of electronic devices often fails to distinguish between amplitude and power bandwidths and some care is required in interpreting specified -3dB frequency limits.

System Frequency Response

Consider the frequency response of a simple resistance-capacitance system which is described by a single time constant τ_s , with no dissipative damping. The response of this measuring system to a step change in input from zero to V_{in} is an exponential rise with time, t

$$V_{out} = V_{in} \left(1 - \exp\left(-\frac{t}{\tau_s}\right)\right) \quad (A3)$$

For a sinusoidal input with amplitude A_{in} and frequency "f" cycles per second, the gain G is

$$G = \frac{A_{out}}{A_{in}} = \left(\frac{1}{1 + (\tau_s 2\pi f)^2} \right)^{1/2} \quad (A4)$$

The -3dB attenuation frequency occurs where $G = 0.5$ at a frequency $f_{0.5}$ which from (A4) is

$$f_{0.5} = \frac{\sqrt{3}}{2\pi \tau_s} \quad (A5)$$

The Markovian Spectrum

If a variable, c' , with no inertia is subjected to random fluctuations, the auto correlation of these fluctuations for varying time delay, t' , will be exponential. The essential characteristic of such inertialess systems is that the time rate of change of c' has no autocorrelation. That is,

$$\frac{\partial c'(t)}{\partial t} \cdot \frac{\partial c'(t+t')}{\partial t}$$

is zero except when $t' = 0$. In simple terms this says that knowing c'

is increasing at time t tells us nothing about whether c' will continue to increase, stay constant, or decrease in the next instant. Hence the term "inertialess". Such first order Markov processes have an exponential auto time correlation given by

$$R_c(t') = \exp\left(\frac{-t'}{\bar{\tau}_c}\right) \quad (A6)$$

where

$$R_c(t) = \frac{\overline{c'(t)c'(t+t')}}{c'^2} \quad (A7)$$

The constant $\bar{\tau}_c$ is the integral time scale of concentration defined by

$$\bar{\tau}_c = \int_0^\infty R_c(t') dt' \quad (A8)$$

Frozen Turbulence

If the turbulent eddies are not too small, they lose their coherence slowly as they are advected past a point. In this case we can assume that the turbulence is "frozen" into the flow and is carried past a point at the local mean velocity, U . Because it is the size of eddies not their time of passage that remains constant when the speed varies, it is more useful to think in terms of the concentration integral length scale Λ_c . For turbulence frozen into the flow which passes at speed U ,

$$\Lambda_c = U \bar{\tau}_c \quad (A9)$$

In all the analysis here, a non-intermittent turbulence is assumed. That is $c > 0$ and $\gamma = 1.0$ at all times. For intermittent fluctuations adjustments are required to deal with the periods of intermittency.

Frequency Spectrum of Concentration Fluctuations

To see the effect of frequency dependent gain G on the input concentration fluctuations, we first use a Fourier transform to express the exponential correlation as a frequency spectrum $E_c(f)$, for frequency, f

$$E_c(f) = 4 c'^{\frac{1}{2}} \int_0^{\infty} R_c(t') \cos(2\pi f t') dt' \quad (A10)$$

which for the exponential correlation is

$$E_c(f) = 4 c'^{\frac{1}{2}} \int_0^{\infty} \exp\left(\frac{-t'}{\tau_c}\right) \cos(2\pi f t') dt' \quad (A11)$$

Integrating this twice by parts gives the Markov spectrum

$$E_c(f) = \frac{4 c'^{\frac{1}{2}} \tau_c}{1 + (\tau_c^2 \pi f)^2} \quad (A12)$$

This can be expressed in terms of the integral length scale of concentration fluctuations Λ_c by using (A9)

$$U E_c(f) = \frac{4 c'^{\frac{1}{2}} \Lambda_c}{1 + (\Lambda_c \frac{2\pi f}{U})^2} \quad (A13)$$

For turbulence "frozen" into the mean flow the fluctuation frequency f increases in direct proportion to the flow speed U . The wave number k_1 defined as

$$k_1 = \frac{2\pi f}{U} \quad \frac{2\pi}{\text{wavelength}} \quad (A14)$$

remains constant with changes in flow speed

Observed Spectrum and Variance with Gain Attenuation

The spectrum is defined in terms of the square of the fluctuation amplitude c' about the mean. The spectrum will be attenuated by the square of the system response gain G so that the observed "effective" spectrum is

$$E_{c,\text{eff}}(f) = G^2(f) \cdot E_c(f) \quad (\text{A15})$$

Combining (A4) and A(12)

$$E_{c,\text{eff}}(f) = \left(\frac{1}{1 + (\tau_s 2\pi f)^2} \right) \left(\frac{4 \overline{c'^2} \bar{\tau}_c}{1 + (\bar{\tau}_c 2\pi f)^2} \right) \quad (\text{A16})$$

This system response attenuation is shown schematically in Figure A1.

To determine the "effective" variance $\overline{c'^2}_{\text{eff}}$ observed by the system, the integral of the spectral density is taken

$$\overline{c'^2}_{\text{eff}} = \int_0^\infty E_{c,\text{eff}}(f) df \quad (\text{A17})$$

Using (A4) and (A16), noting that the integral time scale $\bar{\tau}_c$ is a function of location and not frequency f ,

$$\frac{\overline{c'^2}_{\text{eff}}}{\overline{c'^2}} = 4 \bar{\tau}_c \int_0^\infty \frac{df}{(1 + (2\pi\tau_s)^2 f^2)(1 + (2\pi \bar{\tau}_c)^2 f^2)} \quad (\text{A18})$$

To evaluate the integral, Bara (1983) defines

$$a \equiv \frac{1}{2\pi \tau_s} \quad (\text{A19})$$

and

$$b \equiv \frac{1}{2\pi \bar{\tau}_c} \quad (\text{A20})$$

Then factor these parameters out of the integrand to obtain

$$\frac{\overline{c'^2_{\text{eff}}}}{\overline{c'^2}} = 4a^2 b^2 \int_c^\infty \frac{df}{(a^2 + f^2)(b^2 + f^2)} \quad (\text{A21})$$

Then separate the integrand into two parts using partial fractions

$$\frac{1}{(a^2 + f^2)(b^2 + f^2)} = \frac{A}{(a^2 + f^2)} + \frac{B}{(b^2 + f^2)} \quad (\text{A22})$$

$$1 = Ab^2 + Af^2 + Ba^2 + Bf^2$$

$$1 = (Ab^2 + Ba^2) + (A + B)f^2$$

The only solution of which must be

$$A + B = 0$$

$$Ab^2 + Ba^2 = 1$$

which leads to

$$A = \frac{1}{b^2 - a^2}$$

$$B = \frac{1}{a^2 - b^2}$$

so that (A22) becomes

$$\frac{1}{(a^2 + f^2)(b^2 + f^2)} = \frac{1}{(b^2 - a^2)(a^2 + f^2)} = \frac{1}{(a^2 - b^2)(b^2 + f^2)} \quad (\text{A23})$$

The integral in (A21) then becomes

$$\frac{\overline{c'^2_{\text{eff}}}}{\overline{c'^2}} = \frac{4a^2 b^2 \int_c^\infty df}{(b^2 - a^2)} + \frac{4a^2 b^2 \int_c^\infty df}{(a^2 - b^2)} \quad (\text{A24})$$

The integrals can now be evaluated from standard integral tables as

$$\int_0^{\infty} \frac{df}{(a^2 + f^2)} = \frac{1}{a} \tan^{-1}\left(\frac{f}{a}\right)$$

with a similar equation for the second integral.

Using these in (A24),

$$\frac{\overline{c'^2}_{eff}}{\overline{c'^2}} = 4a^2 b^2 \mathcal{J}_C \left[\frac{1}{a(b^2 - a^2)} \tan^{-1}\left(\frac{f}{a}\right) + \frac{1}{b(a^2 - b^2)} \tan^{-1}\left(\frac{f}{b}\right) \right] \quad (A24)$$

$f=\infty$
 $f=0$

noting $\tan^{-1}(0) = 0$ and $\tan^{-1}(\infty) = \pi/2$

$$\begin{aligned} &= 2\pi a^2 b^2 \mathcal{J}_C \left[\frac{1}{a(b^2 - a^2)} + \frac{1}{b(a^2 - b^2)} \right] \\ &= 2\pi a^2 b^2 \mathcal{J}_C \left[\frac{1}{ab(a+b)} \right] \end{aligned}$$

From (A20) $2\pi \mathcal{J}_C = 1/b$ so that the equation reduces to .

$$\frac{\overline{c'^2}_{eff}}{\overline{c'^2}} = \frac{1}{(1 + \frac{b}{a})}$$

Using the definitions in (A19) and (A20) this reduces to the simple result

$$\frac{\overline{c'^2}_{eff}}{\overline{c'^2}} = \frac{1}{\left(1 + \frac{\tau_s}{\mathcal{J}_C}\right)} \quad (A26)$$

The spectral attenuation is shown in Figure A1.

This can be interpreted in two ways. When applied to the response of a sensing instrument it shows that the actual variance c'^2 is just the measured variance multiplied by $(1 + \tau_s/\bar{\tau}_c)$. On the other hand, for a biological receptor with a response time constant of τ_s , the fluctuation level seen by the receptor is just the actual variance c'^2 divided by this same factor of $(1 + \tau_s/\bar{\tau}_c)$

Effect of Data Averaging Time Interval on Observed Variance

As we have shown in the previous analysis, the response time constant, τ_s of the receptor (a measuring instrument, or biological receptor) causes the observed concentration fluctuation variance to be less than the actual variance. This time constant can seldom be controlled, and must be considered as part of the system.

The variance is also reduced by another quite different parameter; the averaging time selected for sequential data samples. Because of the hour to hour variability of wind speed, direction and stability, full scale data is collected and analyzed over short intervals of duration T_a . Because the variance computed over an interval T_a will exclude low frequency fluctuations with frequencies less than $1/T_a$, some of the full scale variance will be missed. The problem we will deal with here is how to estimate the actual atmospheric fluctuation variance c'^2 from the measured variance $c_a^{T_2}$, an ensemble average of variance each of which is measured over a time interval T_a . Here we will assume that the instantaneous data used to compute the sample averages is taken with an ideal sensor that has a zero response time constant, $\tau_s = 0$, so that there is no attenuation due to sensor response.

The effects of sample averaging time T_a are similar to those of response time constant τ_s . In both cases:

- 1.) The peak concentration excursions are reduced
- 2.) The observed periods of zero concentration (i.e. intermittency) occur for a smaller fraction of time, so observed γ is larger.
- 3.) The observed variance is reduced.

These effects are illustrated in Figure A2. In the following analysis, only the influence of averaging time on variance will be estimated. Pasquill (1974, pp. 12-16) discusses the attenuation of variance for averaging time T_a by analyzing the fluctuation spectrum. The attenuation factor at frequency f for the variance is given by the square of the gain G , where

$$G(f) = \frac{\sin(\pi f T_a)}{\pi f T_a} \quad (A27)$$

This may be compared to (A4) which is the gain for a receptor with a response time constant of τ_s . The attenuated concentration fluctuation spectrum $E_{c,a}(f)$ is given by:

$$E_{c,a}(f) = G^2(f) \cdot E_c(f) \quad (A28)$$

The variance for samples of duration T_a is simply the integral of the spectrum

$$\overline{c_a^2} = \int_0^\infty E_{c,a}(f) df \quad (A29)$$

This variance is the smoothed average of a large ensemble of samples each of duration T_a . For the Markov spectrum in (A12), Shoji and Tsukatani (1973) have evaluated the integral of $G^2 \cdot E_c$ using (A27) to obtain

$$\frac{\overline{c_a^2}}{c^2} = 2 \frac{\sqrt{J_c}}{T_a} \left[1 - \frac{\sqrt{J_c}}{T_a} \left(1 - \exp\left(-\frac{T_a}{\sqrt{J_c}}\right) \right) \right] \quad (A30)$$

For very long averaging times relative to the fluctuation time scale, the exponential approaches zero and the ratio of the observed to actual variance reduces to

$$\begin{aligned} \frac{\overline{c_a^2}}{c^2} &= 2 \frac{\sqrt{J_c}}{T_a} \left(1 - \frac{\sqrt{J_c}}{T_a} \right) \\ &\approx 2 \frac{\sqrt{J_c}}{T_a} \quad \text{for large } \frac{T_a}{\sqrt{J_c}} \end{aligned} \quad (A31)$$

For short times the exponential may be expanded as a Taylor series about $T_a = 0$ to obtain to fourth order

$$\exp\left(-\frac{T_a}{\sqrt{J_c}}\right) \approx 1 - \left(\frac{T_a}{\sqrt{J_c}}\right) + \frac{1}{2}\left(\frac{T_a}{\sqrt{J_c}}\right)^2 - \frac{1}{6}\left(\frac{T_a}{\sqrt{J_c}}\right)^3 + \frac{1}{24}\left(\frac{T_a}{\sqrt{J_c}}\right)^4 \quad (A32)$$

Inserting this in (A30) yields

$$\frac{\overline{c_a^2}}{c^2} = 1 - \frac{1}{3}\left(\frac{T_a}{\sqrt{J_c}}\right) + \frac{1}{12}\left(\frac{T_a}{\sqrt{J_c}}\right)^2 \quad \text{for small } \frac{T_a}{\sqrt{J_c}} \quad (A33)$$

which is correct to fourth order in $T_a/\sqrt{J_c}$. This series approximation in (A33) will be within 1% of the exact ratio predicted by (A30) for $(T_a/\sqrt{J_c}) < 1.0$.

The ratio of observed to actual variance can also be computed directly from the time correlation $R_c(t')$ defined in (A7). This approach gives a better physical insight into the effect of time averaging interval than does the spectral analysis method. Fackrell (1978) presents a concise derivation which we will reproduce here. The concentration fluctuation c' about the mean \bar{c} when averaged over the time interval T_a is

$$\overline{c'_a} = \frac{1}{T_a} \int_0^{T_a} c' dt \quad (A34)$$

The auto correlation of this is

$$\begin{aligned} \overline{c'_a}^2 &= \left(\frac{1}{T_a} \int_0^{T_a} c'(t) dt \right) \left(\frac{1}{T_a} \int_0^{T_a} \tilde{c}'(\tilde{t}) d\tilde{t} \right) \\ &= \frac{1}{T_a^2} \int_0^{T_a} \int_0^{T_a} c'(t) c'(\tilde{t}) dt d\tilde{t} \quad (A35) \end{aligned}$$

For a stationary random variable we can define $t' = \tilde{t} - t$ without loss of generality, and then take the ensemble average to write

$$\overline{c'_a}^2 = \frac{1}{T_a^2} \int_0^{T_a} \int_0^{T_a} \overline{c'(t) c'(t+t')} dt dt' \quad (A36)$$

Using the definition of the auto correlation $R_c(t')$ in (A7) this becomes,

$$\frac{\overline{c'_a}^2}{\overline{c}^2} = \frac{1}{T_a^2} \int_0^{T_a} \int_0^{T_a} R_c(t') dt dt' \quad (A37)$$

This can be manipulated using Kampé de Fériet's transformation (see Hinze (1975), p.52) to a single integral

$$\frac{\overline{c_a'^2}}{c'^2} = \frac{2}{T_a} \int_0^{T_a} \left(1 - \frac{t'}{T_a}\right) R_c(t') dt' \quad (A38)$$

For the exponential correlation in (A6) that produces the Markov spectrum, (A38) can be integrated by parts to produce (A30).

Effect of Response Time Constant and Averaging Time on Measured Fluctuation Scales

Both the system response time constant τ_s and the averaging time T_a attenuate the high frequency end of the fluctuation spectrum, leaving the low frequency fluctuations unaffected. This high frequency attenuation will cause the measured concentration integral scale \overline{J}_{ceff} or \overline{J}_{ca} to be larger than the true value \overline{J}_c . These integral time scales are related to the fluctuation variance through their spectra by the relation from Appendix C, equation (C3)

$$E_c(0) = 4 c'^2 \overline{J}_c \quad (A39)$$

Because the averaging time T_a and the system response time constant affect only the high frequencies, this zero frequency intercept $E_c(0)$ will be the same for spectra of $\overline{c_{eff}'^2}$ and $\overline{c_a'^2}$ with time constant τ_s or averaging time T_a . Equating the spectral densities $E_c(0)$ yields the simple relationship from (A40)

$$\frac{\overline{J}_{ceff}}{\overline{J}_c} = \frac{\overline{c'^2}}{\overline{c_{eff}'^2}} \quad (A40)$$

and

$$\frac{\bar{J}_{ca}}{\bar{J}_c} = \frac{\bar{c}'^2}{\bar{c}_a'^2} \quad (A41)$$

Using (A26) and (A40) produces the remarkable result that the effective fluctuation time scale \bar{J}_{ceff} is simply the sum of the true time scale and the system time constant

$$\boxed{\bar{J}_{ceff} = \bar{J}_c + \tau_s} \quad (A42)$$

for the Markov spectrum. The effect of averaging time T_a may be found by combining (A30) and (A41). However, in many situations the averaging time is much larger than the fluctuation scale \bar{J}_c , and the approximate form in (A31) may be used. This leads to the simple result that the measured integral scale of time averaged data is

$$\boxed{\begin{aligned} \bar{J}_{ca} &\approx \frac{T_a}{2} \\ \text{for } \frac{T_a}{\bar{J}_c} &> 5 \end{aligned}} \quad (A43)$$

when \bar{c}'^2 follows a Markov spectrum. This result is even more remarkable because for long averaging times the measured integral time scale \bar{J}_{ca} has nothing whatever to do with the actual integral scale \bar{J}_c , because the fluctuations which contribute to the scale \bar{J}_c have been smoothed out by the averaging process.

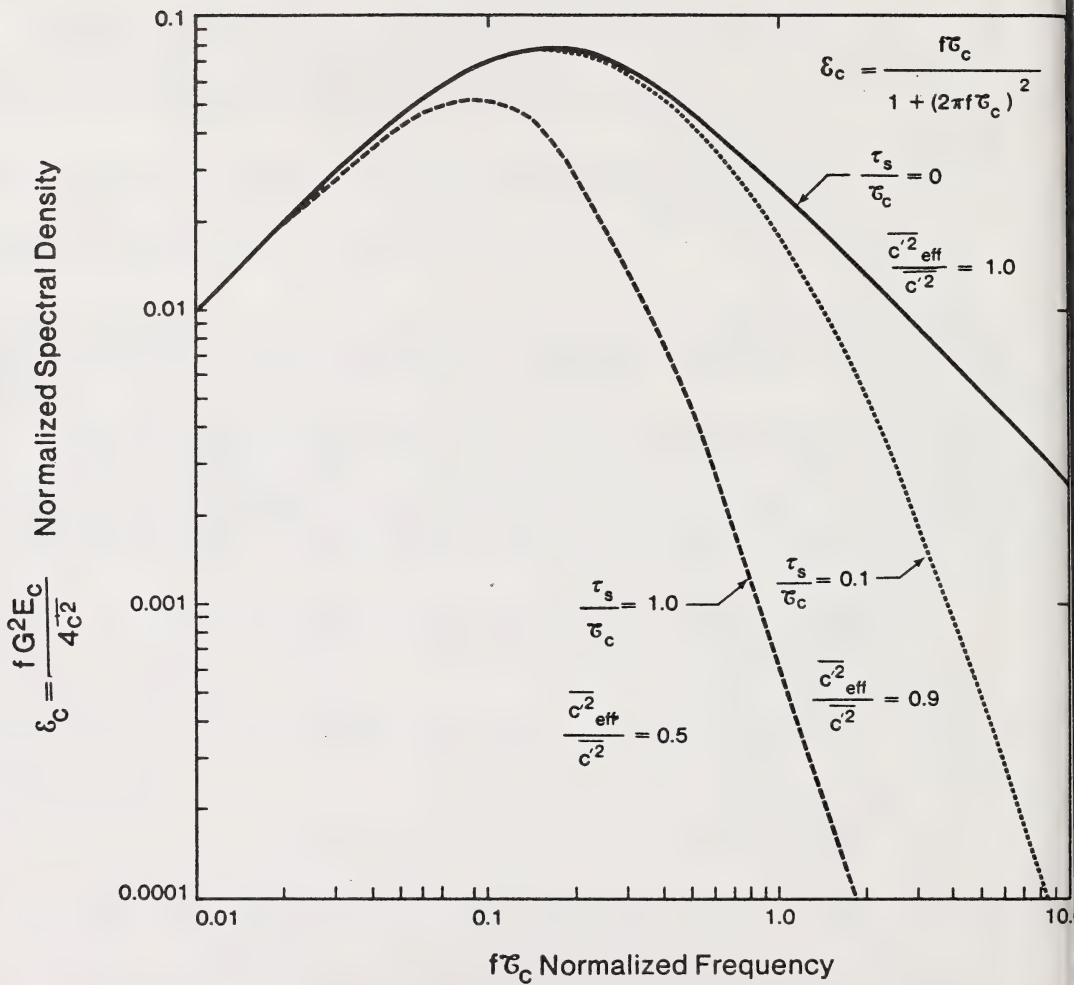


Figure A1 Attenuation of the High Frequency End of the Concentration Fluctuation Spectrum by Receptor Time Response.

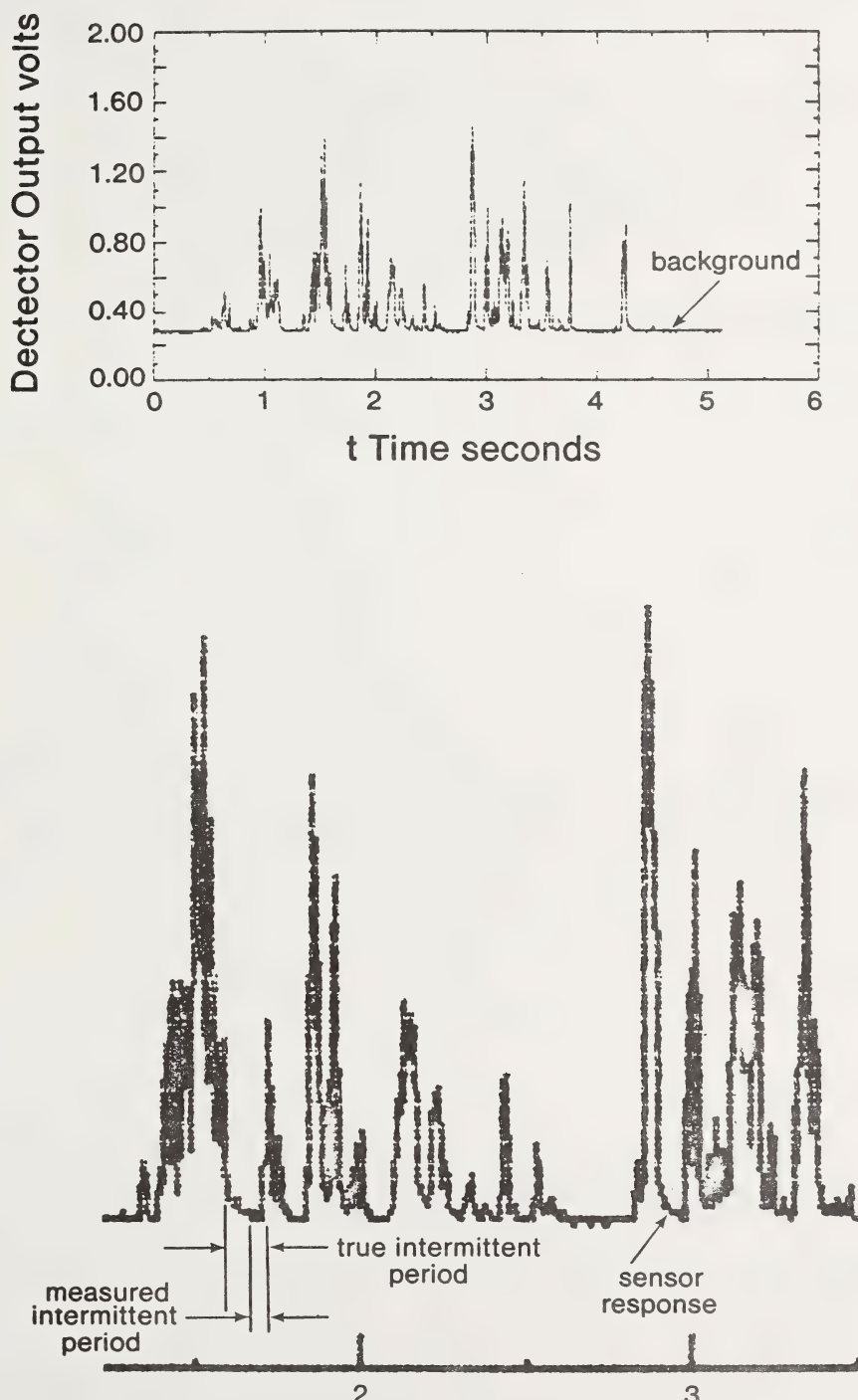
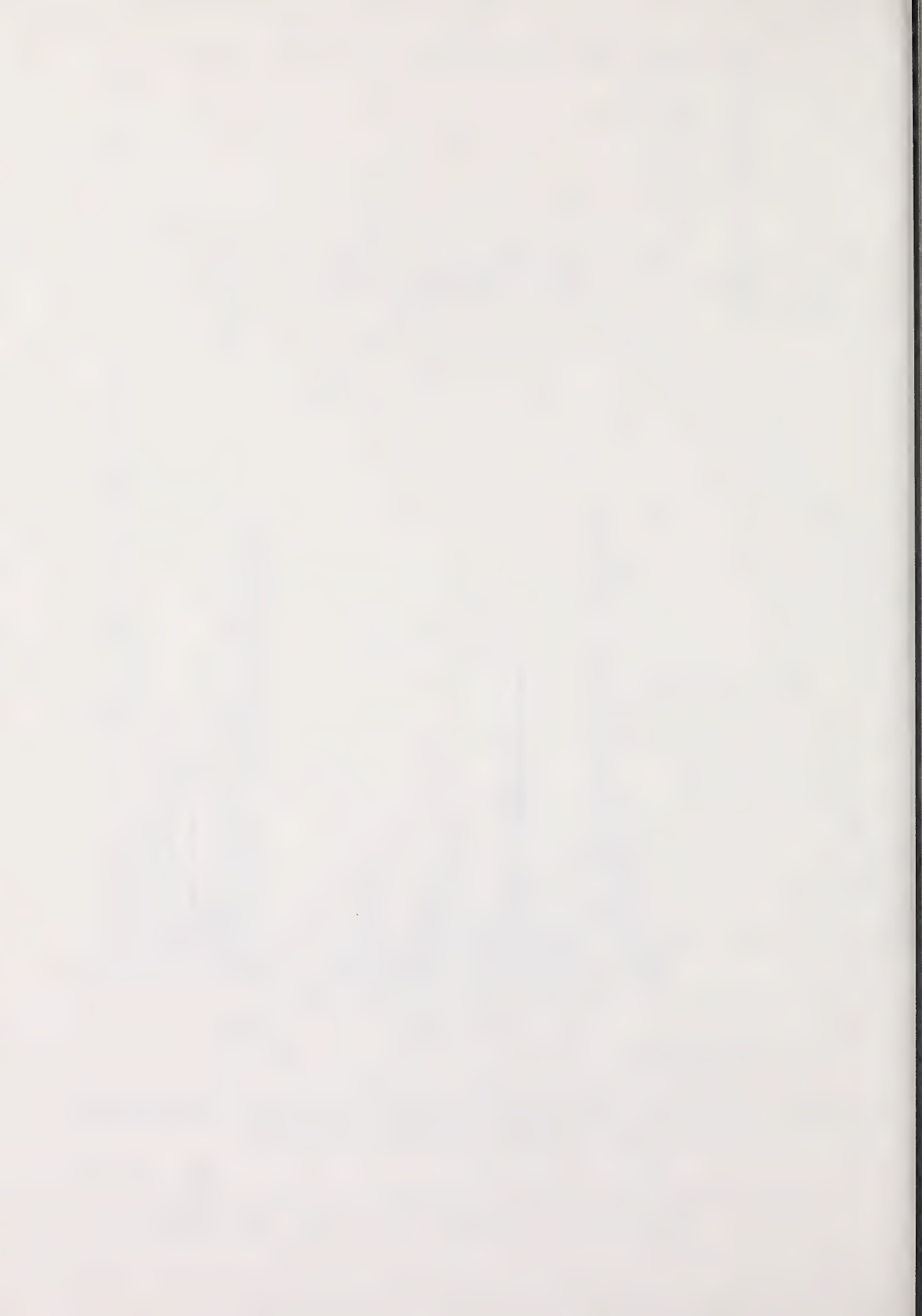


Figure A2 Influence of Sensor Response on Observed Intermittency in Water Channel Simulation of the Plume from a Ground Level Source.



APPENDIX B

UNIVERSAL GROUND LEVEL PROFILES OF MEAN AND FLUCTUATING CONCENTRATION

The objective of this note will be put the along-wind variations of mean concentration and fluctuation intensities in terms of the single dimensionless plume spread parameter λ , where

$$\lambda \equiv \frac{\sqrt{\sigma_y \sigma_z}}{H} \quad (B1)$$

and H is the boundary layer thickness.

Mean Concentration

For a Gaussian plume with plume spreads in the form of power laws.

$$\sigma_y = D_y x^a \quad (B2)$$

$$\sigma_z = D_z x^a \quad (B3)$$

Pasquill (1974, p.273) and Weil and Jepson (1977) find the maximum ground level concentration c_{om} for a given windspeed U and constant source height h to be

$$c_{om} = \frac{Q}{\pi \exp(\frac{\epsilon}{2}) Uh^\epsilon} \cdot \frac{(D_z \sqrt{\epsilon})^\epsilon}{D_z D_y} \quad (B4)$$

at the downwind location x_m

$$x_m = \left[\frac{h}{D_z \sqrt{\epsilon}} \right]^{1/a_z} \quad (B5)$$

$$\text{where } \epsilon = 1 + \frac{a_y}{a_z} \quad (B6)$$

The alongwind variation of ground level mean concentration on the plume axis is given by the normalized equation

$$\frac{c_0}{c_{om}} = \frac{1}{(\frac{x}{x_m})^{a_z}} \exp \left[-\frac{\epsilon}{2} \left(\left(\frac{x}{x_m} \right)^{-2a_z} - 1 \right) \right] \quad (B7)$$

given by Weil and Jepson (1977). These equations can be transformed to plume co-ordinates by combining (B1), (B2) and (B3) to write

$$\lambda^2 = \frac{D_y D_z}{H^2} x^{a_y + a_z} \quad (B8)$$

Then, evaluating (B8) at x_m , the position of maximum mean concentration, to find λ_m

$$\lambda_m^2 = \frac{D_y D_z}{H^2} x_m^{a_y + a_z} \quad (B9)$$

Combining this with (B5)

$$\lambda_m^2 = \frac{D_y D_z}{H^2} \left[\frac{h}{D_z \sqrt{\epsilon}} \right]^{\frac{a_y + a_z}{a_z}}$$

from which

$$\lambda_m = \frac{(D_y D_z)^{0.5}}{H} \left[\frac{h}{D_z \sqrt{\epsilon}} \right]^{\frac{\epsilon}{2}} \quad (B10)$$

Taking the ratio of (B8) to (B9) yields

$$\frac{x}{x_m} = \left(\frac{\lambda}{\lambda_m} \right)^{\frac{2}{a_y + a_z}} \quad (B11)$$

Using this to transform (B7) gives the normalized mean concentration as

$$\frac{c_0}{c_{om}} = \frac{1}{\left(\frac{\lambda}{\lambda_m} \right)^2} \exp \left[- \frac{\epsilon}{2} \left(\left(\frac{\lambda}{\lambda_m} \right)^{-\frac{4}{\epsilon}} - 1 \right) \right] \quad (B12)$$

By solving (B9) for $D_y D_z$ and inserting the result in (B4), the maximum ground level concentration may be expressed as a function of λ_m

$$c_{om} = \frac{Q}{\pi \exp(\frac{\epsilon}{2}) U \lambda_m^2 H^2} \quad (B13)$$

The appearance of the boundary layer thickness, H , is a result of the definition of λ , which uses H as a normalizing factor. Wilson, Fackrell and Robins (1982) suggest that in neutral stability $H \approx 650$ m. In terms of the neutrally stable log-law surface roughness Z_0 they recommend, as a rough estimate

$$H \approx 2500 Z_0 \quad (B14)$$

While the value of H will affect the shape of the alongwind concentration

profile because it changes the scaling between λ and x in (B9), it has no effect on the maximum concentration c_{om} because $\lambda_m^2 H^2 = \sigma_{ym} \sigma_{zm}$, which has no direct dependence on H .

Fluctuation Intensity

The square of the fluctuation intensity is given by

$$i^2 = \left(\frac{q}{Q}\right)^2 \frac{\frac{G_v(\frac{y}{\sigma_y})}{\sigma_y} F_v(\frac{z}{\sigma_z})}{\left[\frac{G_M(\frac{y}{\sigma_y})}{\sigma_y} F_M(\frac{z}{\sigma_z})\right]^2} \quad (B15)$$

At ground level, where $z = 0$ the vertical and crosswind distribution functions reduce to

$$F_M(0) = \exp \left[-\frac{h^2}{2\sigma_z^2} \right] + \exp \left[-\frac{h^2}{2\sigma_z^2} \right] \quad (B16)$$

$$G_M(\frac{y}{\sigma_y}) = \exp \left[-\frac{y^2}{2\sigma_y^2} \right] \quad (B17)$$

$$F_v(0) = \exp \left[-\frac{h_v^2}{2\sigma_z^2} \right] - \alpha \exp \left[-\frac{h_v^2}{2\sigma_z^2} \right] \quad (B18)$$

$$G_v(\frac{y}{\sigma_y}) = \frac{1}{2} \exp \left[-\frac{1}{2} \left(\frac{y}{\sigma_y} - \phi \right)^2 \right] + \frac{1}{2} \exp \left[-\frac{1}{2} \left(\frac{y}{\sigma_y} + \phi \right)^2 \right] \quad (B19)$$

The effective height, h_v , of the variance source in (B18) is

$$h_v = \left(h^2 + \phi_z^2 \sigma_z^2 \right)^{0.5} \quad (B20)$$

Using (B20) in (B18), and then taking the ratio of (B18) to the square of (B16)

$$\frac{F_v(0)}{[F_M(0)]^2} = \left(\frac{1-\alpha}{4}\right) \exp \left[-\frac{h^2}{2\sigma_z^2} - \frac{\phi_z^2}{2} \right] \quad (B21)$$

The ratio of crosswind distribution functions from (B19) and (B17) is

$$\frac{G_v \left(\frac{y}{\sigma_y}\right)}{\left[G_M \left(\frac{y}{\sigma_y}\right)\right]^2} = \frac{1}{2} \exp \left[-\frac{y^2}{2\sigma_y^2} - \frac{\phi^2}{2} \right] \left(\exp \left[\phi \frac{y}{\sigma_y} \right] + \exp \left[-\phi \frac{y}{\sigma_y} \right] \right) \quad (B22)$$

Using these in (B15)

$$\begin{aligned} i^2 \Big|_{z=0} &= \left(\frac{q}{Q}\right)^2 \exp \left[-\frac{h^2}{2\sigma_z^2} - \frac{\phi_z^2}{2} \right] \exp \left[-\frac{y^2}{2\sigma_y^2} - \frac{\phi^2}{2} \right] \left(\frac{1-\alpha}{8} \right) \cdot \\ &\quad \boxed{\rightarrow \left(\exp \left[\phi \frac{y}{\sigma_y} \right] + \exp \left[-\phi \frac{y}{\sigma_y} \right] \right)} \end{aligned} \quad (B23)$$

The ratio h/σ_z can be expressed in terms of plume size λ by writing (B5) as

$$h = \sqrt{\varepsilon} D_z x_m^{a_z} \quad (B24)$$

Using σ_z from (B3) the ratio is

$$\frac{h}{\sigma_z} = \sqrt{\varepsilon} \left(\frac{x_m}{x} \right)^{a_z} \quad (B25)$$

Then using the relation between x and λ in (B11)

$$\frac{h}{\sigma_z} = \sqrt{\varepsilon} \left(\frac{\lambda_m}{\lambda} \right)^{\frac{2}{\varepsilon}} \quad (B27)$$

Using this (B23) becomes

$$i^2 \Big|_{z=0} = \left(\frac{q}{Q} \right)^2 \exp \left[\frac{\varepsilon}{2} \left(\frac{\lambda_m}{\lambda} \right)^{\frac{4}{\varepsilon}} - \frac{\phi_z^2}{2} \right] \exp \left[\frac{y^2}{2\sigma_y^2} - \frac{\phi^2}{2} \right] \left(\frac{1-\alpha}{8} \right) \cdot \boxed{\rightarrow \left(\exp \left[\phi \frac{y}{\sigma_y} \right] + \exp \left[-\phi \frac{y}{\sigma_y} \right] \right)} \quad (B28)$$

Then, along the plume centerline where $y = 0, i = i_0$ the axis ground level intensity, from (B28)

$$i_0^2 = \left(\frac{q}{Q} \right)^2 \exp \left[\frac{\varepsilon}{2} \left(\frac{\lambda_m}{\lambda} \right)^{\frac{4}{\varepsilon}} - \frac{\phi_z^2}{2} \right] \exp \left(-\frac{\phi^2}{2} \right) \left(\frac{1-\alpha}{4} \right) \quad (B29)$$

Conditional Fluctuation Intensity and Intermittency

Far above the influence of ground surface effects, the conditional fluctuation intensity i_{p^∞} is constant across a plume cross section at a fixed x (or λ) location. It is given by

$$i_{p^\infty}^2 = \left(\frac{q}{Q} \right)_\infty^2 \exp \left(-\frac{\phi^2}{2} \right) \quad (B30)$$

where the variance source strength is given by

$$\left(\frac{q}{Q} \right)_\infty = \left[\frac{0.337 \lambda}{\lambda^2 + (0.119)^2} \right] \exp \left(\frac{\phi^2}{4} \right) \quad (B31)$$

The effect of the receptor height z above ground level on the conditionally averaged fluctuation intensity i_p is given by

$$i_p^2 = i_{p^\infty}^2 \frac{\left[1 - \alpha \exp \left[-2 \left(\frac{h}{\sigma_z} \right) \left(\frac{z}{\sigma_z} \right) \right] \right]}{\left[1 + \exp \left[-2 \left(\frac{h}{\sigma_z} \right) \left(\frac{z}{\sigma_z} \right) \right] \right]^2} \quad (\text{B32})$$

At $z = 0$ this reduces to the simple result that

$$i_p^2 \Big|_{z=0} = i_{p^\infty}^2 \left(\frac{1-\alpha}{4} \right) \quad (\text{B33})$$

The plume intermittency may be computed from the general relationship

$$\gamma = \frac{i_p^2 + 1}{i^2 + 1} \quad (\text{B34})$$

Variance Source Strength

The source strength is given by

$$\frac{q}{Q} = \left(\frac{0.337 \lambda}{\lambda^2 + \lambda_0^2} \right) \exp\left(\frac{\phi^2}{4}\right) \quad (\text{B35})$$

with the virtual origin for fluctuations at λ_0 ,

$$\lambda_0 = \frac{0.119}{1 + 0.033 \frac{z_e}{d}} \quad (\text{B36})$$

with the reference height z_e given by

$$\frac{z_e}{d} = \frac{h}{d} \exp \left[- \left(\frac{\sigma_z}{h} \right)^2 \right] \quad (\text{B37})$$

This can be expressed in terms of the plume size parameter λ by using

(B27)

$$\frac{z_e}{d} = \frac{h}{d} \exp \left[-\frac{1}{\varepsilon} \left(\frac{\lambda}{\lambda_m} \right)^{\frac{4}{\varepsilon}} \right] \quad (B38)$$

From this we see that the only parameter other than λ and λ_m needed to characterize the normalized alongwind mean and fluctuating concentration on the plume axis, is the source height to diameter ratio h/d in (B38). The value of λ_m is computed from source height h and the plume spread constants using (B10).

APPENDIX C

LENGTH AND TIME SCALES OF CONCENTRATION FLUCTUATIONS

The time scale of concentration fluctuations is defined by

$$\bar{\tau}_c = \int_0^{\infty} R_c(t') dt' \quad (C1)$$

Because intermittency is like a square wave distribution superposed on plume fluctuations, the random frequency of the intermittency will be superposed on the plume fluctuations, and contribute to both spectrum and scale. For this reason we use $c^{-\frac{1}{2}}$ rather than the conditional average $c_p^{-\frac{1}{2}}$ to characterize scale.

The spectrum and correlation are related by the Fourier integral transform

$$E_c(f) = 4c^{-\frac{1}{2}} \int_0^{\infty} R_c(t') \cos(2\pi ft') dt' \quad (C2)$$

The time scale may be obtained from the zero frequency intercept of the spectrum, obtained experimentally by extrapolating to $f = 0$, and in (C2) simply by setting $f = 0$ to obtain; noting $\cos(0) = 1.0$.

$$\begin{aligned} E_c(0) &= 4c^{-\frac{1}{2}} \int_0^{\infty} R_c(t') dt' \\ &= 4c^{-\frac{1}{2}} \bar{\tau}_c \end{aligned} \quad (C3)$$

Assuming frozen turbulence, convected by at the local mean velocity U , we can define a length scale Λ_c

$$\Lambda_c \equiv \bar{\tau}_c U \quad (C4)$$

Unlike the Eulerian time scale \bar{J}_c which becomes shorter as the convection velocity U increases, the length scale Λ_c measures the physical size of concentration eddies, and remains constant at a given location in the plume. Combining (C3) and (C4)

$$\Lambda_c = \frac{E_c(0) \cdot U}{c^{\frac{1}{2}}} \quad (C5)$$

Variation of Length Scale Across a Plume

Because only a few measurements of length scale are available from the wind tunnel data of Fackrell and Robins (1982), a semi-empirical model must be developed to interpolate between, and extrapolate from existing data. Before proposing a model, it is worthwhile reviewing Fackrell and Robins observations of concentration scale for a ground level and elevated source. Their data has been transformed from a normalized time scale $\bar{J}_c U_H / H$ to length scale Λ_c / H by using (C4) and the mean velocity profile in their boundary layer. The data on the plume centerline $y = 0$ is presented in Figures C1 and C2 for the ground level and elevated sources. The measurements have more scatter than the mean \bar{c} and variance $c^{\frac{1}{2}}$ measurements, emphasizing the difficulty of measuring turbulence scale. This scatter is due to the long sampling periods required to define the low frequency end of the spectrum needed for extrapolation to get $E_c(0)$ in (C5). In spite of this, three features are clear:

- 1) The small scale turbulence and mean wind shear near the ground surface dissipates and smears out the small scale concentration eddies in the plume. This leaves only large scale fluctuations and causes the dramatic increase in Λ_c near the surface.

- 2) Far above the surface dissipation effects, where either z/σ_z or h/σ_z is large, the length scale remains relatively constant across a plume cross section at a fixed downwind distance. Measurements at varying crosswind y/σ_y locations confirm this.
- 3) The scale Λ_c away from the influence of surface effects increases gradually with downwind distance as the plume spread becomes larger.

The effect of surface dissipation on the variance is accounted for by a variance sink term in the Gaussian model for \bar{c}^2 . Because these surface effects decrease \bar{c}^2 while increasing the scale Λ_c , we will assume in the model that the effects are directly related through their effect on the spectrum.

As a physical model of the relationship between Λ_c and \bar{c}^2 we assume that the decreasing turbulence scale and the increasing mean wind shear dU/dz near the surface act only on the smaller concentration eddies, leaving the large eddies at the low frequency end of the spectrum unaffected. Because these surface related dissipation effects act only on the high frequency end of the spectrum, the zero frequency intercept $E_c(0)$ should be the same at all heights above ground when normalized by \bar{c}^2 , the square of the mean concentration. Then (C5) can be written as

$$\frac{E_c(0) U}{\bar{c}^2} = \frac{4\bar{c}^2 \Lambda_c}{\bar{c}^2} \quad (C6)$$

which is constant. Equating values far above the ground where surface dissipation effects are negligible this leads to

$$i^2 \Lambda_c = i_\infty^2 \Lambda_{c\infty} \quad (C7)$$

where the subscript " ∞ " refers to the same location but with the ground plane and surface dissipation effects removed, and "i" is the fluctuation intensity

$$i = \frac{\sqrt{i^2}}{\frac{c}{\bar{c}}} \quad (C8)$$

Wilson (1982) gives the ground surface dissipation effect on the fluctuation intensity as

$$\frac{i}{i_\infty} = \frac{\left[1 - \alpha \exp \left(-2 \frac{h_v z}{\sigma_z^2} \right) \right]^{0.5}}{\left[1 + \exp \left(-2 \frac{h_v z}{\sigma_z^2} \right) \right]} \quad (C9)$$

where h_v is the effective variance source height, which is related to the actual source height by

$$h_v = \left[h^2 + \phi_z^2 \sigma_z^2 \right] \quad (C10)$$

The values of $\phi_z = 0.706$ and $\alpha = 0.6$ were derived by Wilson, Robins, and Fackrell (1982) from experiment. Using (C9) in (C7) gives the scale ratio as

$$\frac{\Lambda_c}{\Lambda_{c\infty}} = \frac{\left[1 + \exp \left(-2 \frac{h_v z}{\sigma_z^2} \right) \right]^2}{\left[1 - \alpha \exp \left(-2 \frac{h_v z}{\sigma_z^2} \right) \right]} \quad (C11)$$

It is interesting to note that regardless of source height, the ground level concentration fluctuation scale at $z = 0$ always takes on the constant values of

$$\left. \frac{\Lambda_c}{\Lambda_{c^\infty}} \right|_{z=0} = \frac{4}{(1-\alpha)} \quad (C12)$$

For $\alpha = 0.6$ this ratio is exactly 10.0, a very large increase indeed.

Alongwind Variation of Concentration Scale

The variation of concentration scale with downwind distance is a complex process in which the turbulence scales of the velocity fluctuations $\overline{u^2}$, $\overline{v^2}$ and $\overline{w^2}$ interact with source size effects and decay of concentration fluctuations to produce the scale Λ_c . Sirivat and Warhaft (1982) measured the decay of concentration variance of tracer gas injected uniformly from a plane source in grid turbulence. They found that the variance decay rate was a function of the ratio of concentration length scale to velocity length scale, showing the interaction. The semi-empirical model proposed here is

$$\frac{\Lambda_{c^\infty}}{H} = B_2(\lambda + \lambda_0) \quad (C13)$$

The effect of velocity fluctuation scale is contained implicitly in λ because

$$\lambda = \frac{\sqrt{\sigma_y \sigma_z}}{H} \quad (C14)$$

and by dimensional reasoning the plume spreads σ_y and σ_z contain the velocity fluctuation length scales Λ_v and Λ_w and turbulence intensities

$$\sigma_y = \left(\frac{\sqrt{v'2}}{U_c} \right)^{a_y} (B_0 \Lambda_v)^{1-a_y} x^{a_y} \quad (C15)$$

and

$$\sigma_z = \left(\frac{\sqrt{w'2}}{U_c} \right)^{a_z} (B_0 \Lambda_w)^{1-a_z} x^{a_z} \quad (C16)$$

where B_0 is the Lagrangian-Eulerian constant. Source size effects are contained in the virtual origin term λ_0 , which is assumed to be the same function used for the along-wind changes in c'^2 . From Wilson (1982), the virtual origin is

$$\lambda_0 \equiv \frac{\sqrt{\sigma_{y0}\sigma_{z0}}}{H} \quad (C17)$$

$$\lambda_0 = \frac{0.119}{1 + 0.033 \frac{z_e}{d}} \quad (C18)$$

The ratio of reference height, z_e , to source diameter, d is

$$\frac{z_e}{d} = \frac{h}{d} \exp \left[- \left(\frac{\sigma_z}{h} \right)^2 \right] \quad (C19)$$

From the definition of λ and λ_0 we see that the concentration length scale Λ_c is not a direct function of the boundary layer thickness H . Equation (C13) can be written using (C14) and (C17) as

$$\Lambda_{c_\infty} = B_2 (\sqrt{\sigma_y \sigma_z} + \sqrt{\sigma_{y0} \sigma_{z0}}) \quad (C20)$$

with no dependence on H , and no explicit dependence on turbulent velocity scale Λ_u , Λ_v or Λ_w .

Comparison With Measurements

Using the data of Fackrell and Robins (1982) from Figures C1 and C2, corrections were applied from (C12) to estimate the scale Λ_{c_∞} for each vertical profile of Λ_c . These values are shown in Figure C3 along with the linear correlation equation. The data suggests that $B_1 = 2.0$ and $B_2 = 0.34$. This figure shows that considerably more uncertainty exists in predicting concentration length scale Λ_c , than in estimating the variance $c^{\frac{1}{2}}$. The final form for estimating scale is

$$\frac{\Lambda_{c_\infty}}{H} = 0.34 (\lambda + \lambda_0) \quad (C21)$$

Using this equation and (C12) vertical profiles of scale Λ_c were calculated, and the predictions are compared with the measurements in Figures C4 and C5. Considering the scatter in the data, the agreement is satisfactory.

Using the semi-empirical theory of (C12) and (C21), concentration fluctuation length scales near the ground can be estimated. However, an uncertainty of about a factor of two may be expected due to data scatter and the use of variance source location and dissipation constants λ_0 from (C18), $\alpha = 0.6$ and $\phi_z = 0.706$. These empirical constants were derived for the variance field to predict $c^{\frac{1}{2}}$, and refined values may be required to optimize their use for both $c^{\frac{1}{2}}$ and Λ_c estimation.

Finally, it should be noted that the behaviour of the concentration and

and velocity length scales near the ground is quite different. The high intensity small scale eddies that are produced by the mean flow wind shear dU/dz near the ground decrease the turbulent velocity scales Λ_u , Λ_v and Λ_w , as shown in Figure C6. At the same time, these mean wind shear and small scale velocity eddies are dissipating concentration fluctuations and increasing the concentration scale Λ_c . Comparing Figure C6 to Figure C1 and C2 clearly shows the different effect of the flow near the ground on velocity and concentration scales.

So far we have considered only the spatial variation of length scale Λ_c for some unspecified sampling time interval. Because these estimates use the wind tunnel data of Fackrell and Robins, the sampling time is probably about 3 to 30 minutes in the full scale atmosphere. We expect that as the sampling time interval T_s increases that the crosswind meandering of the plume will generate low frequency fluctuations that will increase the concentration time scale $\bar{\tau}_c$. These effects are discussed in Appendix D.

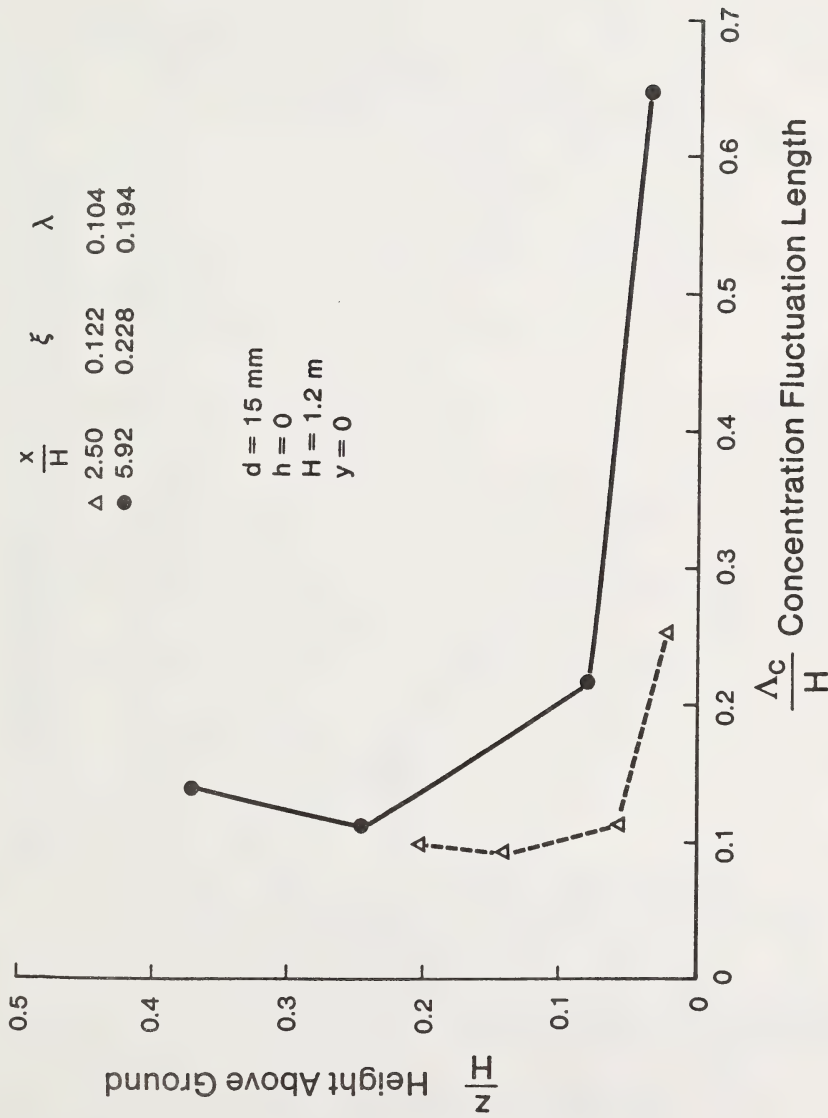


Figure C1 Concentration length scales on plume centerline for a ground level source with $d = 15 \text{ mm}$, in boundary layer thickness $H = 1.2 \text{ m}$.

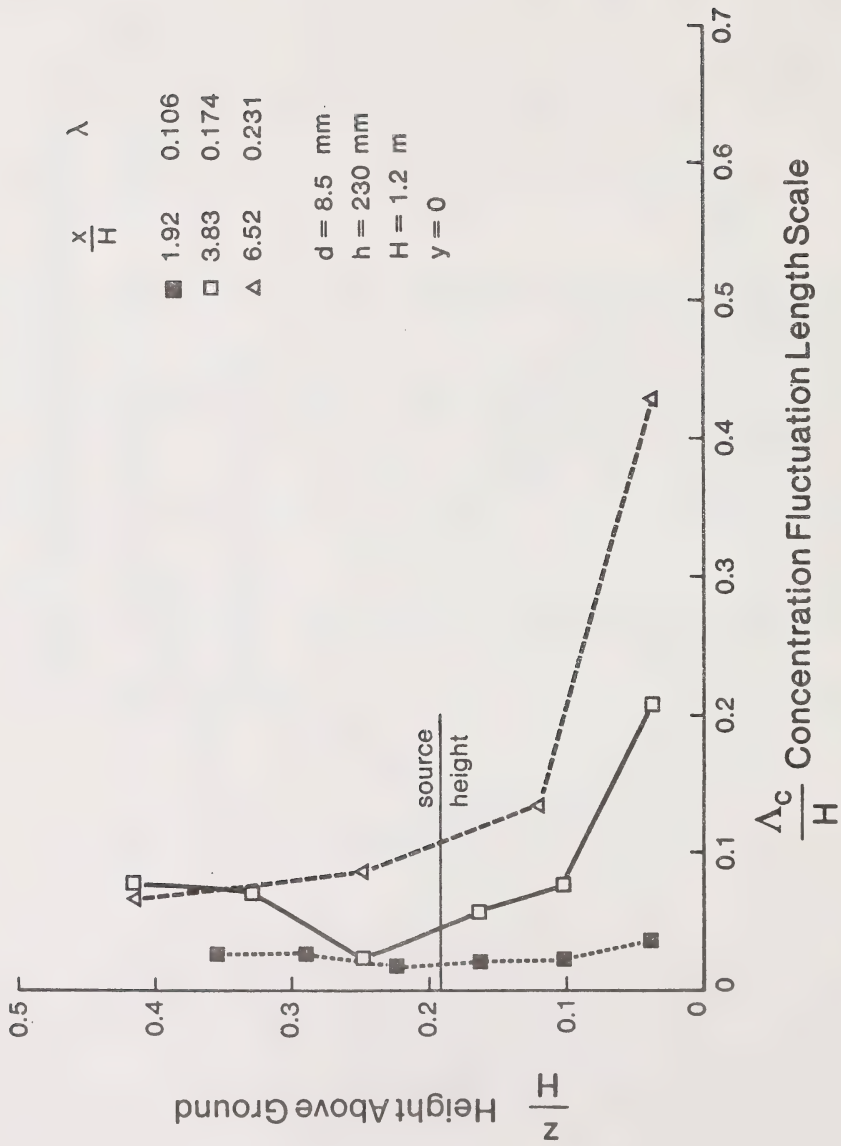


Figure C2 Concentration length scales for an elevated source with $h/H = 0.192$, $d = 8.5 \text{ mm}$ in $H = 1.2 \text{ m}$.

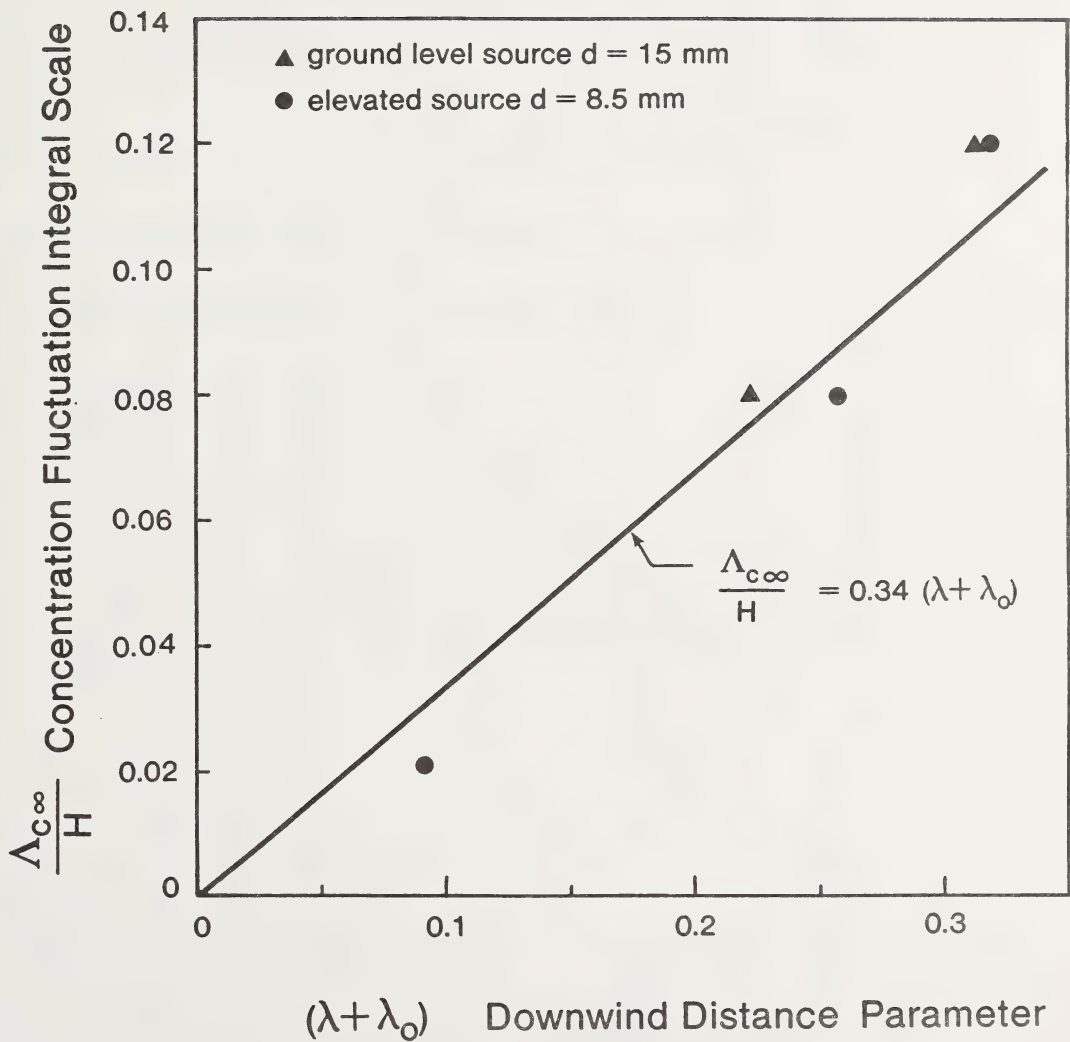


Figure C3 Along-wind variation of concentration length scale $\Lambda_{c\infty}$ above ground surface dissipation region.

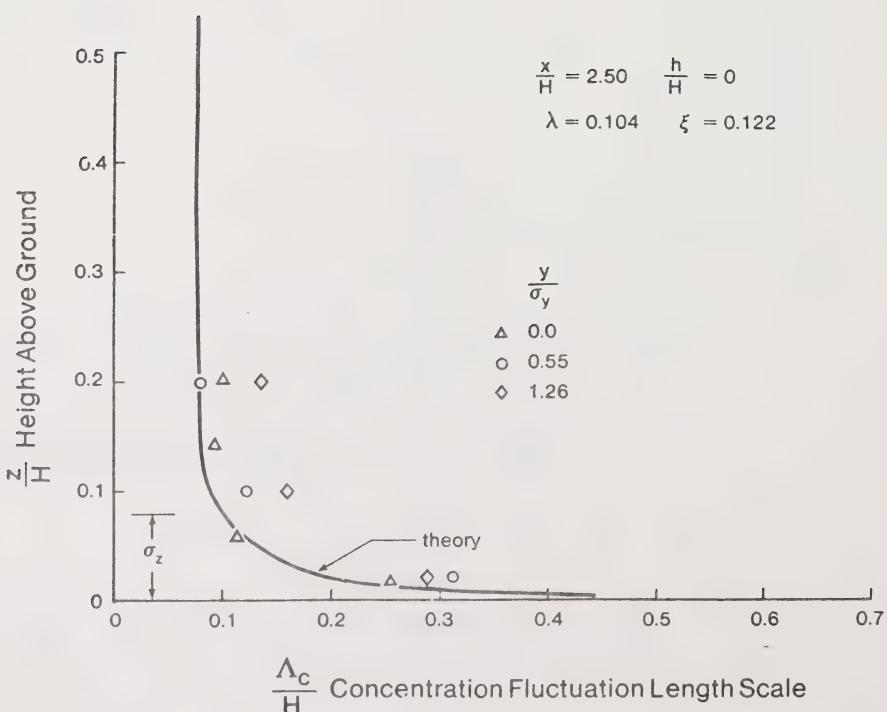
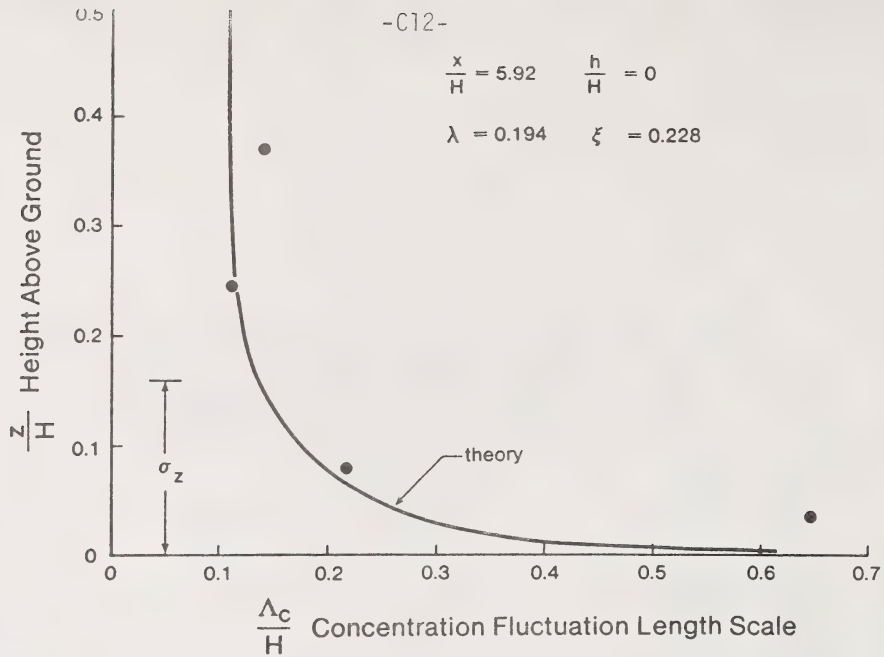


Figure C4 Ground level source: Comparison of concentration length scales with predictions for $h/H = 0$, $d = 15$ mm, $H = 1.2$ m.

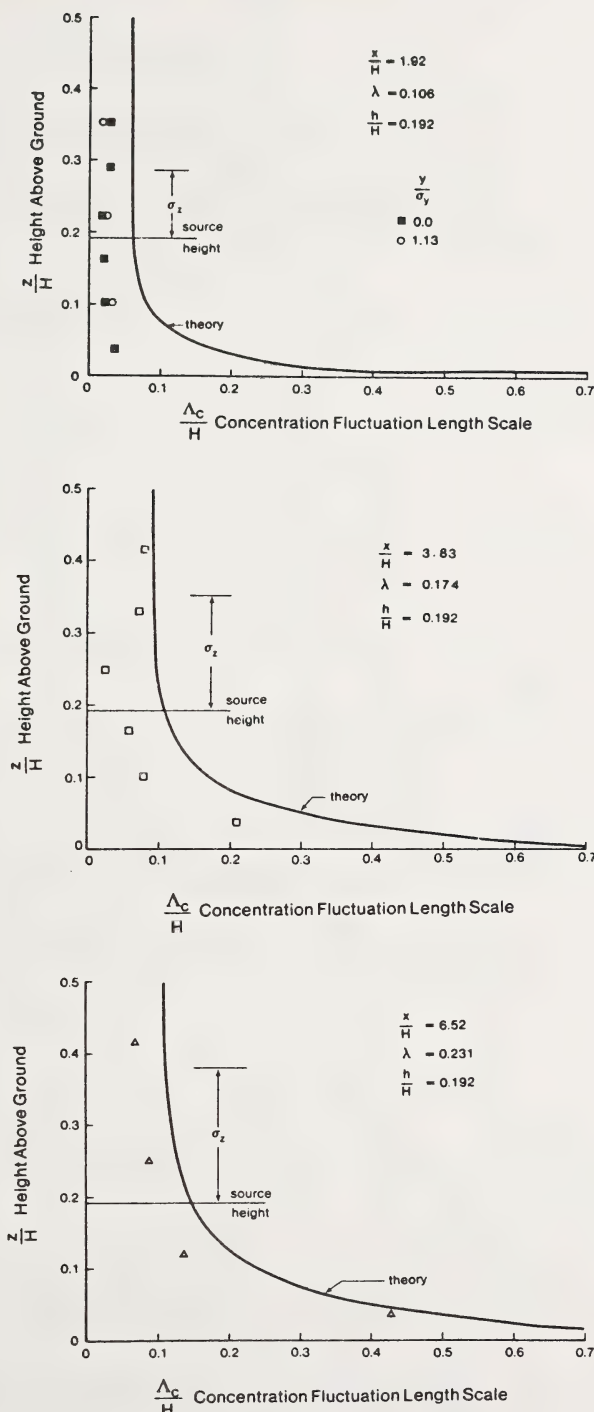


Figure C5 Elevated source: Comparison of concentration length scales with predictions for $h/H = 0.192$, $d = 8.5$ mm, $H = 1.2$ m.

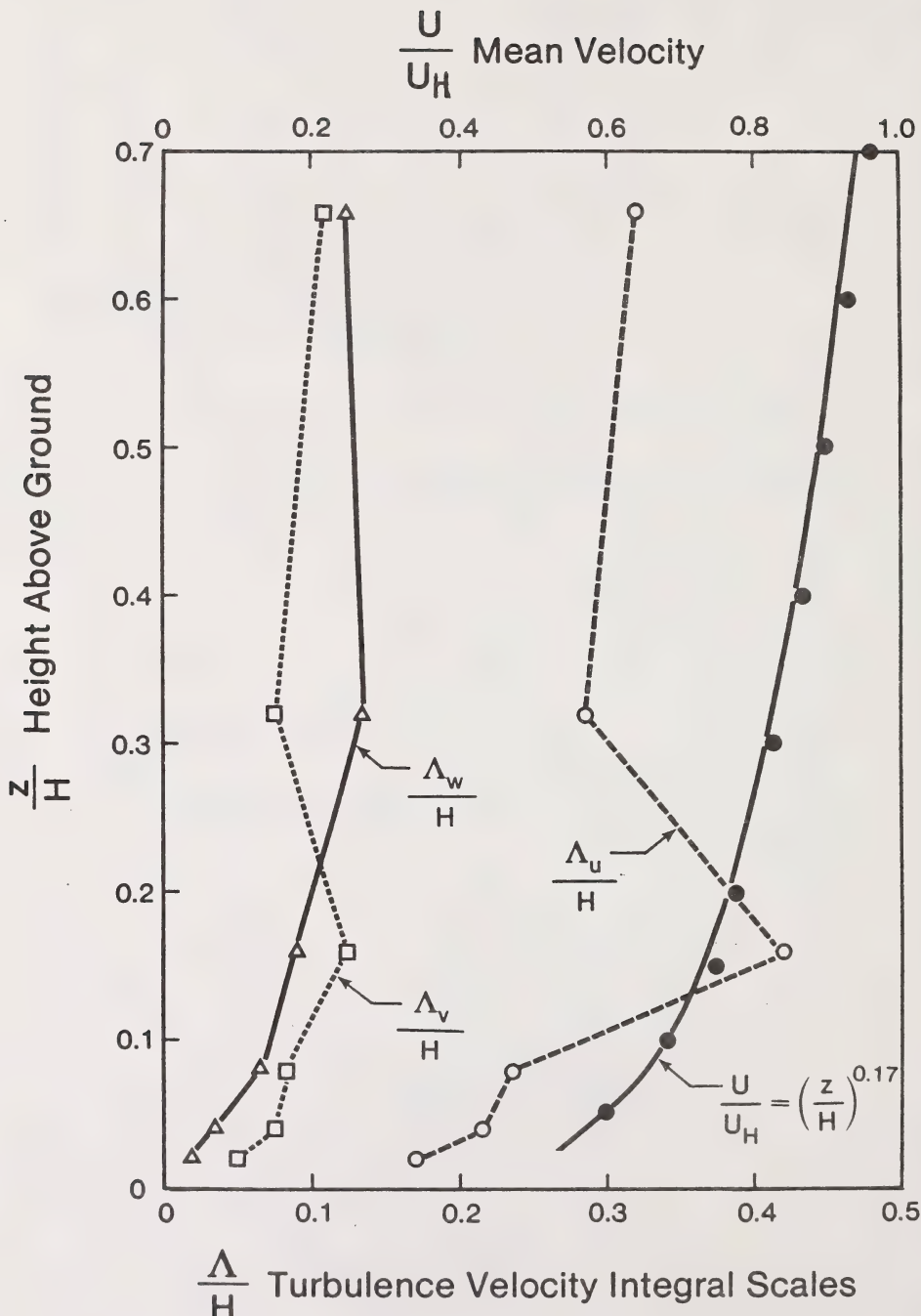


Figure C6 Turbulence velocity length scales and mean velocity profile for wind tunnel boundary layer of Fackrell and Robins (1982).

APPENDIX D

EFFECT OF WIND DIRECTION MEANDERING ON MEAN AND FLUCTUATING CONCENTRATION

As the sample time over which concentrations are observed goes up, the mean concentration goes down due to increased meandering caused by large scale atmospheric turbulence. The decrease in mean concentration continues even at long sample times when the plume has sampled all the large scale atmospheric turbulence. This long term decrease in concentration is caused by shifts in mean wind direction which force the plume centerline to meander back and forth over a fixed receptor location.

Wind tunnel data of plume dispersion and concentration fluctuation, on which the theory in this report is based, is incapable of simulating the plume centre line meandering caused by the two effects of large scale atmospheric turbulence and changing mean wind direction. The wind tunnel data of Fackrell and Robins is limited by the available turbulence scales to simulation of full scale sample times 3 to 30 minutes. This short full scale sample time is appropriate for estimating the risk of exposure to peak concentrations in short term accidental releases, such as a pipeline rupture. However, the long term exposure of plants and animals to pollution from a continuous industrial source cannot be accurately estimated using the theories developed from these wind tunnel simulations. In this appendix we will develop a method for extrapolating predictions from short sample periods to longer exposure times typical of continuous sources. This sampling time T_s for wind meandering will be used to account for the non-stationary decrease in mean \bar{c}_T and variance $c_T^{1/2}$. This effect must be combined with

the variance smoothing caused by sample averaging time T_a for the stationary statistics which have a constant mean \bar{c} for all T_a .

Accounting for Long Sampling Time by Increased Crosswind Spreading

One widely used method of accounting for sampling time is to assume that for samples longer than three minutes the vertical spread remains constant, while the crosswind spread increases as some empirical power function of sample time. For any fixed receptor location under an elevated plume with an effective source height h , ground level mean concentration on the plume centre line is given by

$$\bar{c}_0 = \frac{Q}{\pi U_c \sigma_y \sigma_z} \exp \left[-\frac{h^2}{2\sigma_z^2} \right] \quad (D1)$$

For averaging time T_s , the crosswind spread σ_y is usually assumed to be proportional to averaging time raised to some power, p .

$$\frac{\sigma_y T}{\sigma_{y, \text{ref}}} = \left(\frac{T_s}{T_{s,\text{ref}}} \right)^p \quad (D2)$$

while the vertical spread σ_z remains constant. This model produces the empirically observed result that the mean concentration sample over T_s behaves like

$$\bar{c}_{0T} \propto \frac{1}{T_s^p} \quad (D3)$$

Unfortunately, this approach leads to serious difficulties when it is applied to concentration fluctuation statistics. The difficulty becomes apparent when the plume intermittency is calculated. The intermittency is directly related to the fluctuation intensities by

$$\gamma = \frac{i_p^2 + 1}{i^2 + 1} \quad (D4)$$

which is valid for all sampling times. On the plume axis both the conditional (plume) intensity i_p and the total intensity i of concentration fluctuations depends only on the ratio of variance source strength to mean source strength, and is completely independent of σ_y or σ_z . Using the increased crosswind spread model to account for sampling time, there should be no effect of sampling time on the observed plume intensities or on the intermittency γ . This result is clearly incorrect because we know by observing long time records of full scale concentration that the plume becomes increasingly intermittent with time, as changes in mean wind direction cause the plume to meander back and forth across the receptor. Clearly, the use of increased crosswind spread is an incorrect model for the effects of sampling time.

The reason for the failure of an increased crosswind spread model is that as sampling time increases a plume will meander back and forth allowing a receptor to sample the outer edges of the short term plume fluctuations. Because the concentration statistics on the plume axis carry no information about the structure in the outer edges of the plume it is not possible to account for increased sampling time simply by adjusting crosswind spread and applying this to values computed on the axis. The outer edge of the plume has different turbulence structure than the plume axis, so turbulence properties such as intermittency γ will change as the receptor sees the fringes of the plume. In the following section we will present a more realistic model using crosswind averaging to allow the long term time average statistics to "sample" across the entire width of the plume.

Crosswind Integration to Simulate Long Sampling Times

The effect of increasing the sampling time T_s over which the mean concentration is measured is equivalent to allowing the short sample time plume to meander back and forth over the receptor. This exposes the receptor to the tails of the crosswind distributions of mean and fluctuating concentration, and changes both the mean and fluctuating statistics of the plume. Starting from the short term statistics \bar{c}_o , i_o , i_{p_o} and γ_o measured on the plume centerline for a short sample time T_{sref} the crosswind profiles of these parameters must be averaged to produce \bar{c}_{oT} , i_{oT} , i_{pT} and γ_{oT} for a longer sample time T_s . The following assumptions will be made to model the meandering:

- Correlations of effect of sampling time on full scale data use the maximum mean concentration \bar{c}_{oT} observed for a fixed sampling period T_s . To model these maximum values it will be assumed that the plume blows directly toward a receptor located on the plume centerline at $y = 0$.
- The effect of meandering is to expose the receptor to the entire crosswind profile of the short term plume. The probability that the receptor is exposed to the part of the short term plume located at $\pm y$ off the centerline is $p_m dy$, where the probability density p_m is assumed to be normally distributed.

$$p_m = \frac{1}{\sqrt{2\pi} \sigma_m} \exp \left[-\frac{1}{2} \left(\frac{y}{\sigma_m} \right)^2 \right] \quad (D5)$$

where σ_m is the crosswind meander standard deviation.

- The short term model, derived from wind tunnel measurements, represents a sampling time T_{sref} that is sufficiently long that increasing the sample time will cause no further vertical meandering. Thus, there will be no contribution from the vertical profile to long term meandering effects.
- The additional meander width σ_m acts only on the crosswind concentration profiles. The additional meander width must increase with increasing sample time, and $\sigma_m \rightarrow 0$ as $T_s \rightarrow T_{sref}$, where T_{sref} is the sample period of the short term plume model.

Using our assumption that the probability of observing any part of the short term plume is $p_m dy$, the crosswind average of any appropriate statistic represented by $A(y)$ is

$$A_T = \int_{-\infty}^{\infty} A(y) p_m(y) dy \quad (D6)$$

where A_T is the statistic for a sampling time T_s , and A is the same statistic for the short term sample T_{sref} . Our crosswind averaging model has a great deal in common with Gifford's (1959), (1960) classic fluctuating plume model for predicting peak to mean concentration ratios. There are, however, several fundamental differences between them:

- Gifford assumed an instantaneous gaussian plume profile with vertical and crosswind spreads σ_{zi} and σ_{yi} for sampling time $T_s = 0$. This instantaneous profile, which has no concentration fluctuations, is then allowed to meander over a long but unspecified sample time to produce a total spread that is

the sum of squares of instantaneous σ_{yi}^2 meandering σ_{ym}^2 components. The meandering component σ_{ym}^2 is zero at $T_s = 0$.

- The crosswind averaging method assumes that there is an existing model for the mean and fluctuation statistics, and that this existing model combines both the instantaneous and meandering components for some short sampling time T_{sref} . In the crosswind averaging model σ_m is the additional meandering caused by sampling for times longer than T_{sref} .

Because crosswind averaging relies on an experimentally based model for the short term plume, it should provide a more accurate extrapolation to longer sampling times than the meandering plume model with its hypothetical "instantaneous" profile which has no internal turbulent fluctuations. Sawford (1983) in a Monte-Carlo simulation of puff dispersion and the data of Fackrell and Robins (1982a), suggest that i and i_p may take on a finite value far downwind, rather than going to zero as the meandering component becomes negligible.

Another point that must be clarified is the definition of an "appropriate" statistic which can be crosswind averaged. The mean concentration \bar{c} and the intermittency γ (which represents the fraction of time the plume is present) are two variables which can be crosswind averaged. However, conditional statistics such as \bar{c}_p cannot be obtained by direct crosswind averaging, because the fraction of time they are present varies with crosswind position y . Also, ratios such as the fluctuation intensities i and i_p cannot be averaged because the average ratio is not the same as the ratio of the average value from which it is formed. To compute the average fluctuation intensity i_{OT}

it is first necessary to determine the crosswind averaged mean \bar{c}_{oT} and variance $\overline{c_{oT}^2}$ and use these in the definition

$$i_{oT} = \sqrt{\frac{\overline{c_{oT}^2}}{\bar{c}_{oT}}} \quad (D7)$$

Finally, we will show later than even the total variance $c^{-1/2}$, for which we have an explicit equation, cannot be directly crosswind averaged because each local variance at y is taken with respect to its local mean \bar{c} .

Crosswind Averaging of Mean Concentration

The crosswind concentration at any fixed height z is given by the Gaussian profile for the short sample time T_{sref} .

$$\bar{c} = \bar{c}_0 \exp \left[-\frac{1}{2} \left(\frac{y}{\sigma_y} \right)^2 \right] \quad (D8)$$

where \bar{c}_0 is the concentration on the plume centerline at $y = 0$. Integrating this across the plume using the meandering probability $p_m dy$ from (D5)

$$\bar{c}_{oT} = \int_{-\infty}^{\infty} \frac{\bar{c}_0}{\sqrt{2\pi} \sigma_m} \exp \left[-\frac{1}{2} \left(\frac{y}{\sigma_y} \right)^2 - \frac{1}{2} \left(\frac{y}{\sigma_m} \right)^2 \right] dy \quad (D9)$$

Combining terms and noting the function is symmetric about $y = 0$ produces the single sided integral

$$\bar{c}_{oT} = \sqrt{\frac{2}{\pi}} \frac{\bar{c}_0}{\sigma_m} \int_0^{\infty} \exp \left[- \left(\frac{\sigma_m^2 + \sigma_y^2}{\sigma_y^2 \sigma_m^2} \right) \frac{y^2}{2} \right] dy \quad (D10)$$

Defining a combined "spread" by

$$\sigma^2 = \frac{\sigma_y^2 \sigma_m^2}{\sigma_m^2 + \sigma_y^2} \quad (D11)$$

the crosswind average reduces to

$$\frac{\bar{c}_{OT}}{c_0} = \left[\frac{\sigma_y^2}{\sigma_m^2 + \sigma_y^2} \right]^{0.5} \sqrt{\frac{2}{\pi}} \frac{1}{\sigma} \int_0^\infty \exp \left[-\frac{1}{2} \left(\frac{y}{\sigma} \right)^2 \right] dy \quad (D12)$$

This integral is just the cumulative probability of all y locations and by definition is equal to unity. The crosswind averaged concentration reduces

$$\frac{\bar{c}_{OT}}{c_0} = \left[\frac{1}{\left(\frac{\sigma_m}{\sigma_y} \right)^2 + 1} \right]^{0.5} \quad (D13)$$

Crosswind Averaging of Intermittency

Intermittency is a particularly important parameter because much of the effect of increased sampling time on mean concentration is to reduce the intermittency factor γ by introducing more periods of zero concentration as meandering causes the receptor to see the fringes of the crosswind profile. Most of the reduction of \bar{c}_{OT} with longer T_s is caused by decreasing γ_{OT} . The conditional (plume) concentration \bar{c}_{PT} defined by

$$\bar{c}_{PT} = \frac{\bar{c}_T}{\gamma_T} \quad (D14)$$

remains relatively constant with increasing T_s . Using the definition of γ from (D4) we can write

$$\gamma = \gamma_0 \frac{1 + i_o^2}{1 + i^2} \quad (D15)$$

where γ_0 is the plume centerline concentration for the short term sample time T_{sref}

$$\gamma_0 = \frac{1 + i_p^2}{1 + i_o^2} \quad (D16)$$

For a single variance source the source pair spacing is $\phi = 0$, and the fluctuation intensity varies in the crosswind direction at any fixed height z as a simple exponential

$$i^2 = i_o^2 \exp\left[\frac{1}{2} \left(\frac{y}{\sigma_y}\right)^2\right] \quad (D17)$$

In this appendix only the case of a single variance source ($\phi = 0$) will be presented. The crosswind averaged intermittency γ_{oT} is, from (D5), (D6) and (D15)

$$\gamma_{oT} = \frac{\gamma_0}{\sqrt{2\pi} \sigma_m} \int_{-\infty}^{\infty} \frac{(1 + i_o^2) \exp\left[-\frac{1}{2} \left(\frac{y}{\sigma_y}\right)^2\right]}{1 + i_o^2 \exp\left[\frac{1}{2} \left(\frac{y}{\sigma_y}\right)^2\right]} dy \quad (D18)$$

Using the transformation $\zeta = y/\sigma_y$ and noting that the integrand is symmetric about $y = 0$ leads to

$$\frac{\gamma_{oT}}{\gamma_0} = \sqrt{\frac{2}{\pi}} \left(\frac{\sigma_y}{\sigma_m}\right) \int_0^{\infty} \frac{(1 + i_o^2) \exp\left[-\frac{\zeta^2}{2} \left(\frac{\sigma_y}{\sigma_m}\right)^2\right]}{1 + i_o^2 \exp\left[\frac{\zeta^2}{2}\right]} d\zeta \quad (D19)$$

for variance source spacing $\phi = 0$

This integral may be easily evaluated by numerical methods. Accuracy to four significant figures was obtained using the trapezoidal rule in 50 equal steps from $\zeta = 0$ to $\zeta = 5 \sigma_m / \sigma_y$. An alternative approach, using an explicit approximating function is given in (D53).

Crosswind Averaging of Fluctuation Variance

The fluctuation variance normalized by the plume centerline variance $\overline{c_0^2}$ at $y = 0$ is

$$\frac{\overline{c^2}}{\overline{c_0^2}} = \exp\left[\frac{\phi^2}{2}\right] \left[\frac{1}{2} \exp\left[-\frac{1}{2} \left(\frac{y}{\sigma_y} - \phi\right)^2\right] + \frac{1}{2} \exp\left[-\frac{1}{2} \left(\frac{y}{\sigma_y} + \phi\right)^2\right] \right] \quad (\text{D20})$$

It is tempting to follow the same procedure used for mean concentration and integrate this over the meander width σ_m . However, this would not give the correct value for the variance observed over the sample time T_s . The reason the variance cannot be averaged directly is because the mean value \bar{c} , about which the variance is measured, also varies across the plume. We visualize the averaging process as a series of discrete steps each of duration $T_{sref} = 3$ min. to make up a total sample time T_s . Then, each of these three minute samples will have a different $\overline{c^2}$ and \bar{c} , and the average variance over T_s must include the variance induced by the changing mean \bar{c} from step to step.

To find the crosswind averaged variance, we will first compute the averaged mean square concentration $\overline{\bar{c}^2}$. Because this total mean square concentration is measured relative to zero it can be crosswind averaged in the same way as the mean concentration \bar{c} was. For any sampling time the mean square is related to the mean \bar{c} and variance $\overline{c^2}$ by

$$\overline{\bar{c}^2} = \bar{c}^2 + \overline{c^2} \quad (\text{D21})$$

In particular, for a sample time T_s during which the plume meanders

$$\overline{c_{0T}^2} = \overline{c_{0T}}^2 + \overline{c_{0T}^{'2}} \quad (D22)$$

From this the averaged fluctuation variance $\overline{c_{0T}^{'2}}$ can be determined once $\overline{c_{0T}^2}$ and $\overline{c_{0T}}^2$ are known. Because we already have $\overline{c_{0T}}$ from (D13), it is only necessary to compute the mean square $\overline{c_{0T}^{'2}}$. Integrating (D21) using (D6)

$$\overline{c_{0T}^2} = \int_{-\infty}^{\infty} p_m \overline{c}^2 dy + \int_{-\infty}^{\infty} p_m \overline{c^{'2}} dy \quad (D23)$$

Because both integrands are symmetric about $y = 0$ they may be written as

$$I_1 = 2 \int_0^{\infty} p_m \overline{c}^2 dy \quad (D24)$$

and

$$I_2 = 2 \int_0^{\infty} p_m \overline{c^{'2}} dy$$

With the crosswind meander probability density from (D5) and \overline{c} from (D8)

$$I_1 = \sqrt{\frac{2}{\pi}} \frac{\overline{c}_o^2}{\sigma_m} \int_0^{\infty} \exp \left[-\frac{1}{2} \left(\frac{y}{\sigma_m} \right)^2 - \left(\frac{y}{\sigma_y} \right)^2 \right] dy \quad (D25)$$

Defining $\sigma_* = \sigma_y / \sqrt{2}$ this can be written as

$$I_1 = \sqrt{\frac{2}{\pi}} \frac{\overline{c}_o^2}{\sigma_m} \int_0^{\infty} \exp \left[- \left(\frac{\sigma_m^2 + \sigma_*^2}{\sigma_m^2 \sigma_*^2} \right) \frac{y^2}{2} \right] dy \quad (D26)$$

This is exactly the same form as (D10) with σ_* instead of σ_y . Carrying out the transformation of (D11) and (D12) on (D26) leads to a result exactly like (D13). Then, using $\sigma_* = \sigma_y / \sqrt{2}$ yields

$$I_1 = \overline{c}_o^2 \left[\frac{1}{2 \left(\frac{\sigma_m}{\sigma_y} \right)^2 + 1} \right]^{0.5} \quad (D27)$$

To evaluate the integral I_2 , use (D20) for a single variance source with $\phi = 0$ to write

$$\bar{c}^{'2} = \bar{c}_0^{'2} \exp \left[-\frac{1}{2} \left(\frac{y}{\sigma_y} \right)^2 \right] \quad (D28)$$

This is exactly the same as the form for \bar{c}/\bar{c}_0 so produces the same average as (D13)

$$I_2 = \bar{c}_0^{'2} \left[\frac{\frac{1}{2}}{\left[\frac{\sigma_m}{\sigma_y} \right] + 1} \right]^{0.5} \quad (D29)$$

Then, equate (D22) and (D23) to show

$$\bar{c}_{0T}^{'2} + \bar{c}_0^{'2} = I_1 + I_2 \quad (D30)$$

Dividing by $\bar{c}_{0T}^{'2}$ yields a total crosswind average fluctuation intensity

$$\bar{i}_{0T}^2 + 1 = \frac{I_1 + I_2}{\bar{c}_{0T}^{'2}} \quad (D31)$$

Squaring (D13) and using (D27) and (D29) this becomes

$$\bar{i}_{0T}^2 + 1 = \frac{\left(\frac{\sigma_m}{\sigma_y} \right)^2 + 1}{\left[2 \left(\frac{\sigma_m}{\sigma_y} \right)^2 + 1 \right]^{0.5}} + \bar{i}_0^2 \left[\left(\frac{\sigma_m}{\sigma_y} \right)^2 + 1 \right]^{0.5} \quad (D32)$$

for variance source spacing $\phi = 0$

The conditional "plume" fluctuation intensity i_{pT} may be computed from the exact relation

$$\gamma_{oT} = \frac{i_{pT}^2 + 1}{i_{oT}^2 + 1} \quad (D33)$$

from the known short term values of γ_0 and i_0^2 , using (D19) for γ_{oT} and (D32) for i_{oT}^2 .

Influence of Sampling Time on Integral Scales

As the sampling time period T_s increases, low frequency concentration fluctuations are introduced by the back and forth meandering of the plume centerline. These fluctuations will cause an increase in the integral time scale \bar{J}_{cT} observed over this sampling period. To estimate the effect of T_s on the observed \bar{J}_{cT} let us look first at the concentration spectrum $E_c(f)$ for a sample time T_s , Pasquill (1974) p. 14 shows that the low frequency components in the spectrum are attenuated to produce a spectrum

$$E_{cT}(f) = E_{c\infty}(f) \left[1 - \frac{\sin^2(\pi f T_s)}{(\pi f T_s)^2} \right] \quad (D34)$$

where $E_{c\infty}$ is the spectrum for $T_s = \infty$. The spectral density at zero frequency is related directly to the integral scale, see Appendix C equation (C3) by

$$E_{cT}(0) = 4 c_T^{1/2} \bar{J}_{cT} \quad (D35)$$

However, at $f = 0$ the spectral attenuation in (D34) gives the disconcerting result that $E_{cT}(0) = 0$ implying that $\bar{J}_{cT} = 0$ as well.

A more useful approach is to assume that both the short sample time spectrum E_c for T_{sref} and the spectrum E_{cT} for sampling time T_s may be represented as Markov spectra, which from Appendix A, (A12) are

$$E_c(f) = \frac{4 \bar{c}_0^2 \bar{\sigma}_{co}^2}{1 + (2\pi \bar{\sigma}_{co} f)^2} \quad (D36)$$

on the centerline of the short sample time plume and

$$E_{cT}(f) = \frac{4 \bar{c}_T^2 \bar{\sigma}_{cT}^2}{1 + (2\pi \bar{\sigma}_{cT} f)^2} \quad (D37)$$

for the crosswind meander averaged plume at sample time T_s . Then, the high frequency components of these two spectra must be equal, because these high frequencies are contributed by small scale turbulence in the short time average plume that meanders back and forth to generate the longer sample time statistics. At high frequencies $2\pi \bar{\sigma}_{cT} f \gg 1$ and the spectra reduces to

$$E_c(f) \approx \frac{\bar{c}_0^2}{\pi^2 \bar{\sigma}_{co}^2 f^2} \quad (D38)$$

and

$$E_{cT}(f) \approx \frac{\bar{c}_T^2}{\pi^2 \bar{\sigma}_{cT}^2 f^2} \quad (D39)$$

These two spectra must be the same, once the effect of the non-stationary mean \bar{c}_T is accounted for. We will assume that this may be done by normalizing with the square of the mean so that

$$\frac{E_{cT}}{\bar{c}_T^2} = \frac{E_c}{\bar{c}_0^2} \quad (D40)$$

at high frequencies. Using (D38) and (D39) yields, for sampling time T_s and reference sample time T_{sref} on the plume centerline

$$\frac{i_o^2}{J_{co}} = \frac{i_{oT}^2}{J_{coT}} \quad (D41)$$

where i_o and J_{co} are the intensity and scale on the plume centerline for a sample time T_{sref} and i_{oT} and J_{coT} are values for sample time T_s during which the short term plume is crosswind averaged by meandering.

Relating Meandering Width to Sampling Time

All the analysis developed so far can only be useful if the meander width ratio σ_m/σ_y can be directly related to the sampling time T_s . We will begin by assuming a power law relationship between the crosswind averaged mean concentration, and the sampling time in the form, from (D3)

$$\frac{\bar{c}_{oT}}{\bar{c}_o} = \left(\frac{T_{sref}}{T_s} \right)^p \quad (D42)$$

Pasquill (1974) p. 65 carries out an analysis of the effect of sampling time on the crosswind turbulent velocity spectrum that contributes to $\sigma_y T$ in (D2). For short sampling times where the attenuation factor in (D34) cuts the spectrum off in the inertial subrange he shows that $p = 1/3$. For longer sampling times p will gradually decrease, until when $T_s \rightarrow \infty$, $p \rightarrow 0$. For a Markov spectrum a value of $p = 0.5$ is the upper limit for short sampling times.

The spectral attenuation caused by averaging time T_a is just the complementary value of the sampling time attenuation - compare Appendix A, (A27) with (D34). For this reason, variation of maximum mean concentration

with averaging time T_a will have the same exponent p for a range of averaging and sampling times where they are acting on the same part of the turbulence spectrum, with averaging time cutting off the high frequencies and sampling time the low frequencies. Time averaged air quality data analyzed by McGuire and Noll (1971) gave values of p from 0.175 to 0.369 with a mean of $p = 0.197$ for urban SO_2 concentrations. The power law fit their data for averaging times from a few minutes to a year. Angle (1978) on the basis of other data recommended $p = 0.20$ for averaging times from 3 min. to several hours.

Most of the data for the effect of sampling time on mean concentration is for urban data with many overlapping plumes. The effect of multiple sources ranged around the receptor causes mean concentrations to decrease more slowly than would be the case for a single source. In addition, for sampling times longer than about an hour local terrain and drainage flows will strongly influence the meandering of wind direction, even for large ensemble averages. These factors in mind, the value of the exponent p is expected to lie somewhere between 0.1 and 0.5. Angle's estimate of $p = 0.2$ may be conservative, because it will produce higher dosage and probabilities of threshold exposure by producing a slower decrease in Y_{oT} and \bar{c}_{poT} than would occur for a larger exponent.

The relationship between meander width σ_m and the sampling time is found by simply equating the empirical power law in (D42) to the analytical prediction of (D13) to obtain

$$\frac{1}{\left(\frac{\sigma_m}{\sigma_y}\right)^2 + 1} = \left(\frac{T_s}{T_{sref}}\right)^{2p} \quad (\text{D43})$$

which reduces to

$$\frac{\sigma_m}{\sigma_{yT}} = \left[\left(\frac{T_s}{T_{sref}} \right)^{2P} - 1 \right]^{0.5} \quad (D44)$$

Crosswind Profiles at Long Sample Times

So far, we have used the crosswind profiles of plume statistics at a short sample time T_{sref} to estimate the statistics on the centerline at longer sample times. Once these centerline statistics \bar{c}_{oT} , i_{pT} , i_T are known it is a simple matter to compute off-axis values at time T_s . It seems reasonable to assume that the functional forms for the crosswind profiles are the same at all sampling times, with the only change being the width σ_{yT} of the crosswind spread. With this assumption, the off axis functions for a single variance source ($\phi = 0$) are:

$$i_{pT} = \text{constant} \quad (D45)$$

and

$$i_T = i_{oT} \exp \left[\frac{1}{2} \left(\frac{y}{\sigma_{yT}} \right)^2 \right] \quad (D46)$$

and

$$\bar{c}_T = c_{oT} \exp \left[\frac{-1}{2} \left(\frac{y}{\sigma_{yT}} \right)^2 \right] \quad (D47)$$

and

$$\bar{c}_T^2 = c_{oT}^2 \exp \left[\frac{-1}{2} \left(\frac{y}{\sigma_{yT}} \right)^2 \right] \quad (D48)$$

The intermittency at any off-axis location is found from the definition

$$\gamma_T = \frac{i_{pT}^2 + 1}{i_T^2 + 1} \quad (D49)$$

using (D45) and (D46).

Closed Form Approximation to Crosswind Averaged Intermittency

The intermittency on the plume centerline γ_{0T} for a sampling time T_s is related to the short term centerline intermittency γ_0 (for sample time T_{sref}) by (D19). The basic assumption embedded in this equation is a Gaussian probability density for the meandering spread σ_m . This meander spread σ_m is zero at the short sampling time of T_{sref} and increases with sampling time according to (D44).

A closed form solution to the integral in (D19) could not be found. This is unfortunate, because with this one exception all the other equations used for conditional and time dependent variables are in an explicit closed form. The lack of a closed form for (D19) is one of the major obstacles to developing rapid microcomputer based models for hazard assessment. In the following analysis an approximate equation for the integral in (D19) will be developed to avoid the time-consuming numerical integration.

In order to develop an approximate form we must first look at the asymptotic limits of the integral in (D19) for large and small values of the plume centerline concentration fluctuation intensity i_0 . For very small intensity with $i_0 \ll 1$ we find, setting $i_0 = 0$ in (D19) that

$$\frac{\gamma_{0T}}{\gamma_0} = 1.0 \quad (D50)$$

$$\text{for } i_0 = 0$$

This is the expected result, because, when the plume is spreading by diffusion in very small scale turbulence the centerline intensity i_0 will be small and there will be little meandering so that $\gamma_0 = \gamma_{0T} = 1.0$.

At the other extreme, when the concentration fluctuation intensity i_0 is large, an exact solution of (D19) is possible if

$$i_0^2 \exp \left[\frac{\xi^2}{2} \right] \gg 1 \quad (D51)$$

so that the "1" in the denominator of (D19) can be neglected. The condition in (D51) is quite easy to meet, because in the fringes of the plume where the dummy variable ξ is large, the exponential term in (D51) makes the inequality true even for values of i_0 greater than unity. Neglecting the "1" in the denominator of (D19) leads to the exact asymptotic solution

$$\frac{\gamma_{0T}}{\gamma_0} = \left[\frac{1}{\frac{(\sigma_m)^2}{(\sigma_y)^2} + 1} \right]^{0.5} \quad (D52)$$

for "large" i_0

which, surprisingly, is independent of the concentration fluctuation intensity, i_0 .

To develop an approximating equation that fits smoothly and accurately between the asymptotic limits of (D50) and (D52) requires a large measure of educated guesswork. Using some suggestions for J.W. Rottman (1984, private communication) the integrand in (D19) was transformed from an exponential to a logarithmic form, and then approximated by a power function and integrated. After considerable trial and error the best approximate form was found to be

$$\frac{\gamma_{0T}}{\gamma_0} \approx \left[\frac{1}{\frac{(\sigma_m)^2}{(\sigma_y)^2} + 1} \right]^{0.5} \left[1 + \frac{1}{i_0^2} (1 - N_1^P) \right] \quad (D53)$$

where

$$N_1 = \frac{1 + \left(\frac{\sigma_m}{\sigma_y} \right)^2}{1 + \left[\frac{\sqrt{2} i_0^2}{1 + \sqrt{2} i_0^2} \right] \left(\frac{\sigma_m}{\sigma_y} \right)^2} \quad (D54)$$

and

$$P = \frac{i_0^2 + 0.003 \left(\frac{\sigma_m}{\sigma_y} \right)^3}{2i_0^2 + 0.003 \left(\frac{\sigma_m}{\sigma_y} \right)^3} \quad (D55)$$

The error in using (D53) with (D54) and (D55) as an approximation to (D19) was found to depend on the value of the centerline intensity i_0 . The approximate value of the absolute error (as opposed to the fractional or percent errors) in γ_{0T}/γ_0 is

$$\text{error} < \pm 0.02 \left[1 + \frac{0.1}{i_0} \right] \quad (D56)$$

For values of i_0 greater than 0.05. At very small values of $i_0 \approx 0.01$ the absolute error may be up to twice as large as predicted by (D56).

Relating Meandering of the Instantaneous Plume to Additional Meandering σ_m

The actual meandering component σ_{im} plume spread is usually applied to the ensemble averaged instantaneous spread σ_{iy} which occurs for zero sampling time when $T_s = 0$. Gifford's (1959) meandering plume model uses this definition.

The analysis in this report takes a different approach. Because the concentration fluctuation statistics are only known for the total (instantaneous plus meandering) plume at some reference time T_{sref} , the meandering component σ_m is the additional meandering experienced by the plume for sampling times T_s that are longer than T_{sref} . While it would be better to base the effects of meandering on the instantaneous plume, our ignorance of its concentration fluctuation statistics prevents this.

How is the additional plume meandering σ_m related to the instantaneous plume meandering σ_{im} ? For the plume at sampling time T_{sref} , the mean concentration on the plume axis is

$$\bar{c}_o = \frac{Q}{2\pi U \sigma_y \sigma_z} \quad (D57)$$

For sampling time T_s the axis concentration is

$$\bar{c}_{oT} = \frac{Q}{2\pi U \sigma_y T \sigma_z T} \quad (D58)$$

Vertical meandering is generally less than crosswind meandering. Because vertical meandering involves turbulence scales much smaller than horizontal scales, Pasquill (1974) suggests that there will be no additional vertical meandering for sample times longer than about three minutes. By requiring $T_{sref} > 3$ min. we avoid the need to define additional vertical meandering and $\sigma_{zT} = \sigma_z$. Then, taking the ratio of the above two equations

$$\frac{\bar{c}_{oT}}{\bar{c}_o} = \frac{\sigma_y}{\sigma_y T} \quad (D59)$$

Equating this to the (D13) leads to

$$\sigma_y T^2 = \sigma_m^2 + \sigma_y^2 \quad (D60)$$

This sum of variances is the expected result for the random uncorrelated variables of plume spread σ_y at T_{sref} , and the additional crosswind meandering σ_m . To relate the additional meandering to the instantaneous plume meandering, σ_{im} , we note that the total spread σ_y at T_{sref} must be

$$\sigma_y = \sigma_{iy}^2 + \sigma_{im,ref}^2 \quad (D61)$$

where $\sigma_{im,ref}$ is the instantaneous plume meandering at sample time T_{sref} . Also, by definition, at sample time T_s ,

$$\sigma_{yT}^2 = \sigma_{iy}^2 + \sigma_{im}^2 \quad (D62)$$

Using (D61) in (D60) and then comparing the result with (D62) leads to the simple relationship

$$\sigma_{im}^2 = \sigma_{im,ref}^2 + \sigma_m^2 \quad (D63)$$

That is, the total meandering spread σ_{im}^2 is found by adding the squares of the instantaneous plume meandering $\sigma_{im,ref}^2$ at T_{sref} and the additional meandering σ_m^2 that occurs as the sampling time is increased to T_s .

If a model for the concentration fluctuation statistics can be developed for the instantaneous plume, it may be more useful to express the effects of sampling time on the instantaneous $T_s = 0$ plume than on the rather arbitrary reference sampling time T_{sref} . However, there are difficulties with this approach. For example, the mean concentration on the centerline of the instantaneous plume is

$$\bar{c}_{oi} = \frac{Q}{2\pi U \sigma_{iy} \sigma_{iz}} \quad (D64)$$

Taking the ratio of (D58) to (D64) yields

$$\frac{\bar{c}_{oT}}{\bar{c}_{oi}} = \begin{bmatrix} \bar{\sigma}_{yT} \\ \bar{\sigma}_{iy} \end{bmatrix} \begin{bmatrix} \bar{\sigma}_{zT} \\ \bar{\sigma}_{iz} \end{bmatrix} \quad (D65)$$

from which we see that meandering in both the vertical and crosswind directions must be considered where the instantaneous plume is used as a reference. This isn't a serious drawback because for $T_s > 3$ min. the ratio of σ_{zT}/σ_{iz} becomes constant.

APPENDIX E

DOSAGE FLUCTUATIONS

For a biological receptor the integrated concentration exposure is often a more important factor in determining damage than the peak concentration.

For a receptor that is exposed in the time period from $t = t_1$ to $t = t_1 + T_e$ the exposure dose is defined as

$$D = \int_{t_1}^{t_1 + T_e} c \, dt \quad (E1)$$

The average concentration over the same time period is

$$c_T = \frac{1}{T_e} \int_{t_1}^{t_1 + T_e} c \, dt \quad (E2)$$

From which we see that the dose is related to the exposure time T_e by the simple equation

$$D = c_T T_e \quad (E3)$$

For risk analysis, receptors which appear during the release period are never considered, and all receptors are assumed to be exposed to the entire transient release. Likewise, in a continuous plume the time origin is taken at the instant that the receptor is first exposed. Thus, in both cases $t_1 \equiv 0$ and the dose equations simplify for fluctuating concentration $c = \bar{c} + c'$ to

$$D = \int_0^{T_e} (\bar{c} + c') dt \quad (E4)$$

and

$$c_T = \frac{1}{T_e} \int_0^{T_e} (\bar{c} + c') dt \quad (E5)$$

If we take an ensemble average of many exposures to find the mean dosage \bar{D} caused by a fluctuating concentration, it is easy to show that the fluctuating component c' cancels in the ensemble average to give

$$\bar{D} = \overline{\int_0^{T_e} c' dt} \quad (E6)$$

where the overbar denotes an ensemble rather than a time average. In the same way,

$$\bar{c}_T = \frac{1}{T_e} \overline{\int_0^{T_e} c' dt} \quad (E7)$$

and using (E3)

$$\boxed{\bar{D} = \bar{c}_T T_e} \quad (E8)$$

where \bar{c}_T is the ensemble average concentration over a sample time equal to the exposure time T_e . Comparing (E3) and (E8), $D/c_T = \bar{D}/\bar{c}_T$

Dosage Fluctuations Caused by Concentration Variance

Defining a mean and fluctuating dosage as \bar{D} and D' , the dosage in a single realization of an ensemble is

$$D = \bar{D} + D' \quad (E9)$$

Taking the mean square and carrying out an ensemble average (denoted by an overbar)

$$\overline{D^2} = \bar{D}^2 + \overline{D'^2} \quad (E10)$$

Using the mean dose \bar{D} from (E6), the dosage fluctuation can be found from (E10) by calculating the mean square \bar{D}^2 . Beginning with the square of the dose, and using two time variables t and \tilde{t} as a reminder that one may vary while the other is held constant,

$$\bar{D}^2 = \int_0^{T_e} c(t) dt \int_0^{T_e} c(t) dt \quad (E11)$$

Writing $c = \bar{c} + c'$ in each of the above integrals, and expanding by multiplication

$$\begin{aligned} \bar{D}^2 &= \int_0^{T_e} \bar{c}(\tilde{t}) dt \int_0^{T_e} \bar{c}(t) dt + \int_0^{T_e} c'(\tilde{t}) dt \int_0^{T_e} c'(t) dt \\ &+ \int_0^{T_e} \bar{c}(\tilde{t}) dt \int_0^{T_e} c'(t) dt + \int_0^{T_e} c'(\tilde{t}) dt \int_0^{T_e} \bar{c}(t) dt \end{aligned} \quad (E12)$$

Take an ensemble average, noting that the last two terms will vanish because the ensemble average of c' is zero, and the integrals of \bar{c} and c' are uncorrelated.

Recognizing the first term as the square of the mean dosage reduces the average to

$$\overline{\bar{D}^2} = \bar{D}^2 + \int_0^{T_e} c'(\tilde{t}) dt \int_0^{T_e} c'(t) dt \quad (E13)$$

We may relate the two time variables t and \tilde{t} by defining a new variable t' which is $\tilde{t} = t + t'$. By direct comparison with (E10), and using t' , the dosage variance is, for t held constant while t' varies

$$\overline{D'^2} = \int_0^{T_e} \int_0^{T_e} \overline{c'(t)c'(t+t')} dt dt' \quad (E14)$$

This is related to the fluctuation variance $\overline{c_a'^2}$ with an averaging time T_a

equal to the dosage exposure time T_e . By direct comparison with equation (A36) in Appendix A we see from (E14), defining $\overline{c_e^2}$ when $T_a = T_e$

$$\boxed{\overline{D^2} = T_e^2 \overline{c_e^2}} \quad (E15)$$

where, from Appendix A, (A30) relates the time averaged variance $\overline{c_e^2}$ to the true variance $\overline{c_T^2}$ for a sampling time duration T_s and averaging time T_a equal to the dose exposure time T_e

$$\boxed{\frac{\overline{c_e^2}}{\overline{c_T^2}} = 2 \frac{\overline{J}_{cT}}{T_e} \left[1 - \frac{\overline{J}_{cT}}{T_e} \left(1 - \exp \left(-\frac{T_e}{\overline{J}_{cT}} \right) \right) \right]} \quad (E16)$$

where \overline{J}_{cT} is the integral time scale of concentration fluctuations. For exposure times T_e that are long compared to the concentration time scale \overline{J}_{cT} (A31) shows that the variance ratio reduces to

$$\boxed{\frac{\overline{c_e^2}}{\overline{c_T^2}} \approx 2 \frac{\overline{J}_{cT}}{T_e} \quad \text{for} \quad \frac{T_e}{\overline{J}_{cT}} \text{ large}} \quad (E17)$$

Values of $T_a/\overline{J}_{cT} > 5$ may be taken as "large". Combining (E15) and (E17) the dosage variance is

$$\boxed{\overline{D^2} \approx 2 T_e \overline{J}_{cT} \overline{c_T^2} \quad \frac{T_e}{\overline{J}_{cT}} > 5} \quad (E18)$$

Taking the ratio of the square root of (E18) to (E8) gives the dosage fluctuation intensity i_D

$$\boxed{i_D \equiv \sqrt{\frac{\overline{D^2}}{\overline{D}}} \quad (E19)}$$

The variance $\overline{c_T^2}$ and scale $\sqrt{J_{cT}}$ may be related to the values in the short term plume by Appendix D, (D42)

$$\sqrt{J_{cT}} = \sqrt{J_{co}} \frac{i_T^2}{i_0^2} \quad (E20)$$

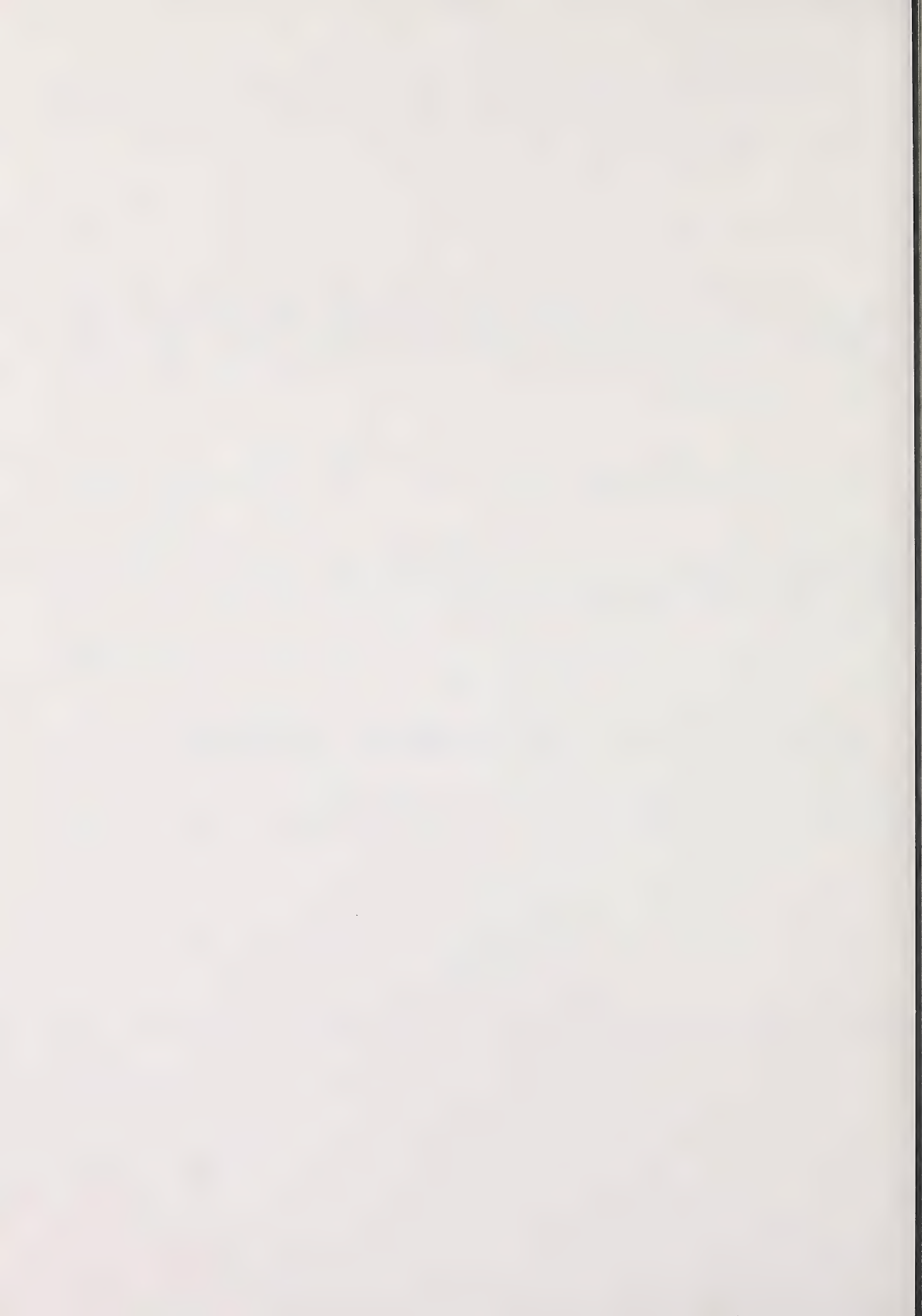
where i_0 and $\sqrt{J_{co}}$ are the concentration fluctuation intensities for the short sampling time T_{sref} appropriate for the wind tunnel simulation. Using (E8) and (E18) in (E19) ,

$$i_D^2 = \frac{\overline{c_T^2}}{\overline{c_e^2}} \left[2 \frac{\sqrt{J_{cT}}}{T_e} \right] \quad (E21)$$

Then, using (E20)

$$i_D^2 = 2 i_T^2 \left(\frac{i_T^2}{i_0^2} \right) \sqrt{J_{co}} \quad (E22)$$

The ratio i_T^2/i_0^2 can be computed from Appendix D, (D32) while the short term time scale is evaluated in Appendix C for $T_{sref} = 3$ min.



APPENDIX F

PROBABILITY OF THRESHOLD LEVEL

CROSSING DURING EXPOSURE

For pollutants whose effects are cumulative, a receptor responds to the total integrated dose to which the receptor is exposed during a time interval T_e . At the other extreme, exposure to highly toxic gases such as hydrogen sulphide may be best described by a threshold concentration level, c^* below which there is no response and above which any short exposure will be fatal. Here, estimating the chance of not once exceeding c^* during the time T_e is complicated by the need to determine the probability of getting through the entire exposure without ever crossing the threshold concentration. The statistical information that is currently available only allows us to compute the fraction of time, V , that the concentration will be more than the threshold for a large ensemble average of exposures, and not the probability of a first threshold crossing occurring during an ensemble of exposures. Some assumptions will be necessary to allow "fraction of time" probabilities to be used to predict time dependent "first crossing" probabilities.

Fraction of Time Over a Threshold

Before dealing with the "first crossing" problem it is useful to review the statistical analysis in current use. The only way in which concentration time series are now analyzed is to sort the time series measurements into concentration bins to specify probability density $p(c)dc$ as the fraction of time the concentration falls in the bin from c to $c + dc$. Periods of zero concentration are usually dealt with separately through the intermittency factor γ and a conditional "plume" probability density $p_p(c)$ which describes all concentrations greater than zero,

$$p(c) = (1 - \gamma) \delta(c) + \gamma p_p(c) \quad (F1)$$

where $(1 - \gamma)$ is the fraction of time with zero concentration and $\delta(c)$ is the delta function, which is a spike at $c = 0$ with the properties that $\delta(c) = 0$ except at $c = 0$ and an area under $\delta(0)$ of unity. The fraction of time that the concentration is less than some threshold c^* , is given by the cumulative distribution function $\Omega(c^*)$.

$$\Omega(c^*) \equiv \int_0^{c^*} p(c) dc \quad (F2)$$

$$\Omega(c^*) = (1 - \gamma) + \gamma \int_0^{c^*} p_p(c) dc \quad (F3)$$

The fraction of time during which the threshold c^* is exceeded is $V(c^*)$, and is simply the complementary cumulative distribution of $\Omega(c^*)$

$$V(c^*) = 1 - \Omega(c^*) \quad (F4)$$

Threshold Crossing Probability for a Series of Short Exposures

The probability $V(c^*)$ may be thought of as the probability of exceeding the threshold c^* at any instant during an exposure time T_e . To estimate the probability of crossing this threshold for the first time we must specify the hazard rate r . This is the probability per unit time of exceeding the threshold c^* for the first time, and this "first time of passage" condition requires that we have always had c less than c^* . The probability of exceeding the threshold for a short exposure of length Δt for the first time is just $r\Delta t$, and the probability of not crossing the threshold is

$$S_1 = (1 - r\Delta t) \quad (\text{F5})$$

To calculate the probability of not crossing for N successive exposures each of equal duration Δt , two assumptions are required.

- 1) The hazard rate r for a unit time of exposure is equal to the probability V of exceeding the threshold for an instant.
- 2) The probability that the j^{th} short exposure exceeds the threshold is independent of the probabilities of exceeding the threshold in any previous interval.

The first assumption implies that the time interval Δt of each exposure is short enough that the probability of exceeding c^* remains constant over the time from t to $t + \Delta t$.

The second assumption; that successive exposures are statistically independent, requires more justification. We know that the concentration time series is strongly autocorrelated, with a correlation coefficient $c'(t) c'(t+\tau)$ having an integral time scale τ_c of 30 to 100 seconds. It would appear from this highly correlated time series that the probability of observing a concentration greater than c^* in the j^{th} exposure should be strongly dependent on the value of c in the previous exposure period ($j-1$). In fact this is true, and if we knew the value of the concentration during the $(j-1)$ exposure interval, the assumption of independence would be incorrect. However, all we know from the previous exposure interval is that c lies somewhere in range $0 \leq c < c^*$, not the specific value of c . As long as the threshold concentration is large enough for a wide range of possible c values to occur in the previous interval then assumption #2 is reasonable. As a rough estimate, successive exposure intervals should be statistically independent as long as c^* is larger than the mean concentration \bar{c} during an interval. For most risk analysis this condition is easily met.

Using these assumptions, the hazard rate for any exposure is just

$$r_j = V_j \quad (F6)$$

and for N statistically independent exposures the probability of exposure without once crossing the threshold is just the product of the series of probabilities of not crossing during each Δt

$$S_N = \prod_{j=1}^N (1 - V_j \Delta t) \quad (F7)$$

where \prod indicates the product of N terms. Often the time interval is expressed in terms of the respiration frequency of an exposed person. This breathing rate B expressed in "breaths per second" defines the exposure time interval as

$$\Delta t = \frac{1}{B} \quad (F8)$$

For a series of N breaths, combining (F7) and (F8)

$$S_N = \prod_{j=1}^N \left(1 - \frac{V_j}{B}\right) \quad (F9)$$

Steady Release With Long Exposure Time

For a continuous steady source, the plume mean concentration \bar{c}_p , fluctuation intensity i_p and intermittency γ all remain constant with time. For a given threshold level c^* , let the exceedance probability V_j be a constant, V , for each exposure time interval. For N breaths the probability (F9) is

$$S_N = \left(1 - \frac{V}{B}\right)^N \quad (F10)$$

In terms of the total exposure time T_e , the number of breaths N depends on the breathing rate B

$$N = B T_e \quad (\text{F11})$$

so that in terms of exposure time we can write (F10) as

$$S(T_e) = \left(1 - \frac{V T_e}{N} \right)^N \quad (\text{F12})$$

For long exposure times, the number of breaths becomes large and we use the fundamental definition of an exponential function

$$\lim_{N \rightarrow \infty} \left(1 - \frac{x}{N} \right)^N \equiv \exp(-x) \quad (\text{F13})$$

to write the probability S of not once exceeding c_* as

$$\boxed{S(T_e) = \exp(-V T_e)} \quad (\text{F14})$$

for large N

Note that the survival probability S is independent of the breathing rate B for sufficiently long exposure times. Assuming successive time intervals are statistically independent for exposure probability, the exposure time does not need to be continuous but may be the sum of a series of short exposure times (such as might occur if a subject was entering and leaving a contaminated area several times).

Generalized Model for Continuous Exposure

Conceptually it is easier to visualize the exposure as a series of discrete events rather than a continuous process. The advantage of regarding the exposure as a continuous process is that a time varying hazard rate that

occurs for a transient release can be easily accounted for. If we define the following continuous probability functions:

$f(t)dt$ = the probability that the time to the first passage over the threshold will occur in the interval from t to $t + dt$

$f(t)$ = the probability density function for the first passage time over the threshold c^*

$F(t)$ = the probability that the threshold c^* has been exceeded at least once before time t .

$S(t)$ = the probability of being exposed to c from $t = 0$ to t without exceeding the threshold c^* .

$r(t)dt$ = the probability of exceeding the threshold at time t given that the first passage over the threshold c^* has not yet occurred.

These probabilities can be related using the hazard rate r , which we now allow to be a time varying function $r(t)$. We know that the probability $f(t)dt$ of first crossing the threshold is simply the product of the probability $S(t)$ of being exposed from $t = 0$ to t without crossing the threshold and time probability $r(t)dt$ of exceeding the threshold in the current time step from t to $t + dt$. That is

$$f(t) dt = S(t)r(t)dt \quad (\text{F15})$$

By definition $S(t)$ is just the complementary probability of $F(t)$

$$S(t) = 1 - F(t) \quad (\text{F16})$$

and $F(t)$ must be the time cumulative probability distribution of the time probability density $f(t)$. That is,

$$F(t) = \int_0^t f(t') dt' \quad (F17)$$

where t' is a dummy time variable of integration. By differentiating (F17) we find the usual relation between the cdf and pdf

$$\frac{dF(t)}{dt} = f(t) \quad (F18)$$

Then, combine (15) and (16) to obtain

$$f(t) = \left(1 - F(t) \right) r(t) \quad (F19)$$

Equate (18) and (19) and transpose terms to obtain a differential equation for the cdf

$$\frac{dF(t)}{1 - F(t)} = r(t) dt \quad (F20)$$

We then use our first assumption that the hazard rate $r(t)$ is equal to the instantaneous probability of exceedance $V(t)$ and integrate (F20) over an exposure time from $t = 0$ to $t = T_e$

$$\int_0^{T_e} \frac{dF}{1 - F} = \int_0^{T_e} V(t) dt \quad (F21)$$

From which

$$-\ln (1 - F(T_e)) \Big|_0^{T_e} = \int_0^{T_e} V(t) dt \quad (F22)$$

Because $F(0) = 0$ this becomes

$$\ln(1 - F(T_e)) = - \int_0^{T_e} V(t)dt \quad (F23)$$

Using the definition of the survival probability in (F16), the final result is

$$S(T_e) = \exp \left[- \int_0^{T_e} V(t)dt \right] \quad (F24)$$

which shows that all that is required to estimate the survival probability for an exposure time T_e is the integrated probability of exceedance over the time interval. For the case where $V(t)$ is constant in a steady release, (F24) reduces immediately to (F14). If we define an average probability of exceedance over an exposure time T_e as

$$V_{avg} \equiv \frac{1}{T_e} \int_0^{T_e} V(t)dt \quad (F25)$$

The survival probability S is then

$$S(T_e) = \exp \left[- V_{avg} T_e \right] \quad (F26)$$

which simplifies the task of estimating risk of exposure to time varying releases.

APPENDIX G
STOCHASTIC MODEL OF GAS CONCENTRATIONS

I. Introduction

A mathematical model will be proposed which will predict concentrations of a target gas released as a result of either a pipeline rupture or a continuous plume. The model, when provided with estimates of several basic parameters, will be used to specify;

- a) the steady state probability distribution of gas concentration $p(c)$,
and
- b) the probability $F(T_e)$ that the passage to a concentration higher than a specified threshold will occur at least once during a given exposure time T_e .

The perspective taken is that the initial gas concentration on exit from the source is c_0 , the gas exits in a continuous process but is quickly transformed into a series of discrete eddies, and each eddy undergoes a dilution process as a result of air entrainment and diffusion. During the dilution process and as function of the time t since release, the gas concentration of each eddy is a random variable and the average concentration decreases.

The analysis will be carried out as follows:

- a) In section II the dilution process will be modeled as a continuous random walk Wiener process. It will be shown that if the gas concentrations follow this type of process then the probability density function of gas concentration in the short run will be normal (Gaussian) and in the long run an exponential. The Gamma probability density function is suggested as an approximation to the steady state probability distribution of gas concentration.

- b) In section III it is noted that the plume over a sample site is not continuous and because of meandering and holes in the plume there are intervals of time that the plume is not at the sample site. The meandering process is modeled as a two stage Markov process and the characteristics of the model are highlighted.
- c) In section IV the time to first passage past a concentration threshold will be discussed and an expression developed for the probability that a concentration threshold will be exceeded, as a function of time.
- d) In section V numerical routines will be given which are required for calculation of the relevant variables of the model.

II. The Dilution Process

The Wiener process has been used as a model for many physical processes, including the diffusion of one gas into another. The Wiener process may be regarded as a limiting form of the random walk in one dimension. Consequently, no discrete jumps occur and in a small interval of time the process is restricted to local transitions and has independent increments. The displacement per interval Δt is of the order of magnitude $\Delta t^{1/2}$, and in any single realization of this continuous process one would expect to find an infinite number of small spikes in any finite time interval.

The equations describing the gas concentration at time t from release from the source $c_p(t)$, for a Wiener process are also a solution of the Fokker-Planck equation for diffusion.

$$\frac{1}{2} \overline{c_{op}^2} \frac{d}{dc_p} p(c_p, t | c_0) - \frac{\overline{dc_p(t)}}{dt} \frac{d}{dc_p} p(c_p, t | c_0) = \frac{d}{dt} p(c_p, t | c_0), \quad G1$$

where $\frac{\overline{dc_p(t)}}{dt} = \text{constant}$, and $\overline{c_{op}^2} \equiv \text{variance defined by the process.}$

This one-dimension diffusion equation with an external field of force, such as gravity, is normally used to calculate the density of particles at a point x at time t given the initial position x_0 , $p(x,t|x_0)$. For the dilution process the point is fixed to the frame of reference, an eddy in the plume, and the distribution for the concentration within the eddy is required. Given the initial condition $c_p(0)=c_0$, and unrestricted values for $c_p(t)$; $-\infty < c_p(t) < \infty$, the probability density function of gas concentration will be Gaussian with:

$$\bar{c}_p = c_0 + \frac{\overline{dc_p(t)}}{dt} t, \text{ where } \frac{\overline{dc_p(t)}}{dt} \text{ is sometimes called the drift} \quad G2$$

and

$$\overline{c_p^2} = \overline{c_{op}^2} t.$$

For notational convenience, define $\overline{\frac{dc_p}{dt}} = \frac{\overline{dc_p(t)}}{dt}$,

$$\text{and } p(c_p, t | c_0) = \frac{1}{\sqrt{\overline{c_{op}^2} 2\pi t}} \exp \left\{ -\frac{(c_p - c_0 - \overline{\frac{dc_p}{dt}} t)^2}{2 \overline{c_{op}^2} t} \right\}. \quad G3$$

For the dilution process, however, the gas concentration in the eddy is restricted to be greater than zero; $c_p(t) > 0$. The appropriate boundary equation for this case is

$$\left| \frac{1}{2} \overline{c_{op}^{-2}} \frac{dp(c_p, t | c_0)}{dc_p} - \frac{\overline{dc_p}}{dt} p(c_p, t | c_0) \right|_{c_p=0} = 0. \quad G4$$

It is known that the solution to the resulting diffusion equation is (e.g., Cox and Miller, [1965], p.224);

$$\begin{aligned}
 p(c_p, t | c_0) = & \frac{1}{\sqrt{\frac{c_{op}}{2} t}} \left[\exp \left\{ -\frac{(c_p - c_0 - \frac{\bar{dc}_p}{dt} t)^2}{2 \frac{c_{op}}{2} t} \right\} \right. \\
 & + \exp \left\{ \frac{-4c_0 \frac{\bar{dc}_p}{dt} t - (c_p + c_0 - \frac{\bar{dc}_p}{dt} t)^2}{2 \frac{c_{op}}{2} t} \right\} \\
 & - \frac{2 \frac{\bar{dc}_p}{dt}}{\frac{c_{op}}{2}} \exp \left\{ \frac{2 c_p \frac{\bar{dc}_p}{dt}}{\frac{c_{op}}{2}} \right\} \left\{ 1 - \Phi \left(\frac{c_p + c_0 + \frac{\bar{dc}_p}{dt} t}{\sqrt{t \frac{c_{op}}{2}}} \right) \right\}, \quad G5
 \end{aligned}$$

where $\Phi(z)$ is the cumulative density function for the standardized normal variate Z . The equilibrium or steady state distribution exists only for $\frac{\bar{dc}_p}{dt} < 0$, and

$$p(c_p, \infty | c_0) = \frac{2 \left| \frac{\bar{dc}_p}{dt} \right|}{\frac{c_{op}}{2}} \exp \left\{ -\frac{2 \left| \frac{\bar{dc}_p}{dt} \right|}{\frac{c_{op}}{2}} c_p \right\}; \quad c_p > 0, \quad G6$$

which is the exponential probability density function.

If examined closely it becomes apparent that $p(c_p, t | c_0)$ is a combination of an exponential, a normal and another distribution which is normal-like. For the dilution process, the drift is expected to be negative since, due to air entrainment and diffusion, the tendency is for the average gas concentration to decrease as time since emission from the source t , increases.

When the product $\frac{\bar{dc}_p}{dt} t$ is small the distribution of gas concentration is predicted to be approximately Gaussian, When $\frac{\bar{dc}_p}{dt} t$ is

large the distribution of gas concentration approaches an exponential probability density function. An example of the changing shape of the gas concentration distribution as a function of time as predicted by the model is shown in Figure G.1. Also note that $\overline{\frac{dc_p}{dt}}$ is assumed to be a constant and is independent of the initial condition c_0 , but it is dependent on the process being analyzed. $\overline{c_p}(0)=c_0$ will be higher than the final value of $\overline{c_p}(\infty)$, since

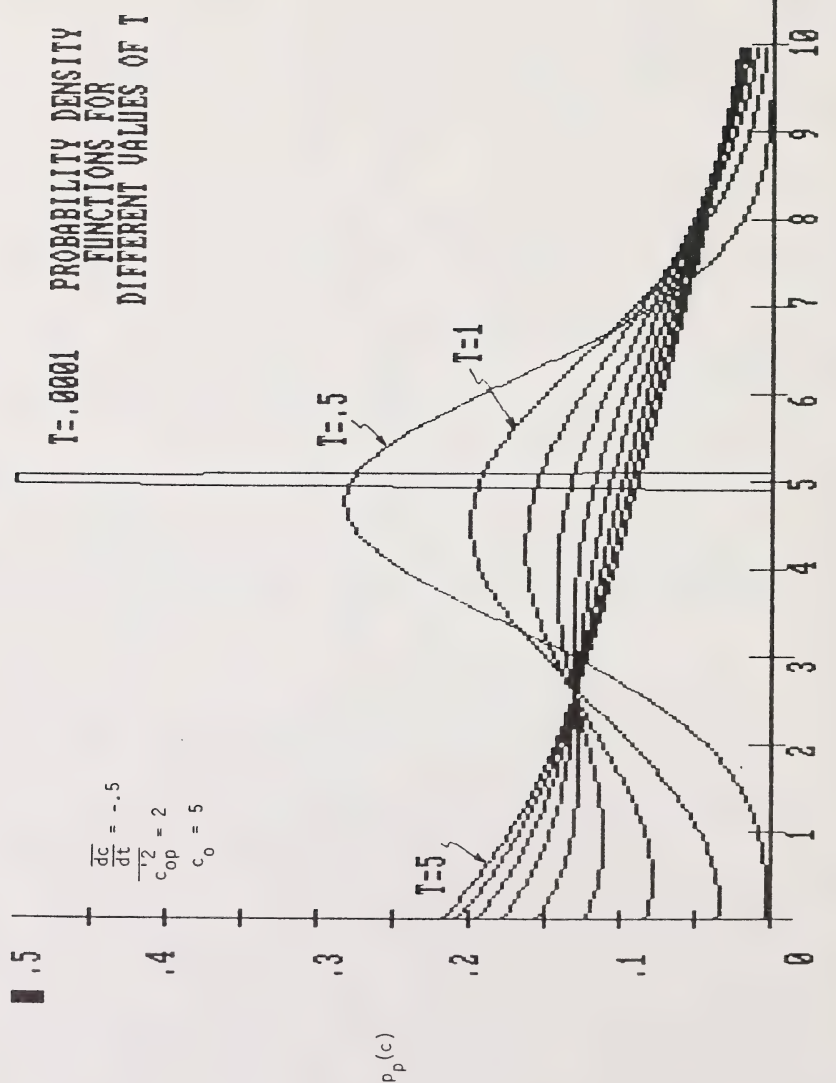
$$\overline{c_p}(\infty) = 2 \frac{\left| \frac{dc_p}{dt} \right|}{\frac{c_{op}}{\sqrt{2}}} \quad G7$$

$\overline{\frac{dc_p}{dt}}$ may be either positive, zero, or negative, but for the dilution process studied here c_0 is expected to be relatively high, $\overline{\frac{dc_p}{dt}}$ to be negative and the average concentration will decrease to a final value of $\overline{c_p}(\infty)$.

The principal predictions of the model are:

- a) Immediately after release, and for some time period from release, the distribution of gas concentrations is approximately Gaussian.
- b) When time since exit from the source is large the distribution of gas concentrations will follow the exponential probability density function.
- c) If gas concentrations are examined from a sample site which is positioned such that the gas has been subject to the dilution process for time t , then the steady state probability distribution of gas concentrations for non-zero concentrations $p_e(c)=p(c_p,t|c_0)$. This is also known as the ensemble average in the literature.

The probability density function for gas concentration which has been derived from the Wiener process is too complex for use in measurement experiments and it will be approximated by the Gamma family of probability



density functions. This family was chosen because it has as special cases the exponential and deterministic distributions and in some cases (when the probability of values less than zero is small) it may be used to approximate the normal distribution. The Gamma distribution will be referred to as $G(\alpha, k)$ and its general form is;

$$\frac{\alpha^k c^{k-1} e^{-\alpha c}}{\Gamma(k)} ; \quad c > 0 .$$

G8

For this application the distribution becomes $G(\alpha, k)$ where

\bar{c}_e = expected concentration for non-zero concentrations , and

k = shape parameter of the Gamma distribution.

$$p_e(c) = \frac{\left(\frac{k}{\bar{c}_e}\right)^k c^{k-1} e^{-k\left(\frac{c}{\bar{c}_e}\right)}}{\Gamma(k)} ; \quad c > 0 ,$$

G9

See Figure G.2 for examples of the Gamma distribution for different values of the shape parameter k . Note that for $k=1$, the resulting distribution is the exponential probability density function.

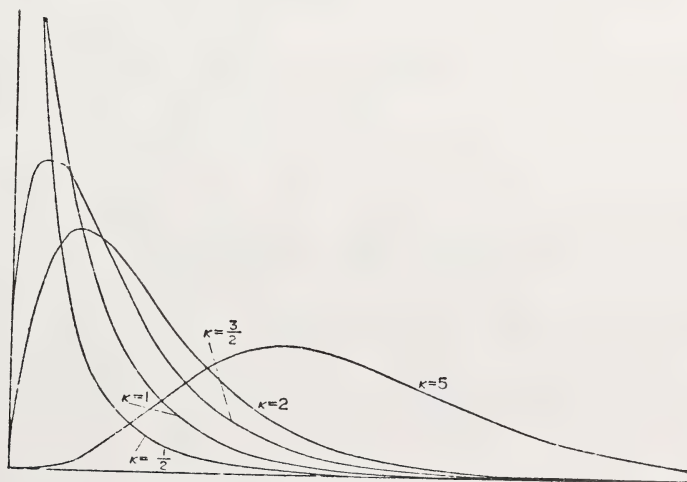


FIGURE G.2 The Gamma Probability Density Function

III. The Meander Process Model

The plume may meander, with the result that a sample site in a stationary geographical location will not experience a continuous plume, but rather will experience a series of intervals when the plume is present and then not present. A two stage markov process is used to model the meandering process. Define

$P_{ij}(t)$ = The transition probability; the probability that the process is in state j at time t , given that the process was in state i at $t=0$.

r_{ij} = The rate of transition from state i to j ; $r_{ij} \Delta t$ is the probability that the process is in state j after some small increment of time Δt , given that it is currently in state i .

Let the state $i=0$ represent the event that the plume is not present and the state $i=1$ represent the event that the plume is present, then it can be shown that

$$p_{00}(T_e) = \frac{r_{10}}{r_{01} + r_{10}} + \frac{r_{01}}{r_{01} + r_{10}} e^{-(r_{01} + r_{10}) T_e},$$

$$p_{01}(T_e) = \frac{r_{01}}{r_{01} + r_{10}} - \frac{r_{01}}{r_{01} + r_{10}} e^{-(r_{01} + r_{10}) T_e},$$

$$p_{10}(T_e) = \frac{r_{10}}{r_{01} + r_{10}} - \frac{r_{10}}{r_{01} + r_{10}} e^{-(r_{01} + r_{10}) T_e},$$
G10

$$p_{11}(T_e) = \frac{r_{01}}{r_{01} + r_{10}} + \frac{r_{10}}{r_{01} + r_{10}} e^{-(r_{01} + r_{10}) T_e}.$$

In steady state as t

$$P_0 = \frac{r_{10}}{r_{C1} + r_{10}} \quad \text{and} \quad P_1 = \frac{r_{01}}{r_{01} + r_{10}} . \quad G11$$

Consequently, the steady state probability distribution $p(c)$ can be written as,

$$p(c) = P_0 + (1-P_0)p_p(c), \quad G12$$

where $p_p(c)$ = the steady state probability that the gas concentration is c given that the plume is present.

When the plume is present, the gas is not a completely homogeneous mixture, but consists of a number of discontinuous eddies, and the dilution process within each eddy is assumed to follow a Wiener process. In steady state the probability distribution of gas concentrations in the eddy $p_e(c)$, will be distributed according to the Gamma distribution as developed in section II and expressed by Equation G9. The steady state probability distribution of gas concentrations can now be written as,

$$p(c) = 1-\gamma + \gamma p_e(c) \quad \text{and} \quad \Omega(c^*) = \int_0^{c^*} p(c,t)dt = 1-\gamma + \gamma \int_0^{c^*} p_e(c) \quad \text{where}$$

$$p_e(c) = \frac{\left(\frac{k}{c_e}\right)^k c^{k-1} e^{-\frac{kc}{c_e}}}{\Gamma(k)} ; \quad k = \frac{1}{i_p^2} ,$$

and $1-\gamma$ is the probability that an eddy is not present.

Since $\Omega_e(c^*) = \int_0^{c^*} p_e(c)dc$ is not available directly a numerical routine shown in section V will be required for calculations.

IV First Passage Times

Define $\{N(t); t > 0\}$ as a counting process for the number of events occurring by time t . If the arrival rate of events is r ; $r > 0$ and if;

- a) $N(0)=0$,
- b) the process has stationary and independent increments,
- c) $P\{N(h)=1\}=rh+O(h)$ for h small, and
- d) $P\{N(h)>2\}=O(h)$.

then $N(t)$ is a Poisson process. A function is of order $O(h)$ if

$\lim_{h \rightarrow 0} f(h)/h = 0$. A process has independent increments if the number of events occurring in disjoint time intervals are independent. The increments are stationary if the number of events occurring in the interval depends only on the length of the interval.

It is argued that the arrival process of the eddies when the plume is present satisfy the conditions specified above and eddies arrive at the sample site according to a Poisson process if the plume is present. An important characteristic of the sampling process is the probability that some threshold value of gas concentration c^* , has been exceeded by time T_e . In the study of stochastic processes this is called the first passage time distribution. The probability of threshold exceedance $F(T_e)$ will depend on whether the plume is present or not at $T_e=0$. The following derivation will assume the plume is present at time $T_e=0$ although the cases of plume not present and no information can also be dealt with using this type of analysis.

Consider that a threshold exceedance can only occur when the plume is present. Using an absorbing state for the event of a threshold exceedance a three state Markov process can be defined. It is important to note that if eddies arrive according to a Poisson process with rate r , and the probability is $1-\Omega_e(c^*)$ that the gas concentration of the eddy is greater

than c^* , then the process of threshold exceedance is also Poisson with rate $r(1 - \Omega_e(c^*))$.

Defining state 2 as the state of a threshold exceedance and r_{12} as the rate of threshold exceedance when the plume is present, then the one-step transition equation can be written as,

$$\{P_0(t + \Delta t), P_1(t + \Delta t), P_2(t + \Delta t)\} = \{P_0(t), P_1(t), P_2(t)\} \{p_{ij}\} \quad G15$$

where $\{p_{ij}\}$ is the one-step transition matrix with elements p_{ij} defined by

$$\{p_{ij}\} = \begin{bmatrix} 1-r_{01} \Delta t & r_{01} \Delta t & 0 \\ r_{10} \Delta t & 1-(r_{10}+r_{12}) \Delta t & r_{12} \Delta t \\ 0 & 0 & 1 \end{bmatrix} \quad G16$$

The resulting set of simultaneous differential equations are;

$$P_0'(t) = r_{01}P_1(t) - r_{10}P_0(t)$$

$$P_1'(t) = -(r_{12}+r_{01})P_1(t) + r_{10}P_0(t) \quad G17$$

$$P_2'(t) = r_{12}P_1(t)$$

Examining the first two differential equations it is noted that $P_2(t)$ does not appear and the solution to this smaller set of simultaneous first order differential equations can be reduced to a single, second order equation. Isolating $P_1(t)$ in the resulting second order differential equation has the general solution;

$$P_1(t) = B_1 \exp(b_1 t) + B_2 \exp(b_2 t)$$

where $b_1 = [-(r_{10}+r_{01}+r_{12})-\text{sqr}((r_{01}+r_{10}+r_{12})^2-4r_{01}r_{12})]/2$, and $G18$

$$b_2 = [-(r_{10}+r_{01}+r_{12})+\text{sqr}((r_{01}+r_{10}+r_{12})^2-4r_{01}r_{12})]/2.$$

B_1 and B_2 are found from the boundary conditions for $P_1(0)$ and $P_2(0)$. For the case where the exposure interval begins with the plume overhead $P_1(0)=1$ and $P_0(0)=0$. Using these boundary conditions, a solution was found for Equation G18. Noting that $P_2(T_e)=F(T_e)$ is the probability that the threshold has been exceeded at least once in exposure time T_e and is equal

to $1 - P_0(T_e) - P_1(T_e)$, then

$$F(T_e) = 1 - (B_1 b_2 / r_{01}) \exp(-b_1 T_e) - (B_2 b_1 / r_{01}) \exp(-b_2 T_e) \quad G19$$

where $B_1 = 1/2 + (r_{10} - r_{01} + r_{12}) / \{2\sqrt{(r_{01} + r_{10} + r_{12})^2 - 4r_{01}r_{12}}\}$ and $B_2 = 1 - B_1$.

A mathematical model of the discontinuous dilution process has been proposed. Distributions of gas concentration in an eddy as a function of time since emission from the source were developed from the Wiener process model. From the mathematical model the steady state distribution of gas concentrations at a stationary location was specified. The Gamma family of probability density functions were recommended as an approximation to the derived gas concentration distribution. An expression for the probability of threshold exceedance for some exposure time T_e was derived assuming that the meandering process is a two stage Markov process and the arrival process for eddies when the plume is present is Poisson. Numerical techniques for calculating the steady state probability of exceeding a threshold concentration at any instant for the Gamma probability density function are shown in section V.

V. Numerical Routines

The general form of the Gamma used in the report, $G\left(\frac{k}{c_p}, k\right)$ where $k = \frac{1}{i_p^2}$ is

$$p_p(c) dc = \frac{\left(\frac{k}{c_p}\right)^k c^{k-1} e^{-\frac{kc}{c_p}}}{\Gamma(k)} dc \quad G20$$

The cumulative distribution is

$$\Omega_p(c_p) = \int_0^c \frac{\left(\frac{k}{c_p}\right)^k c^{k-1} e^{-\frac{kc}{c_p}}}{\Gamma(k)} dc \quad G21$$

Normalizing by defining a new variable $\frac{c}{\bar{c}_p}$, then

$$c = \bar{c}_p \frac{c}{\bar{c}_p} \quad \text{and} \quad dc = \bar{c}_p d \left(\frac{c}{\bar{c}_p} \right) ,$$

such that

$$p_p \left(\frac{c}{\bar{c}_p} \right) d \left(\frac{c}{\bar{c}_p} \right) = \frac{\left(\frac{k}{\bar{c}_p} \right)^k \left(\bar{c}_p \frac{c}{\bar{c}_p} \right)^{k-1} e^{-\frac{kc}{\bar{c}_p}}}{\Gamma(k)} \bar{c}_p d \left(\frac{c}{\bar{c}_p} \right) , \quad G22$$

and

$$p_p \left(\frac{c}{\bar{c}_p} \right) d \left(\frac{c}{\bar{c}_p} \right) = \frac{k^k \left(\frac{c}{\bar{c}_p} \right)^{k-1} e^{-k \frac{c}{\bar{c}_p}}}{\Gamma(k)} d \frac{c}{\bar{c}_p} , \quad G23$$

$$\Omega_p \left(\frac{c}{\bar{c}_p} \right) = \int_0^{\frac{c}{\bar{c}_p}} \frac{k^k \left(\frac{c}{\bar{c}_p} \right)^{k-1} e^{-k \frac{c}{\bar{c}_p}}}{\Gamma(k)} d \left(\frac{c}{\bar{c}_p} \right) . \quad G24$$

When provided with \bar{c}_p and i_p , $p_p(c)$ and $\Omega_p(c)$ can be found.

Subroutine For $\Gamma(k)$:

For $k \geq 10$ Stirlings formula will be used :

$$\ln[\Gamma(k)] = \left(k - \frac{1}{2} \right) \ln k - k + \frac{1}{2} \ln (2\pi) + \frac{1}{12k} - \frac{1}{360k^3} + \frac{1}{1260k^5} .$$

Then

$$\Gamma(k) = \exp [\ln \Gamma(k)]$$

and for

$$k < 10,$$

$$\Gamma(k) = \Gamma(a + \varepsilon).$$

Where a is an integer and $0 < \varepsilon < 1$.

Therefore,

$$\Gamma(a + \varepsilon) = (a + \varepsilon - 1) (a + \varepsilon - 2) \times \dots \times (\varepsilon + 1)(\varepsilon) \Gamma(\varepsilon),$$

where

$$\Gamma(\varepsilon) = \left[\sum_{n=1}^{\infty} c_n \varepsilon^n \right]^{-1}.$$

The computer listing is shown in Table G1.

The subroutine for

$$p_p \left(\frac{c}{c_p} \right) = \frac{k^k \left(\frac{c}{c_p} \right)^{k-1} e^{-k} \frac{c}{c_p}}{\Gamma(k)}$$

G25

$$= k \left[\frac{x^{k-1} e^x}{\Gamma(k)} \right]$$

where $x = \frac{kc}{c_p}$, is found from

$$\ln [p_p \left(\frac{c}{c_p} \right)] = \ln k + (k - 1) \ln (x) - x - \ln (\Gamma(k)),$$

G26

and

$$p_p \left(\frac{c}{c_p} \right) = \exp [\ln [p_p \left(\frac{c}{c_p} \right)]].$$

The subroutine for,

$$\Omega_p \frac{c}{c_p} = \int_0^{\frac{c}{c_p}} \frac{(k)^k \left(\frac{c}{c_p} \right)^{k-1} e^{-k \frac{c}{c_p}} d \left(\frac{c}{c_p} \right)}{\Gamma(k)}$$

G27

is proposed by BURGIN [1975], and

$$\begin{aligned} &= \int_0^{\frac{ck}{c_p}} \frac{\left(\frac{kc}{c_p} \right)^{k-1} e^{-k \frac{c}{c_p}} d \frac{ck}{c_p}}{\Gamma(k)} \\ &= \int_0^{\frac{kc}{c_p}} \frac{x^{k-1} e^{-x} dx}{\Gamma(k)} \end{aligned}$$

G28

$$\Omega_p \left(\frac{c}{c_p} \right) = \left| \frac{\left(\frac{kc}{c_p} \right)^{k-1} e^{-\frac{kc}{c_p}}}{\Gamma(k)} \right| \sum_{n=0}^{\infty} \left| \frac{\left(\frac{ck}{c_p} \right)^{n+1}}{\frac{n!}{r!} (k+r)} \right|.$$

G29

Computer listings for $p_p(c)$ and $\Omega_p(c)$ are shown in Tables G2 and G3.

Table G1 Subroutine for $\Gamma(k)$

```
10 PRINT "THIS PROGRAM CALCULATES VALUES FOR THE GAMMA"
20 PRINT "FUNCTION WHEN SUPPLIED WITH THE ARGUMENT K"
30 PRINT "WHAT IS THE VALUE OF K?"
40 INPUT K
50 DIM C(12)
60 FOR L=1 TO 12
70 READ C(L)
80 NEXT L
90 IF K <= 10 GOTO 120
100 LGAMMA=(K-.5)*LOG(K)-K+.5*LOG(2*3.1416)+(1/(12*K))-(1/(360*K))
110 GOTO 270
120 LGAMMA=0
130 FOR L=1 TO 10
140 K1=K-L
150 IF K1=0 GOTO 190
160 LGAMMA=LGAMMA+LOG(K1)
170 IF K1<1 GOTO 190
180 NEXT L
190 K2=0
200 K3=1
210 IF K1=0 GOTO 260
220 FOR L=1 TO 12
230 K2=C(L)*(K1^L)+K2
240 NEXT L
250 K3=1/K2
260 LGAMMA=LGAMMA+LOG(K3)
270 GAMMA=EXP(LGAMMA)
280 PRINT "THE VALUE OF GAMMA(K) IS";GAMMA
300 END
310 DATA 1.0,.57721,-.65587,-.042,.16653,-.04219,-.00962
320 DATA 7.2189E-03,1.1652E-03,2.1524E-04,1.2805E-04,2.0125E-05
```

Table G2 Subroutine for the Gamma Distribution $p_p(c)$

```
10 PRINT "THIS PROGRAM CALCULATES VALUES FOR THE NORMALIZED"
20 PRINT "GAMMA PROBABILITY DENSITY FUNCTION WHEN GIVEN THE "
30 PRINT "CONCENTRATION FLUCTUATION PARAMETER i AND THE LENGTH"
40 PRINT "AND INTERVAL OF THE NORMALIZED CONCENTRATION VALUES"
50 PRINT "WHAT IS THE VALUE OF i";
60 INPUT IP
70 PRINT "WHAT IS THE LOWER VALUE FOR THE NORMALIZED CONCENTRATION";
80 INPUT R1
85 PRINT "WHAT IS THE UPPER VALUE FOR THE NORMALIZED CONCENTRATION";
86 INPUT R2
90 PRINT "WHAT IS THE STEP SIZE FOR THE NORMALIZED CONCENTRATIONS";
100 INPUT ITE
110 K=1/(IP^2)
120 GOSUB 1040
130 FOR L=R1 TO R2 STEP ITE
140 LNG=(K-1)*(LOG(L)-LOG(IP^2))-L*K-LGAMMA
145 LNC=LNG-LOG(IP^2)
146 CONC=EXP(LNC)
150 LPRINT L,CONC
160 NEXT L
170 END
1040 DIM C(12)
1050 FOR L=1 TO 12
1060 READ C(L)
1070 NEXT L
1080 IF K <= 10 GOTO 1110
1090 LGAMMA=(K-.5)*LOG(K)-K+.5*LOG(2*3.1416)+(1/(12*K))-(1/(360*K))
1100 GOTO 1260
1110 LGAMMA=0
120 FOR L=1 TO 10
130 K1=K-L
140 IF K1<0 GOTO 1180
150 LGAMMA=LGAMMA+LOG(K1)
160 IF K1<1 GOTO 1180
170 NEXT L
180 K2=0
185 IF K1<0 THEN K1=K
190 K3=1
200 IF K1=0 GOTO 1250
210 FOR L=1 TO 12
220 K2=C(L)*(K1^L)+K2
230 NEXT L
240 K3=1/K2
250 LGAMMA=LGAMMA+LOG(K3)
260 RETURN
280 STOP
290 END
300 DATA 1.0,.57721,-.65587,-.042,.16653,-.04219,-.00962
310 DATA 7.2189E-03,1.1652E-03,2.1524E-04,1.2805E-04,2.0125E-05
```

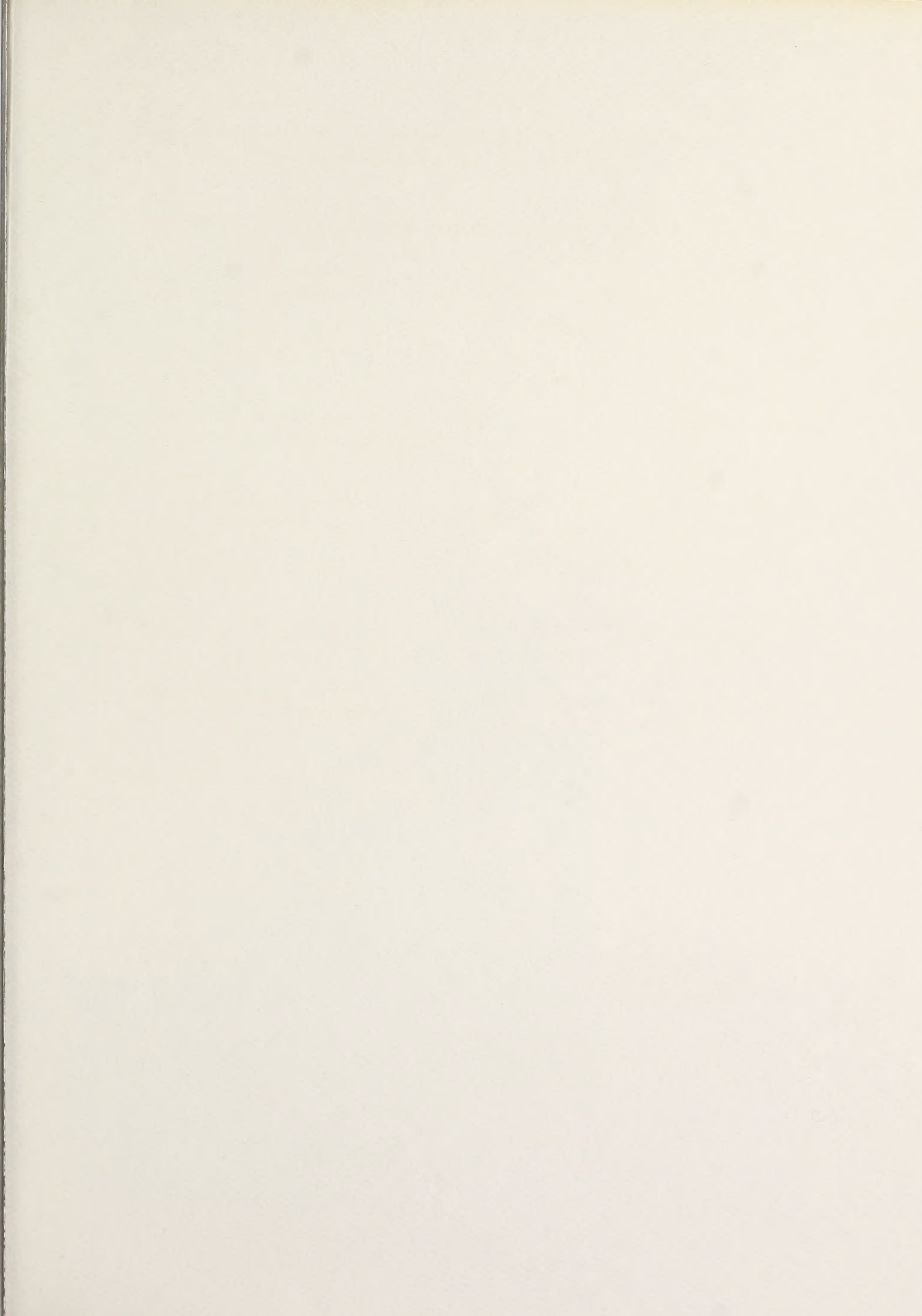
Table G3 Subroutine for $\Omega(c)$ and $v(c)$

```
10 PRINT "THIS PROGRAM CALCULATES THE PDF AND CDF OF THE NORMALIZED"
20 PRINT "GAMMA PROBABILITY DISTRIBUTION"
30 PRINT "WHAT IS THE VALUE OF THE FLUCTUATION INTENSITY i";
40 INPUT IP
50 PRINT "WHAT IS THE RANGE OF VALUES OF THE NORMALIZED PARAMETER; MIN, MAX";
60 INPUT RR1,RR2
70 PRINT "WHAT IS THE STEP SIZE ACROSS THE INTERVAL";
80 INPUT IITE
90 PRINT "WHAT IS THE ACCURACY REQUIRED FOR THE NUMERICAL ROUTINE";
100 INPUT EPS
110 PRINT "WHAT IS THE VALUE OF THE INTERMITTENCY";
120 INPUT MIT
130 LPRINT "THE FLUCTUATION INTENSITY IS";IP
135 LPRINT "THE INTERMITTENCY IS";MIT
140 LPRINT "CONC", "CDF", "VCDF"
150 R1=RR1*MIT
160 R2=RR2*MIT
170 ITE=IITE*MIT
180 K=1/(IP^2)
190 GOSUB 450
200 SUM1=0
210 FOR L=R1 TO R2 STEP ITE
220 SUM=0
230 N=0
240 LSUM=(N+1)*LOG(L*K)
250 FOR R=0 TO N
260 LSUM=LSUM-LOG(K+R)
270 NEXT R
280 SUM=EXP(LSUM)+SUM
290 IF (EXP(LSUM)/SUM)<EPS GOTO 320
300 N=N+1
310 GOTO 240
320 GOSUB 410
330 GAM=EXP(LNG)*SUM
340 SUM1=SUM1+(CONC*ITE)
350 CUM=1-MIT +MIT*GAM
360 VCUM=1-CUM
370 L1=L/MIT
380 LPRINT L1,CUM,VCUM
390 NEXT L
400 END
410 LNG=(K-1)*(LOG(L)-LOG(IP^2))-L*K-LGAMMA
420 LNC=LNG-LOG(IP^2)
430 CONC=EXP(LNC)
440 RETURN
450 DIM C(12)
460 FOR L=1 TO 12
470 READ C(L)
480 NEXT L
490 IF K<=10 GOTO 520
500 LGAMMA=(K-.5)*LOG(K)-K+.5*LOG(2*3.1416)+(1/(12*K))-(1/(360*K))
510 GOTO 680
520 LGAMMA=0
530 FOR L=1 TO 10
540 K1=K-L
550 IF K1<=0 GOTO 590
560 LGAMMA=LGAMMA+LOG(K1)
570 IF K1<1 GOTO 590
580 NEXT L
590 K2=0
600 IF K1<0 THEN K1=K
610 IF K1=0 GOTO 670
620 FOR L=1 TO 12
630 K2=C(L)*(K1^L)+K2
640 NEXT L
650 K3=1/K2
660 LGAMMA=LGAMMA+LOG(K3)
680 RETURN
690 DATA 1.0,.57721,-.65587,-.042,.16653,-.04219,-.00962
700 DATA 7.2189E-03,1.1652E-03,2.1524E-04,1.2805E-04,2.0135E-05
```

REFERENCES

- Angle, R. (1978) "Guidelines for Plume Dispersion Calculations" Alberta Dept. of Environment, Standards and Approvals Division.
- Bara, B. (1985) "Water Channel Simulation of Concentration Fluctuations from a Ground Level Source" M.Sc. Thesis, Dept. of Mech.Eng., University of Alberta, Edmonton.
- Barry, P.J. (1977) "Stochastic Properties of Atmospheric Diffusivity" Chap. 7 in Sulphur and Its Inorganic Derivatives in the Canadian Environment, National Research Council of Canada pp 313-358.
- Bencala, K.E. and Seinfeld, J.H. (1976) "On Frequency Distribution of Air Pollutant Concentrations" Atmospheric Environment 10 pp. 941-950.
- Berger, A., Melice, J.L. and Demuth, Cl. (1982) "Statistical Distribution of Daily and High Atmospheric SO₂ Concentrations" Atmospheric Environment 16 pp. 2863-2877.
- Burgin, T.A. (1975) "The Gamma Distribution and Inventory Control" Opl. Res. Q., Vol. 26, 3, i.
- Cox, D.R. and Miller, H.D. (1965) "The Theory of Stochastic Processes" Chapman and Hall, London.
- Fackrell, J.E. (1978) "Plume Concentration Statistics Measured on the Tilbury-Northfleet Model" Central Electricity Generating Board Research Memorandum R/M/N1016.
- Fackrell, J.E. and Robins, A.G. (1982 a.) "Concentration Fluctuations and Fluxes in Plumes from Point Sources in a Turbulent Boundary Layer" Journal of Fluid Mechanics 117 pp. 1-26.
- Fackrell, J.E. and Robins, A.G. (1982 b.) "The Effects of Source Size on Concentration Fluctuations in Plumes" Boundary Layer Meteorology 22 pp. 335-350.
- Gifford, F.A. (1959) "Statistical Properties of a Fluctuating Plume Dispersion Model" in Advances in Geophysics 6 pp. 117-138 F.N. Frenkiel and P.A. Sheppard (eds.) Academic Press, New York.
- Gifford, F.A. (1960) "Peak to Average Concentration Ratios According to a Fluctuating Plume Dispersion Model" Int. Jour. Air Pollution 3 pp. 253-260.
- Gross, D. and Harris, C.M. (1975) "Fundamentals of Queueing Theory" J. Wiley and Sons, New York.
- Hanna, S.R. (1983) "Concentration Fluctuations in Smoke Plumes" Environmental Research and Technology Inc. Document No. PB-811-000, 30 pp.

- Hinds, W.T. (1969) "Peak-to-Mean Concentration Ratios from Ground Level Sources in Building Wakes" Atmospheric Environment 3 pp. 145-156.
- Hinze, J.O. (1975) Turbulence, 2nd Edition, McGraw Hill, New York.
- McGuire, T. and Noll, K.E. (1971) "Relation Between Concentrations of Pollutants and Averaging Time" Atmospheric Environment 5 pp. 291-298.
- Pasquill, F. (1974) Atmospheric Diffusion, 2nd ed. Halsted Press (John Wiley and Sons).
- Ramsdell, J.V. and Hinds, W.T. (1971) "Concentration Fluctuations in Plumes from a Ground-Level Continuous Point Source" Atmospheric Environment 5 pp. 483-495.
- Sawford, B.L. (1983) "The Effect of Gaussian Particle-Pair Distribution Functions in the Statistical Theory of Concentration Fluctuations in Homogeneous Turbulence" Quarterly Journal Royal Meteorological Society 109 pp. 339-354.
- Shoji, J. and Tsukatani, T. (1973) "Statistical Model of Air Pollutant Concentration and Its Application to Air Quality Standards" Atmospheric Environment 7 pp. 485-501.
- Sirivat, A. and Warhaft, Z. (1982) "The Mixing of Passive Helium and Temperature Fluctuations in Grid Turbulence" Journal of Fluid Mechanics 120 pp. 475-504.
- Weil, J.C. and Jepsen, A.F. (1977) "Evaluation of the Gaussian Plume Model at the Dickerson Power Plant" Atmospheric Environment 11 pp. 901-910.
- Wilson, D.J. (1982) "Predicting Risk of Exposure to Peak Concentrations in Fluctuating Plumes" Alberta Environment Technical Report, December 1982, 90 pp.
- Wilson, D.J., Fackrell, J.E. and Robins, A.G. (1982) "Concentration Fluctuations in an Elevated Plume: A Diffusion-Dissipation Approximation" Atmospheric Environment 16 pp. 2581-2589.
- Wilson, D.J., Robins, A.G. and Fackrell, J.E. (1982) "Predicting the Spatial Distribution of Concentration Fluctuations from a Ground Level Source" Atmospheric Environment 16 pp. 497-504.



N.L.C. - B.N.C.



3 3286 06942251 3